

Summer 2012

Biomechanical analysis of the cervical spine following total disc arthroplasty : an experimental and finite element investigation

Anup Anil Gandhi
University of Iowa

Copyright 2012 Anup Anil Gandhi

This dissertation is available at Iowa Research Online: <https://ir.uiowa.edu/etd/3296>

Recommended Citation

Gandhi, Anup Anil. "Biomechanical analysis of the cervical spine following total disc arthroplasty : an experimental and finite element investigation." PhD (Doctor of Philosophy) thesis, University of Iowa, 2012.
<https://doi.org/10.17077/etd.0jz9v30>

Follow this and additional works at: <https://ir.uiowa.edu/etd>

Part of the [Biomedical Engineering and Bioengineering Commons](#)

BIOMECHANICAL ANALYSIS OF THE CERVICAL SPINE FOLLOWING TOTAL
DISC ARTHROPLASTY: AN EXPERIMENTAL AND FINITE ELEMENT
INVESTIGATION

by
Anup Anil Gandhi

An Abstract

Of a thesis submitted in partial fulfillment
of the requirements for the Doctor of
Philosophy degree in Biomedical Engineering
in the Graduate College of
The University of Iowa

July 2012

Thesis Supervisor: Professor Nicole M. Grosland

ABSTRACT

Disc degeneration is a natural process and is widely prevalent. The severity of disc degeneration and the type of treatment varies from person to person. Fusion is a commonly chosen treatment option. However, clinical and biomechanical studies have shown that intervertebral discs adjacent to a fusion experience increased motion and higher stress which may lead to adjacent-segment disease. Cervical disc arthroplasty achieves similar decompression of the neural elements, but preserves the motion at the operated level and may potentially decrease the occurrence of adjacent segment degeneration.

Computationally, a validated intact 3D finite element model of the cervical spine (C2-T1) was modified to simulate single (C5-C6) and bi-level (C5-C7) degeneration. The single level degenerative model was modified to simulate single level fusion and arthroplasty with the Bryan and Prestige LP artificial discs. The bi-level degenerative model was modified to simulate a bi-level fusion, bi-level arthroplasty with Bryan and Prestige LP discs and a disc replacement adjacent to fusion.

An in-vitro biomechanical study was also conducted to address the effects of arthroplasty and fusion on the kinematics of the cervical spine. A total of 11 specimens (C2-T1) were divided into two groups (Bryan and Prestige LP). The specimens were tested in the following order; intact, single level TDR at C5-C6, bi-level TDR C5-C6-C7, fusion at C5-C6 and TDR at C6-C7 (Hybrid construct) and finally a bi-level fusion. The intact state was tested up to a moment of 2Nm. After surgical intervention, the specimens were loaded until the primary motion (C2-T1) matched the motion of intact state (hybrid control).

In all cases; computational and experimental, an arthroplasty preserved motion at the implanted level and maintained normal motion at the nonoperative levels. A fusion,

on the other hand, resulted in a significant decrease in motion at the fused level and an increase in motion at the un-fused levels. In the hybrid construct, the TDR adjacent to fusion preserved motion at that level, thus reducing the demand on the other levels.

The computational models were used to analyze disc stresses at the adjacent levels and facet forces at the index and adjacent levels. The disc stresses followed the same trends as motion. Facet forces though, increased considerably at the index level following a TDR. There was a decrease in facet forces however at the adjacent levels. The adjacent level facet forces increased considerably with a fusion. The hybrid construct had adjacent level facet forces between the bi-level TDR and bi-level fusion models.

To conclude, this study highlighted that cervical disc replacement with both the Bryan and Prestige LP discs not only preserved the motion at the operated level, but also maintained the normal motion at the adjacent levels. Under hybrid loading, the motion pattern of the spine with a TDR was closer to the intact motion pattern, as compared to the degenerative or fusion models. Also, in the presence of a pre-existing fusion, this study shows that an adjacent segment disc replacement is preferable to a second fusion.

Abstract Approved: _____
Thesis Supervisor

Title and Department

Date

BIOMECHANICAL ANALYSIS OF THE CERVICAL SPINE FOLLOWING TOTAL
DISC ARTHROPLASTY: AN EXPERIMENTAL AND FINITE ELEMENT
INVESTIGATION

by

Anup Anil Gandhi

A thesis submitted in partial fulfillment
of the requirements for the Doctor of
Philosophy degree in Biomedical Engineering
in the Graduate College of
The University of Iowa

July 2012

Thesis Supervisor: Professor Nicole M. Grosland

Copyright by
ANUP ANIL GANDHI
2012
All Rights Reserved

Graduate College
The University of Iowa
Iowa City, Iowa

CERTIFICATE OF APPROVAL

PH.D. THESIS

This is to certify that the Ph.D. thesis of

Anup Anil Gandhi

has been approved by the Examining Committee
for the thesis requirement for the Doctor of Philosophy
degree in Biomedical Engineering at the July 2012 graduation.

Thesis Committee:

Nicole M. Grosland, Thesis Supervisor

Joseph D. Smucker

Tae Hong Lim

David G. Wilder

Salam Rahmatalla

To my family and friends

ACKNOWLEDGMENTS

It gives me great pleasure to present my Doctoral thesis titled ‘Biomechanical Analysis of the Cervical Spine Following Total Disc Arthroplasty: An Experimental and Finite Element Investigation’. This dissertation is a result of three years of hard work, which would not have been possible without support and encouragement of many people. I would like to thank each and everyone.

First and foremost, I would like to express profound gratitude to my advisor, Dr. Nicole Grosland, for her invaluable support, encouragement, supervision and useful suggestions throughout the research work. Her moral support and continuous guidance enabled me to complete my work successfully.

Special thanks to Douglas Fredericks for performing all the surgeries, and all his help and support throughout the project. I would like to thank Dr. Joseph Smucker for providing valuable clinical insights for this project. Dr. Tae-Hong Lim, Dr. David Wilder and Dr. Salam Rahmatalla: thank you for serving on my committee and providing valuable suggestions.

I am grateful to the Bone Healing Research Lab for their financial support over the years and to Medtronic Sofamor Danek, USA for supporting this project by providing the necessary implants and the CAD files.

I am thankful to all my MIMX labmates; Dr. Swathi Kode, Dr. Nicole DeVries and Amy Criswell for all the help with testing and Dr. Kiran Shivanna, Dr. Srinivas Tadepalli and Dr. Nicole Kallemeyn for assistance with FE modeling and analysis. It has been a pleasure working with all the members of MIMX and BHRL lab.

A big thank you to all my friends for supporting me and making my life outside the lab a fun filled one. Last but not the least I would like to thank my family, especially my parents and my sister. Their unconditional love and support helped me reach my goals.

TABLE OF CONTENTS

LIST OF TABLES	vi
LIST OF FIGURES	vii
LIST OF DEFINITIONS	x
CHAPTER 1: INTRODUCTION	1
1.1 Relevant Anatomy	1
1.1.1 Human Spine	1
1.1.2 Cervical Spine	3
1.2 Cervical Disc Degeneration	6
1.3 Operative Management.....	9
1.3.1 Anterior Cervical Decompression and Fusion (ACDF)	9
1.3.2 Cervical Disc Replacement	11
1.3.2.1 Bryan Cervical Disc	12
1.3.2.2 Prestige Cervical Disc	14
CHAPTER 2: SIGNIFICANCE AND SPECIFIC AIMS	17
2.1 Significance	17
2.2 Specific Aims.....	18
CHAPTER 3: MATERIALS AND METHODS	19
3.1 Finite Element Study	19
3.1.1 Intact (Non-degenerative) Model	20
3.1.2 Degenerative Model	22
3.1.3 Simulation of Fusion	23
3.1.3.1 Single level fusion	23
3.1.3.2 Bi-level fusion	24
3.1.4 Simulation of TDR: Bryan Cervical Disc	24
3.1.4.1 Modeling the Bryan Disc	24
3.1.4.2 Simulation of single level TDR surgery.....	25
3.1.4.3 Simulation of bi-level TDR surgery.....	27
3.1.5 Simulation of TDR: Prestige LP.....	28
3.1.4.4 Modeling the Prestige LP Disc.....	28
3.1.4.5 Simulation of single level TDR surgery.....	29
3.1.4.6 Simulation of bi-level TDR surgery.....	31
3.1.6 Simulation of TDR adjacent to Fusion	32
3.1.7 Flexibility Test.....	33
3.2 In-vitro cadaveric testing	34
3.2.1 Testing Protocol.....	37
3.2.1.1 Specimen Preparation.....	38
3.2.1.2 Surgical Procedure: Total Disc Replacement.....	39
3.2.1.3 Surgical Procedure: Total Disc Replacement – Bi-level.....	40
3.2.1.4 Surgical Procedure: Disc replacement adjacent to fusion	41
3.2.1.5 Surgical Procedure: Bi-level Fusion	42
3.2.2 Data Analysis.....	43

CHAPTER 4: RESULTS	44
4.1 Finite Element Analysis Results	44
4.1.1 Comparison of Intact and Degenerative Models	44
4.1.1.1 Range of Motion.....	45
4.1.1.2 Disc Stresses.....	47
4.1.2 Comparison of single level degenerative, disc replacement and fusion models.....	49
4.1.2.1 Range of Motion.....	49
4.1.2.2 Moments.....	51
4.1.2.3 Disc Stresses.....	52
4.1.2.4 Facet Forces.....	53
4.1.3 Comparison of bi-level degenerative, disc replacement and fusion models.....	54
4.1.3.1 Range of motion	54
4.1.3.2 Moments.....	56
4.1.3.3 Disc Stresses.....	57
4.1.3.4 Facet Forces.....	58
4.1.4 Comparison of bi-level degenerative, fusion and hybrid models.....	60
4.1.4.1 Range of Motion.....	60
4.1.4.2 Moments.....	61
4.1.4.3 Disc Stresses.....	62
4.1.4.4 Facet Forces.....	63
4.2 In-vitro Cadaveric Testing Results	65
4.2.1 TDR using Bryan Cervical Disc.....	65
4.2.1 TDR using Prestige LP Cervical Disc	69
CHAPTER 5: DISCUSSION.....	73
5.1 Finite Element Analysis.....	73
5.1.1 Intact Model.....	73
5.1.2 Degenerative Model	73
5.1.3 Single, Bi-level and Hybrid Models	74
5.2 <i>In-vitro</i> Cadaveric Testing	76
5.3 Comparison of computational and experimental results	78
CHAPTER 6: FUTURE WORK	80
APPENDIX A: SURGICAL TECHNIQUE FOR IMPLANTATION	81
A.1 Bryan® Cervical Disc system.....	81
A.2 Prestige LP® Cervical Disc system.....	88
APPENDIX B: DETAILED FE ANALYSIS RESULTS	94
B.1 Single Level Models	94
B.1 Bi-level Models.....	97
REFERENCES	101

LIST OF TABLES

Table 1: Hyperelastic Mooney-Rivlin material properties for different regions of annulus ground substance in intact and degenerative models	22
Table 2: Hybrid moments (Nm) required in various single level models to achieve overall range of motion equal to the intact model.	51
Table 3: Magnitude of facet contact forces at the altered and adjacent levels for intact and various single level models under hybrid moments	53
Table 4: Hybrid moments (Nm) required in various bi-level models to achieve overall range of motion equal to the intact model.	56
Table 5: Magnitude of facet contact forces at the altered and adjacent levels for intact and various bi-level models under hybrid moments	58
Table 6: Hybrid moments (Nm) required in various bi-level degenerative, fusion and hybrid models to achieve overall range of motion equal to the intact model.....	61
Table 7: Magnitude of facet contact forces at the altered and adjacent levels for intact, bi-level degenerative, hybrid (Bryan and Prestige) and bi-level fusion models under hybrid moments.....	64
Table 8: Hybrid moments (Nm) required after various surgeries to achieve overall range of motion equal to the intact state.	68
Table 9: Hybrid moments (Nm) required after various surgeries to achieve overall range of motion equal to the intact state.	72
Table B-1: Range of motion (degrees) values for all single level models in all six directions.....	95
Table B-2: Range of motion (degrees) values for all bi-level models in all six directions.....	99

LIST OF FIGURES

Figure 1: The Human Spine - Anterior, Posterior and Lateral Views [1].....	1
Figure 2: Cervical Spine [4].....	3
Figure 3: A human cervical vertebra [5].....	4
Figure 4: Diagrammatic illustration of the Intervertebral Disc [9].....	5
Figure 5: Grading system for cervical intervertebral disc degeneration.[15]	8
Figure 6: Anterior Cervical Decompression and Fusion [25].....	10
Figure 7: Bryan Cervical Disc (Left), Exploded view showing various components (Right)	12
Figure 8: Bristol-Cummins (Left), Prestige ST (middle) and Prestige LP (Right) cervical discs	15
Figure 9: C2-T1 Intact Finite Element Model	21
Figure 10: Meshes of individual components of Bryan disc.	24
Figure 11: 3D FE model of the Bryan cervical disc (left) and section view of the Bryan disc showing the different contact pairs.....	25
Figure 12: Figure showing the C5-C6 mesh after simulation of milling operations ready for implantation of Bryan disc.	26
Figure 13: Cervical spine model highlighting the implanted Bryan cervical disc at C5-C6 (left) and a sectioned view of the model (right)	27
Figure 14: : C2-T1 FE mesh with bi-level TDR using Bryan discs at C5-C6 and C6- C7	28
Figure 15: 3D FE model of the Prestige LP cervical disc (left) and section view of the Prestige LP disc showing the contact pair	29
Figure 16: Figure showing the C5-C6 mesh after simulation of cutting operations ready for implantation of Prestige LP disc	30
Figure 17: C2-T1 FE model with Prestige LP disc implanted at C5-C6	31
Figure 18: C2-T1 FE mesh with bi-level TDR using Prestige LP discs at C5-C6 and C6-C7 levels.....	32
Figure 19: Human cervical spine in the MTS Bionix System with two Spine Simulators	35
Figure 20: Flowchart of the Experimental Protocol	37

Figure 21: Specimen ready to be tested with C2 and T1 levels potted in Bondo.	38
Figure 22: Specimens implanted with Prestige LP (left) and Bryan (right) discs at the C5-C6 level	39
Figure 23: Bi-level disc replacement with Bryan (left) and Prestige LP (right) discs.....	40
Figure 24: Specimen with a 360 fusion at C5-C6 level and a disc replacement at C6-C7 level	41
Figure 25: Specimen with a bi-level 360 fusion at C5-C6-C7 levels.	42
Figure 26: Comparison of Range of Motion in all 6 directions between intact (non-degenerative), single level degenerative and bi-level degenerative models.	46
Figure 27: Comparison of annular stresses between Intact and single level degenerative models at the levels cranial and caudal to the degenerated level.....	47
Figure 28: Comparison of annular stresses between Intact and bi-level degenerative models at the levels cranial and caudal to the degenerated levels	48
Figure 29: Percent change in motion after fusion and arthroplasty with Bryan and Prestige LP with respect to degenerated motion (C5-C6 level).....	50
Figure 30: Percent change in disc stresses after disc replacement (Bryan and Prestige LP) and fusion in comparison to the degenerative model at the cranial and caudal levels	52
Figure 31: Percent change in motion after bi-level fusion and bi-level arthroplasty with Bryan and Prestige LP discs.	55
Figure 32: Percent change in disc stresses after bi-level disc replacement (Bryan and Prestige LP) and bi-level fusion in comparison to the bi-level degenerative model at the cranial and caudal levels.....	57
Figure 33: Comparison of percent change in motion between Bryan Hybrid, Prestige LP Hybrid and bi-level fusion models.	60
Figure 34: Percent change in disc stresses after a hybrid surgery (Bryan and Prestige LP) and bi-level fusion in comparison to the bi-level degenerative model at the cranial and caudal levels.....	62
Figure 35: Mean intervertebral rotations (\pm standard deviation) for various surgical constructs (Bryan) for each level during Flexion-Extension, lateral bending and axial rotation.....	66
Figure 36: Mean intervertebral rotations (\pm standard deviation) for various bi-level surgical constructs (Bryan)	67
Figure 37: Mean intervertebral rotations (\pm standard deviation) for various surgical constructs (Prestige LP) for each level during Flexion-Extension, lateral bending and axial rotation.....	69

Figure 38: Mean intervertebral rotations (\pm standard deviation) for various bi-level surgical constructs (Bryan)	71
Figure A-1: Excision of disc (A), and removal of osteophytes using a high speed burr (B)	82
Figure A-2: Figure showing transverse alignment (A), sagittal alignment (B) and securing of the Dual Track Milling Guide.	83
Figure A-3: Figure showing burring of the end-plates	84
Figure A-4: End-plate milling operation.....	85
Figure A-5: Insertion of implant spacer (A), and distraction (B)	86
Figure A-6: Bryan disc being filled with saline (A) and tightening of seal plug (B)	87
Figure A-7: A: Implant being inserted in the disc space; B: Disc fully seated in the disc space.....	88
Figure A-8: Anterior surface being milled to create a flat surface.	89
Figure A-9: A rasp being used to prepare the endplates	90
Figure A-10: Rail cutter guide inserted in the disc space	91
Figure A-11: Rail cutting	92
Figure A-12: A: Implant being inserted in the disc space. B: Prestige LP disc fully seated in the disc space.....	93
Figure B-1: Comparison of range of motion in all six directions between single level degenerative, Bryan, Prestige LP and fusion models.	94
Figure B-2: Comparison of range of motion in all six directions between bi-level degenerative, Bryan, Prestige LP and fusion models.....	97
Figure B-3: Comparison of range of motion in all six directions between bi-level degenerative, Bryan Hybrid, Prestige LP Hybrid and bi-level fusion models.	98

LIST OF DEFINITIONS

FE	Finite Element
FEA	Finite Element Analysis
TDR	Total Disc Replacement
ACDF	Anterior cervical decompression and fusion
3D	Three Dimensional
ALL	Anterior Longitudinal Ligament
PLL	Posterior Longitudinal Ligament
CL	Capsular Ligament
LF	Ligamentum Flavum
IS	Interspinous Ligament
CT	Computed Tomography
MRI	Magnetic Resonance Imaging
MTS	Materials Testing Machine
IREDD	Infrared Light Emitting Diodes
Hybrid Construct	Surgical construct with fusion at one level and a disc replacement at the adjacent level
Hybrid Protocol/Control	Loading protocol where the specimen/model is loaded until its motion matches the motion in intact state

CHAPTER 1: INTRODUCTION

1.1 Relevant Anatomy

1.1.1 Human Spine

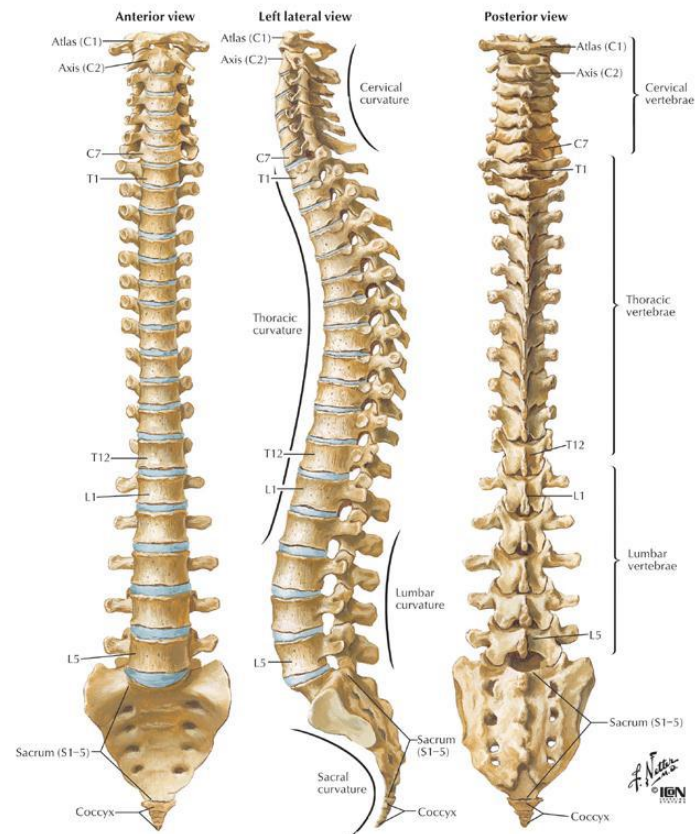


Figure 1: The Human Spine - Anterior, Posterior and Lateral Views [1]

The spine is one of the most important weight bearing structures of the human skeleton. It is comprised of 33 vertebrae connected by ligamentous soft tissue and intervertebral discs forming a segmented column (Figure 1). It is this segmentation that allows the spine to be as flexible as it is. Although the spine is flexible, it is a complex

structure extending from the base of the skull to the pelvis. Most of the weight of the thorax is transferred to the pelvis by the vertebral column.

The first 7 vertebrae of the vertebral column that comprise in the neck region are known as the cervical vertebrae and are numbered from C1 to C7. The next 12 vertebrae make up the thoracic region. The ribs attach to these vertebrae forming a cage which protects the heart and the lungs. These vertebrae are numbered from T1 to T12. The region in the lower back is known as the lumbar spine. It consists of 5 vertebrae numbered from L1 to L5. The lumbar region plays a very important role since it has to support most of the body weight. After the lumbar spine is the Sacrum; it is formed by the fusion of 5 sacral vertebrae. Finally, the last 4 bones fuse to form the coccyx or the tail bone. Since the last 9 bones of the spine are fused to form 2 bones, the spine is also referred to as been made up of 24 bones instead of 33 bones.

Although the spine appears to be straight in the coronal plane, it has four major curves when seen laterally. These curves are very important to balance, flexibility, and stress absorption and distribution. Spinal curves are either kyphotic or lordotic. A kyphotic curve that is concave anteriorly and convex posteriorly where as a lordotic curve is convex anteriorly and concave posteriorly. Normal lordosis is seen in the neck (cervical spine) and low back (lumbar spine) while normal kyphosis is seen in the chest (thoracic spine) and hip areas (sacral spine) (Figure 1). Each of the naturally occurring and normal soft curves serves to distribute mechanical stress incurred as the body is at rest and during movement [2,3].

The smallest possible representation of the spine that can demonstrate the biomechanical characteristics is known as the functional spinal unit (FSU). It is made up of two adjacent vertebrae along with the connecting intervertebral disc and interconnecting ligaments. Each individual FSU has a normal range of motion, the limits of which help contribute to the stability of the spine. When one or more parts of a FSU are affected by disease, trauma, or degeneration, the tissues do not interact normally.

1.1.2 Cervical Spine

The first seven vertebrae (C1 to C7) make up the cervical spine (Figure 2). The cervical spine supports the skull and protects the spinal cord in addition to allowing a diverse head movement.

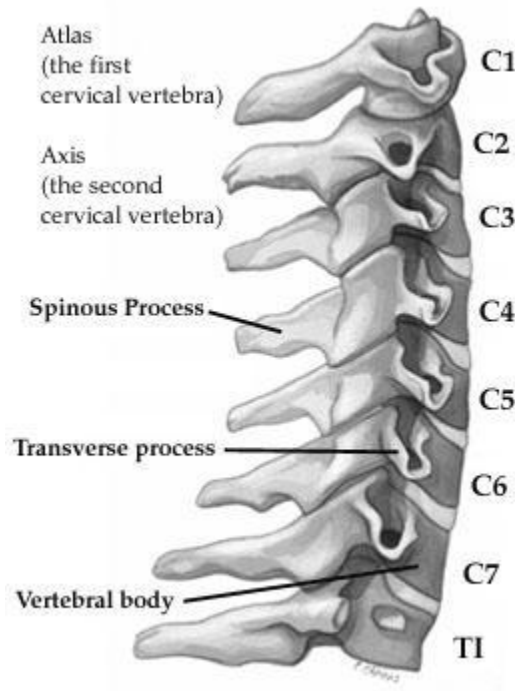


Figure 2: Cervical Spine [4]

The cervical spine is classically divided into the upper atypical vertebrae (C1, C2) and the subaxial spine (C3-C7) as shown in Figure 2. The atlas (C1) and axis (C2) differ from all other vertebrae. There is a diarthrodial articulation between the anterior articular surface of the dens of C2 and the posterior surface of the anterior arch of C1 where the majority of the rotation in the cervical spine occurs. Each vertebra is made of the same parts and consists of a vertebral body on the anterior and a bony ring made of articular, transverse, and spinous processes on the posterior. The vertebral body is a cylindrical

structure containing the outer cortical and the inner cancellous bone. The vertebrae of the subaxial spine have a consistent osseous anatomy, with slight variations in size and orientation of the lateral mass, lamina and a relative consistency to the size of the vertebral bodies (Figure 3). The spinous processes of the cervical spine gradually changes from a bifid spinous process at C2 to a single prominent spinous process at C7. The vertebral bodies of the subaxial cervical spine articulate with one another through the unique joints of Luschka also known as uncovertebral joint.

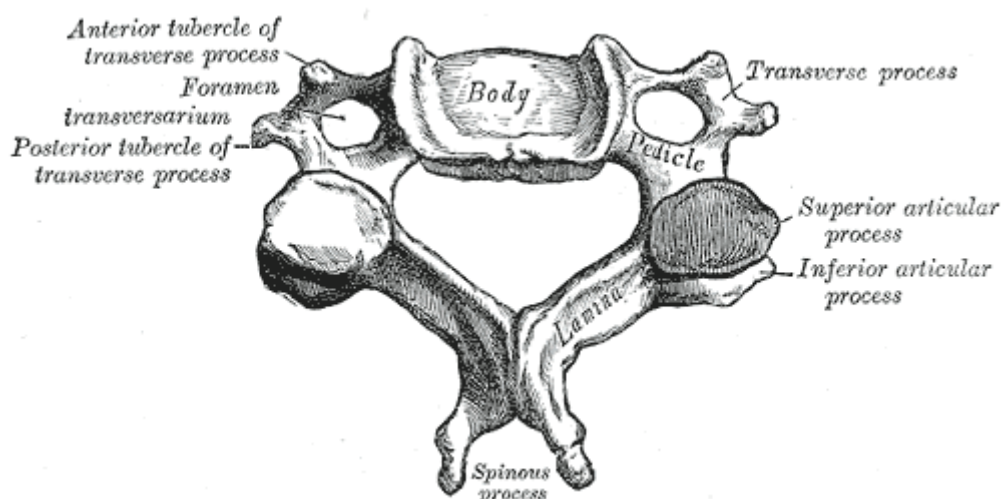


Figure 3: A human cervical vertebra [5]

The intervertebral disc is located between the vertebral bodies beginning at the C2-C3 level (Figure 4). The cervical annulus is well developed anteriorly; but it tapers laterally and posteriorly towards the anterior edge of the uncinate process on each side. The disc functions as a shock absorber between their respective vertebral bodies with axial loads. The facet joints of the subaxial spine are true diarthrodial articulations encapsulated in a thick fibrous sheath, the facet capsule. They allow small degrees of flexion and extension, limit rotation and ultimately serve to protect the disc from

translational shear stresses [6]. It has been shown in the past that the anterior body carries most of the load placed on the spine with only 18% of the compressive load carried by the facets [7]. Few others have shown that the load carried by the facets can vary from zero to 33% depending on the posture. In certain postures the facets will be unloaded and the capsular ligaments will be under tension [8].

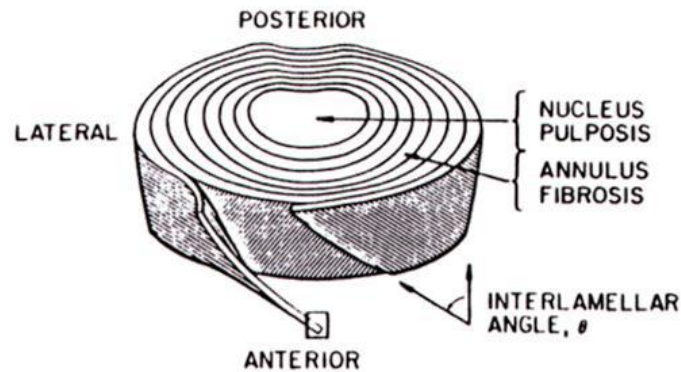


Figure 4: Diagrammatic illustration of the Intervertebral Disc [9]

The cervical spine also features a complex arrangement of ligaments to supplement its structure and mobility. Ligaments are uniaxial structures that are mostly effective in carrying loads along the fiber direction. They can resist tensile forces but buckle under compression. The key function of the ligaments is to allow adequate physiologic motion under different directions while limiting excessive motion to protect the spinal cord. The cervical spinal ligaments include mainly anterior longitudinal ligament (ALL) and posterior longitudinal ligament (PLL) that line the anterior and posterior surfaces of disc and vertebral bodies respectively, the capsular ligaments (CL) that are generally oriented in a direction perpendicular to the plane of the facet joints, the Ligamentum Flavum (LF) that is a thick elastic connective tissue connecting the adjacent

laminae together and interspinous (IS) and intertransverse ligaments that pass between the spinous and transverse process respectively.

1.2 Cervical Disc Degeneration

The intervertebral discs, undergo dramatic changes in structure, composition, and mechanical function with age. The intervertebral discs are also susceptible to degenerative disc disease. The effects of normal aging and of degenerative disc disease are very similar and difficult to differentiate [10].

Cervical disc degeneration is a common pathology which may require surgical intervention as a final treatment. The intervertebral discs play a very important role in mobility and load transfer through the spinal column. Any load through the spinal column is transmitted to the intervertebral disc from the vertebral body [2]. The normal intervertebral disc is anisotropic in structure, the jelly-like nucleus pulposus acts like a fluid filled bag and swells under pressure. The interaction between the intervertebral disc components is similar to a thick-walled pressure vessel, and allows the intervertebral discs to act as shock absorbers, absorbing and transmitting the loads experienced by the spine.

With degeneration however, the biomechanical properties of the disc are altered [11]. Once degeneration sets in, the intervertebral disc goes through a cascade of degenerative changes resulting in a loss of demarcation between the nucleus pulposus and annulus fibrosus, loss of disc height, a decrease in height as the intervertebral disc loses its ability to rehydrate after loading, and altered loading on the intervertebral disc and surrounding tissues [2,10,11].

Though, the exact pathogenesis of the degenerative process is still unknown, several factors that might cause degeneration are: aging, mechanical factors due to occupational exposure, abnormal loading conditions, and the loss of nutrition to the disc [11-13]. Disc degeneration might also be predetermined genetically [14].

Depending on where the degeneration occurs, in the nucleus pulposus or the annulus; there are different ways a degenerated disc can lead to neck pain. Loss of disc height and structure may result in pain in the intervertebral disc itself because of increased innervation in degenerated intervertebral discs. This loss of disc height along with gradual ossification of the endplate and protrusion of the disc tissue leads to stenosis which may lead to neck pain. Loss of disc height may also contribute to altered loading on the vertebral bodies and facet joints of the spine, resulting in pain and possibly arthritis in the facet joints. Bulging of the intervertebral disc can result in nerve root impingement, causing pain in areas of the body innervated by the impinged nerve. Degeneration of the nucleus combined with the annular degeneration may cause disc herniation into the spinal canal causing radiation and neck pain due to nerve pinching. Some authors have devised methods of grading the level of disc degeneration in the cervical spine based on the MRI images [15]. Figure 5 depicts the images of various levels of disc degeneration. Based on the classification of the disc degeneration, surgeons can diagnose the degree of degeneration from the images themselves.

Disc degeneration is a natural process and happens to most individuals [16]. The level of disc degeneration and the type of treatment varies from person to person. Treatments vary from conservative or non-invasive treatments like bed rest or pain killers to invasive treatments or surgeries.

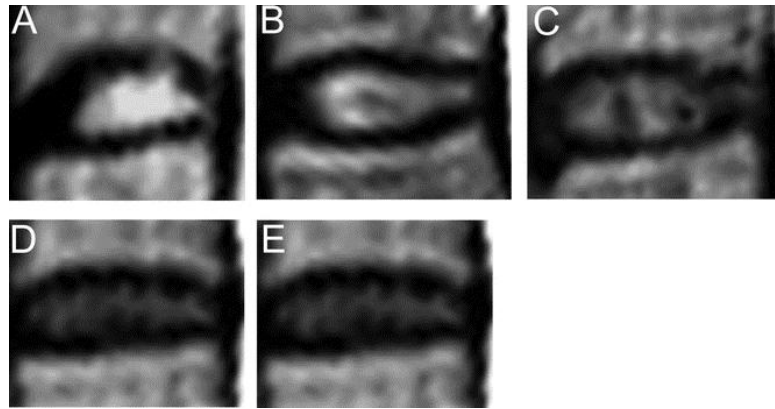


Figure 5: Grading system for cervical intervertebral disc degeneration.[15]

- A. Grade I: Nucleus signal intensity is hyper-intense and nucleus structure is homogeneous, white. Distinction of nucleus and annulus is clear. Disc height is normal.
- B. Grade II: Nucleus signal intensity is hyper-intense and nucleus structure is inhomogeneous with horizontal band, white. Distinction of nucleus and annulus is clear. Disc height is normal.
- C. Grade III: Nucleus signal intensity is intermediate and nucleus structure is inhomogeneous, gray to black. Distinction of nucleus and annulus is unclear. Disc height is normal to decrease.
- D. Grade IV: Nucleus signal intensity is hypo-intense and nucleus structure is inhomogeneous, gray to black. Distinction of nucleus and annulus is lost. Disc height is normal to decrease.
- E. Grade V: Nucleus signal intensity is hypo-intense and nucleus structure is inhomogeneous, gray to black. Distinction of nucleus and annulus is lost. Disc height is collapsed.

Grading was performed on T2-weighted midsagittal images.

(Adapted from: Miyazaki M et al. Kinematic analysis of the relationship between sagittal alignment and disc degeneration in the cervical spine.)

Conservative or non-invasive treatments are usually attempted first, leaving surgery as the last resort. These treatments include medications; pain relievers in addition to anti inflammatory medications, physical therapy and exercise, cervical traction, use of cervical collar or brace and epidural steroid injections [17]. In cases of severe disc

degeneration or herniation, these treatments fail to alleviate the pain. If the pain and disability is severe, spine surgery is a reasonable option.

1.3 Operative Management

1.3.1 Anterior Cervical Decompression and Fusion (ACDF)

The goal of cervical spine surgery is to relieve pain, numbness, tingling and weakness, restore and preserve nerve function and stop or prevent abnormal motion in the spine. Anterior Cervical Decompression and Fusion (ACDF) has been the most commonly preferred method to treat herniated discs, radiculopathy and myelopathy for more than 50 years [18,19].

ACDF involves the excision of disc and bone material causing spinal cord compression and thereafter, stabilizing the spine with autograft /allograft/ or titanium mesh cages with plate fixation (Figure 6).. The main advantages of this approach are the ability to directly remove the majority of compressive pathologies encountered in the cervical spine (e.g., disc herniations, ventral osteophytes), and the ability to decompress the spinal cord. ACDF has served as the standard by which other cervical and spinal disorders may be judged as the result of its high rate of success. The consistent ability of this procedure to relieve symptoms related to neurologic dysfunction and the clinical results with regard to the patient's index complaint are outstanding.

However, this procedure has some drawbacks. Biomechanical studies have shown that spinal levels adjacent to a fusion experience increased intradiscal pressure, increased motion, high facets loads and higher shear stresses [20,21]. These higher stresses may lead to higher incidence of disc degeneration and possibly instability [22]. In 1999, an extensive study by Hilibrand et al comprising of 374 patients with a total of 409 ACDFs reported occurrence of adjacent-segment disease at the rate of 2.9% per year, with a cumulative of 25% over 10 years [23]. A long term followup on patients after

ACDF by Goffin et al reported an adjacent segment degenerative change to be as high as 92% [24].



Figure 6: Anterior Cervical Decompression and Fusion [25]

Pseudoarthrosis, or the lack of fusion after surgery is another drawback that has been reported in some patients [26,27]. Ideally, over time the graft facilitates bone growth in the disc space fusing the two vertebrae. However, if the fusion does not occur, the implant loosens over time. There are chances of implant breakage or even pullout. This phenomenon is known as pseudoarthrosis. Treating it in some cases might even require a revision surgery. Incidences of pseudoarthrosis reported in literature range from 0-50% depending on the number of levels fused [28-33].

To summarize, immobility, adjacent segment disease and pseudoarthrosis are some of the drawbacks of fusion due to which investigators have developed surgical

alternatives to fusion that attempt to address the kinematic and biomechanical issues inherent in it. Cervical disc arthroplasty achieves similar decompression of the neural elements, but preserves the motion and elasticity at the operated level and may potentially decrease the occurrence of adjacent segment degeneration.

1.3.2 Cervical Disc Replacement

Attempts to provide functional substitute for intervertebral discs date back to 1950s, but the unique anatomic features and biomechanical properties of the spinal segment are considerably more challenging to reproduce than the simple ball-and-socket hip joint or the hinged knee joint. The first attempt at cervical arthroplasty reported by Fernstrom in 1966 involved the placement of metallic ball bearings into the disc space of the treated segments. Clinical results were, however, disappointing because of high incidence of segmental hypermobility, endplate subsidence, and clinical failure.

Interest in cervical arthroplasty waned until the 1980s when a renewal of efforts was spurred by progress in lumbar arthroplasty with the Charite prosthesis. Gradually, with reported success of lumbar arthroplasty, renewed enthusiasm has emerged for the prospects of a cervical prosthesis. The first human trial of the cervical prosthesis was the Cummins-Bristol disc (two piece, metal-on-metal, ball and socket) that was developed at Frenchay Hospital, Bristol, United Kingdom.

In contrast to metal-on-metal design of the Bristol disc, a metal-on-plastic design called the Bryan disc emerged in the late 1990s, followed by the Porous coated motion (PCM) artificial disc. With the success of lumbar Prodisc device, a similar construct called Prodisc-C was designed for cervical arthroplasty. Despite the issuance of over 100 separate patents for various artificial disc designs, fewer than 10 designs have led to the implanted devices. This study focuses on the Bryan Cervical Disc (Medtronic Sofamor Danek, Memphis, TN, USA) and the Prestige LP Cervical Disc (Medtronic Sofamor Danek, Memphis, TN, USA).

1.3.2.1 Bryan Cervical Disc

The Bryan Cervical Disc was conceived and developed in the early 1990s by the neurosurgeon Vincent Bryan. After extensive research and testing, the first Bryan Cervical Disc was implanted in January 2000 [34].



Figure 7: Bryan Cervical Disc (Left), Exploded view showing various components (Right)

The Bryan Cervical Disc is an artificial cervical disc made up of two titanium shells, a polycarbonate polyurethane nucleus, a polyether polyurethane sheath, two titanium retaining wires, and two titanium seal plugs (Figure 7). The plastic nucleus is shaped to fit between the two dome-shaped shells. The side of the shell that rests against the bone includes a rough-textured coating to allow for potential attachment to the bone. The articulating surfaces of the device are polyurethane and titanium. The nucleus is designed to fit between the two shells. The bone contacting side of each shell includes a sintered titanium porous coating to provide for bony ingrowth. The nucleus-contacting side of each shell has a center pin which interacts with a central hole in the nucleus to control the range of motion and help prevent nucleus expulsion. A stop or wing on the anterior aspect of the device, which extends superiorly on the cephalad shell and

inferiorly on the caudal shell, is intended to prevent migration of the device into the spinal canal. A polyurethane sheath surrounds the nucleus and is attached to each shell with titanium retaining wires, forming a closed compartment.

The disc is available in five diameters: 14, 15, 16, 17, and 18mm. There is only one height (~6mm after implantation). The insertion technique involves multiple steps and is complex, allowing for precise placement of the prosthesis and preparation of the endplates.

One of the primary goals of cervical disc replacement is to reproduce the normal kinematics after implantation. Bryan cervical disc system is one of the most commonly implanted artificial cervical discs and since it has been successfully implanted for a long time, there have been multiple studies. Sasso et al. conducted a randomized clinical trial comparing the kinematics for Bryan disc arthroplasty and fusion where he observed that following Bryan disc arthroplasty, flexion/extension range of motion (ROM) was maintained at the operated level when compared to the arthrodesis group. Though the ROM at the adjacent levels was similar in both groups, greater anterior-posterior translation was observed at the cephalad adjacent level following fusion. Hence, the authors concluded that Bryan disc may delay adjacent level degeneration by preserving preoperative kinematics at adjacent levels [35]. Goffin et al. published results from a multicenter European study and found success rates in single-level Bryan Cervical Disc replacement at 6 months, 12 months and 24 months of 90%, 86% and 90% respectively. In a bilevel study, success rates at 6 months and 1 year were 82% and 96% respectively. At 1 year, flexion/extension range of motion per level averaged 7.9° in the single level and 7.4° in the bilevel [36].

Galbusera et al. did two finite element studies to determine the biomechanics of C5-C6 spinal unit before and after the placement of the prosthesis [37,38]. The first study included a single FSU whereas the second study had three levels (C4-C7) in the finite element model. Both studies concluded that the moment-rotation curves after the

placement of prosthesis were comparable to the curves obtained from the intact model. The second study which involved the C4-C7 FE model also concluded that the influence of the Bryan disc on mechanics of the adjacent segments resulted to be not significant, in terms of both facet forces and ROMs.

Clinical studies corroborate the conclusions of the biomechanical studies. Several clinical studies have shown significant improvement for Bryan in the post-operative values of VAS (Visual analog scale), SF-36 (Short form-mental component), SF-36, (Short form-physical component) and NDI (Neck disability index) when compared to arthrodesis, making Bryan cervical disc prosthesis a reliable and safe treatment for patients with cervical spondylosis [39-42].

1.3.2.2 Prestige Cervical Disc

The pioneering efforts of Cummins, working in collaboration with the Department of Medical Engineering at Frenchay Hospital, Bristol, U.K, resulted in the invention of metal-on-metal artificial cervical disc with a ball and socket articulation also known as the Bristol-Cummins disc. Developed in the early 1990s, the Bristol-Cummins disc was modified to the Prestige I disc (Medtronic Sofamor Danek) in 1998, to the Prestige II disc (Medtronic Sofamor Danek) in 1999, to the Prestige ST device in 2002, to the Prestige STLP in 2003 and ultimately to the Prestige LP device. The Bristol-Cummins disc, the Prestige I, the Prestige II, the Prestige ST and the Prestige STLP devices are all stainless steel implants. The first four use vertebral body screws to fix their position in the interspace. However, to maintain its implanted position, the Prestige STLP and Prestige LP discs use rails to provide initial friction against migration of the implant and a plasma spray coating on its superior and inferior surfaces to allow bony ingrowth from the vertebral endplates onto the device. This eliminates the anterior profile of the device allowing multilevel implantation. The main difference between Prestige STLP and Prestige LP is the material. The Prestige LP disc is made of titanium and

ceramic composite making it MRI compatible. This device is currently being evaluated in a FDA IDE trial.



Figure 8: Bristol-Cummins (Left), Prestige ST (middle) and Prestige LP (Right) cervical discs

The original Bristol-Cummins disc had a metal-on-metal stainless steel ball-and-socket articulation. Eighty-nine percent of patients exhibited significant clinical improvement and motion preservation up to 5 years postoperation [43]. The second generation device (Prestige I) incorporated a ball-and-trough articulation that allowed for anterior-posterior translation to be coupled with flexion-extension motion which was more similar to the normal physiological motion. Prestige I was able to maintain motion with improved clinical outcomes [44,45]. The Prestige II included a roughened endplate design to promote bony ingrowth. It was shown to alleviate pain and symptoms comparable to fusion while maintaining motion at the treated level [46]. The Prestige ST had a reduction in the height of each anterior flange. It was shown to maintain physiologic segmental motion at 24 months after implantation and was associated with improved neurologic success, improved clinical outcomes, and a reduced rate of secondary surgeries compared with ACDF [47].

The fifth generation Prestige LP disc has a low anterior profile allowing the possibility of multilevel implantation. Recently a clinical study was conducted involving

forty patients (21 females and 19 males) with a mean follow-up of 2.9 years [48]. Cervical range of motion, Neck Disability Index, Visual Analogue, Short Form-36, Modified American Academy of Orthopedic Surgeons, and Japanese Orthopedic Association scores and radiographs were evaluated. Based on the study, the AAOS, VAS, NDI, and JOA scores improved significantly at 6 months and 2 years postoperation. There was significant improvement in all aspects of the SF-36 scores except general health at 6 months and 2 years postoperation. There was significant segmental motion at 6 months and 2 years postoperation compared to the preoperation based on dynamic radiographs.

CHAPTER 2: SIGNIFICANCE AND SPECIFIC AIMS

2.1 Significance

Degenerative disc disease of the cervical spine is a prevalent condition in the population. Studies have shown that by age 65, 95% of men and 70% of women will have some sort of degenerative change as evident on X-ray [49]. Fusion is the accepted gold standard treatment. Unfortunately, arthrodesis lacks the prospect of intervertebral mobility and hence may lead to adjacent segment degeneration. Motion-sparing technologies, such as total disc replacements, offer an alternative to fusion. According to a new Life Science Intelligence (LSI) Report, the U.S. market for artificial disc replacement will grow from \$55 million in 2007 to \$440 million by the year 2013. Initially, these technologies were expected to rapidly penetrate the market for spinal fusion patients due to their potential to preserve motion, limit further degeneration, and avoid the need for fusion; but growth has been restrained by reimbursement challenges, limited long-term data, and various clinical concerns.

The literature is lacking information on kinematics of multilevel arthroplasty and arthroplasty adjacent to fusion. According to AAOS, approximately a quarter-million spinal fusions are performed each year, of which almost half are cervical spine procedures [50]. Also, an increasing number of cases presenting with degenerative changes at levels adjacent to a previous fusion have been reported [28,51-53]. These patients with adjacent level degeneration would be potential patients for Total Disc Replacement (TDR). Hence, studying the behavior of an artificial disc adjacent to fusion is critical.

There have been various studies involving experimental and computational models for evaluating the biomechanics of the cervical spine after arthroplasty [37,54-57]. Most of these studies focused on comparing artificial discs to fusion based on intradiscal pressures and ranges of motion [57-59]. These studies ascertain the ability of

these discs to retain motion at the treated level, minimally affecting the motion patterns at adjacent spinal levels. This may represent as an important step in reducing the incidence of adjacent segment disease. Nevertheless, there is still a good deal of biomechanical data that needs to be determined as far as multilevel disc replacement and disc replacement adjacent to fusion is concerned.

The native disc tissue is composed of a highly hydrated nucleus surrounded by a fiber-reinforced annulus. The mechanical behavior of these tissues is highly nonlinear and involves the use of fluid flow and hydrostatic support to counterbalance stresses that are seen during the activities of daily living. The currently available arthroplasty disc designs in no way resemble the native disc from a geometric or material property standpoint. From an engineering perspective, one would expect the load transmission profile in the cervical spine to be altered after implantation of these devices. This study will attempt to fill this void in knowledge with the use of experimental and computational techniques.

2.2 Specific Aims

The specific aims of the current study can be summarized as follows:

Specific Aim 1: To simulate a single (C5-C6) bi-level (C5-C6-C7) degeneration in a C2-T1 Finite Element model and compare it with the Intact model.

Specific Aim 2: To simulate a single-level TDR at C5–C6 level by modifying the single level degenerative model and to compare it with experimental data and fusion model.

Specific Aim 3: To simulate a bi-level TDR at C5-C6-C7 levels by modifying the bi-level degenerative model and to compare it with experimental data and bi-level fusion model.

Specific Aim 4: To simulate a TDR adjacent to fusion and compare it to bi-level fusion model and experimental data.

CHAPTER 3: MATERIALS AND METHODS

This chapter describes the methods used to gain insight into biomechanics of the cervical spine following disc replacement and fusion. Both *in-vitro* cadaveric testing and finite element analysis were used in this study. Cadaveric testing provides the most direct and obvious way to obtain information on spinal biomechanics and performance, whereas computational models prove to be very useful in quantifying variables not directly measurable with experimental studies (e.g., local stresses and strains). Thus, by using computational models in supplement with experimental research, we gain some valuable insight in understanding the clinical biomechanics of the cervical spine.

3.1 Finite Element Study

In-vitro and *in-vivo* experiments give valuable data, but unfortunately, little information can be obtained about the internal responses. Hence, a commonly employed technique to study the spinal biomechanics is the finite element (FE) method.

Finite element analysis is an essential part of today's engineering activities. Over the years as FE software capabilities have expanded, the number of applications has grown tremendously. The irregular geometry of vertebral bodies, complex nature of the disc, and facet contact between the adjacent vertebrae, all make the spine a very complex structure. Hence, an enormous effort has been put in over the years to generate accurate models that provide a true representation of the spinal behavior. Advanced FE meshers are now able to accurately mesh complex structures like the spine. Also, the commercially available FEA packages available today are capable of handling the complex geometry and non-linearity found in the spine.

Finite element models have been demonstrated to be very useful in quantifying variables not directly measurable with experimental studies (e.g., local stresses and strains). It is also a powerful tool to access the constraints in the FSU, specifically the facet loading, stresses at the adjacent segments, and the contact forces at the prosthesis-

bearing surface. Another important advantage of FE models is that, once validated, a number of parametric studies can be performed at minimal costs.

3.1.1 Intact (Non-degenerative) Model

A previously validated 3D finite element model of the cervical spine (C2-T1) was used [60]. The vertebral bodies were segmented from CT images of the cadaveric spine while MR images provided the approximate boundaries of the intervertebral disc. Thereafter the regions of interest were converted into triangulated surfaces as described by DeVries et al [61]. The resultant surfaces were meshed with hexahedral elements using the multi-block meshing technique (IA-FEMesh) [62]. The meshing technique used is similar to the one described by Kallemeyn et al [63]. The vertebral body was divided into cortical and cancellous regions and a Young's modulus of 10GPa and 450MPa was assigned to each region respectively. All the 5 major spinal ligaments (PLL, ALL, LF, IS, CL) were included in the model and were defined as 3D Truss elements acting in tension only using hypoelastic material definition in ABAQUS.

A finite-sliding surface interaction was used to model the facet joint with a tabular pressure-overclosure relationship used to simulate the cartilage layer. The interaction works towards increasing the contact pressure with the narrowing initial gap distance between the facet surfaces. The intervertebral disc was divided into annular and nucleus regions and was modeled with hybrid linear hexahedral elements. The annulus region of the disc which included grounds substance and fibers was modeled with hexahedral and rebar elements respectively. The annular grounds were further divided into anterior, lateral, and posterior regions for better control of the material properties in these regions. The grounds were defined using isotropic, incompressible, hyperelastic Mooney–Rivlin (c_1 , c_2) formulation. The annular fibers were oriented at approximately $\pm 25^\circ$ from the transverse plane and were assigned a nonlinear hypoelastic material definition based on experimental collagen fiber studies [64]. The nucleus was represented by fluid elements.

The C2-C7 part of model was validated with specimen-specific experimental data under a moment of 1Nm [65]. The T1 vertebra was later on added to the model and this updated model was validated with literature data under a moment of 2Nm in flexion extension [66].

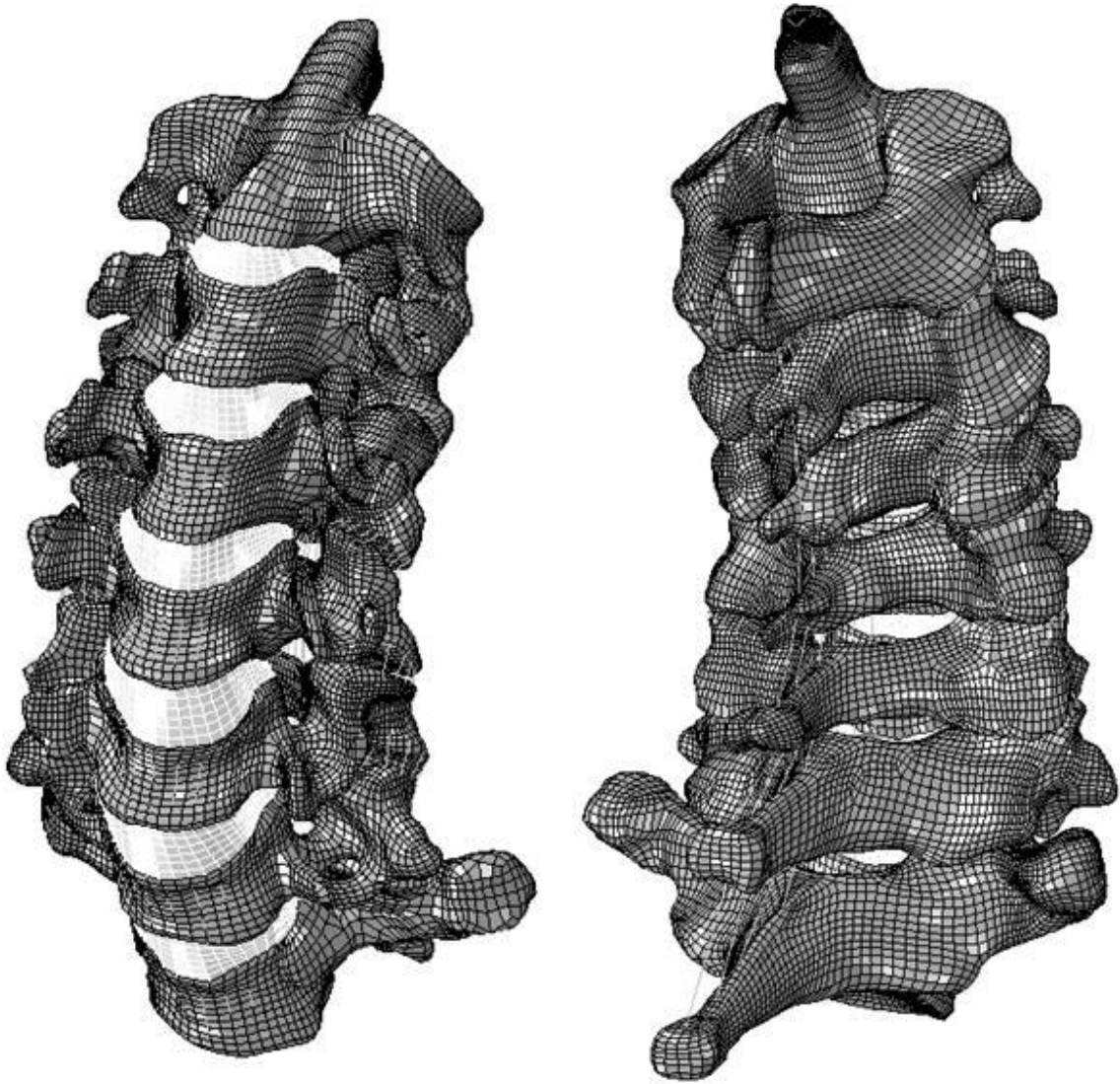


Figure 9: C2-T1 Intact Finite Element Model

3.1.2 Degenerative Model

Degenerative disc disease of the cervical spine is a prevalent condition in the population. Studies have shown that by age 65, 95% of men and 70% of women will have some sort of degenerative change as evident on X-ray [49]. Patients with degenerated discs often times undergo surgery of some sort; fusion or disc replacement in most cases. Thus, instead of simulating fusion/TDR in intact (normal) model, the model was first modified to account for degenerative conditions.

Table 1: Hyperelastic Mooney-Rivlin material properties for different regions of annulus ground substance in intact and degenerative models

	Anterior		Posterior		Lateral	
	c1	c2	c1	c2	c1	c2
Intact Model						
C5-C6	0.2	0.05	0.133	0.033	0.133	0.033
C6-C7	0.2	0.05	0.3	0.075	0.133	0.033
Degenerative Model						
C5-C6	1.05	0.2625	0.7	0.175	0.7	0.175
C6-C7	1.05	0.2625	1.5	0.375	0.7	0.175

Consequently, the intact model was modified to simulate degenerative models by changing the material properties of the disc. Two different models were created; degeneration at C5-C6, and degeneration at C5-C6-C7.

A moderately degenerated disc was simulated by removing the hydrostatic capabilities of the nucleus and by making the nucleus and annulus stiffer [67] (Table 1).summarizes the hyperelastic Mooney-Rivlin material properties of the three regions of

the annulus. The degenerated nucleus was assigned linearly elastic material property with a Young's Modulus of 1.66MPa and a Poissons ratio of 0.4. Although studies have shown that the disc height and disc area also change nominally as disc degeneration progresses, the same disc geometry was used for simplicity [68].

3.1.3 Simulation of Fusion

Spinal fusion is one of the most common procedures performed on the cervical spine. A fusion procedure consists of removing a degenerated intervertebral disc and inserting some form of cage or graft material into the disc space to restore/maintain disc height and appropriate lordotic curvature of the cervical spine. Sometimes an additional anterior plate system is used. Interbody fusion cages are hollow implants that restore physiological disc height, allowing bone growth within and around them, thus stimulating bone fusion. They have been developed to prevent disc space collapse and its relevant clinicoradiological consequences, as well as the donor-site morbidity reported in conjunction with autologous bone graft procedures [69]. Interbody fusion cages have a load-sharing function and stabilize the spine to increase segmental stiffness, thus achieving fusion rates similar to those associated with bone grafts, even in multilevel disease [70].

3.1.3.1 Single level fusion

The degenerative model was modified to a simulate fusion at the C5-C6 level. This was done by changing the material properties of the disc to that of bone ($E = 5\text{GPa}$) [71]. The nucleus of the disc was replaced by a rigid body to simulate the presence of a metal cage. An anterior plate was not included in the model since studies have shown that cage assisted cervical interbody fusion without the use of plates is as effective as interbody fusion with graft and plate [70].

3.1.3.2 Bi-level fusion

A bi-level fusion was simulated at the C5-C6 and C6-C7 levels by modifying the bi-level degenerative model. The steps involved were exactly same as the single level fusion i.e. replacing nucleus by a rigid body and changing the material properties of annulus to that of bone.

3.1.4 Simulation of TDR: Bryan Cervical Disc

3.1.4.1 Modeling the Bryan Disc

The Bryan cervical disc contains a polycarbonate polyurethane nucleus which articulates with a titanium shell on the top and bottom. A polyurethane sheath surrounds the nucleus and is attached to each shell using titanium wires. The polyurethane sheath and titanium wires were not modeled since they are functionally inert. A CAD model of the disc was obtained from Medtronic (Medtronic Sofamor Danek, Memphis, TN). The titanium shells and polyurethane nucleus were imported into IA-FEMesh for meshing with hexahedral elements [62]. The meshes of the individual components can be seen in Figure 10.

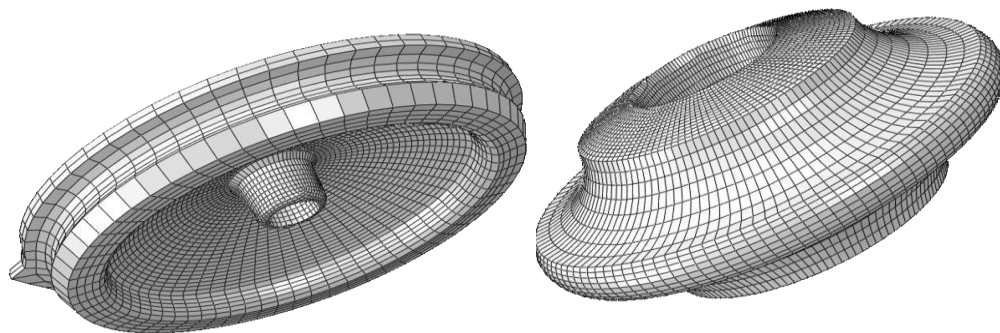


Figure 10: Meshes of individual components of Bryan disc.

The titanium shells were assigned a Young's Modulus of 110GPa and a Poisson's ratio of 0.3 and the polyurethane nucleus was assigned a Young's Modulus of 30MPa and a Poisson's ratio of 0.45. Four contact pairs were defined; two each for contact between the nucleus- upper shell and nucleus-lower shells (Figure 11). The contact between the shells and the nucleus was modeled as finite sliding with coefficient of friction of 0.1.

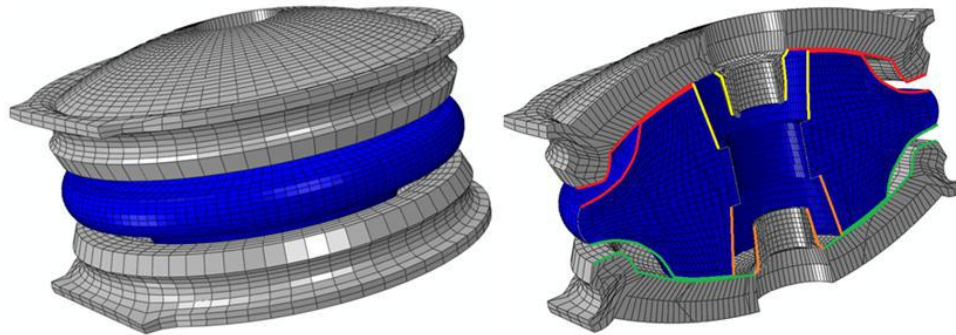


Figure 11: 3D FE model of the Bryan cervical disc (left) and section view of the Bryan disc showing the different contact pairs.

3.1.4.2 Simulation of single level TDR surgery

The single level degenerative model was modified to simulate a TDR at C5-C6. First, a proper size disc was chosen by analyzing the CT scan data. Then the ALL at the C5-C6 level was removed. Next, the nucleus and anterior and posterior parts of the annulus were removed in order to create space for the disc. The maximum possible portions of the lateral annulus and uncinat processes were preserved. The endplates were removed, and a spherical socket fitting the Bryan disc was created in the vertebrae simulating the milling operation performed during the surgical procedure (Figure 12). This was done using an in house Surgical Simulation Suite [72].

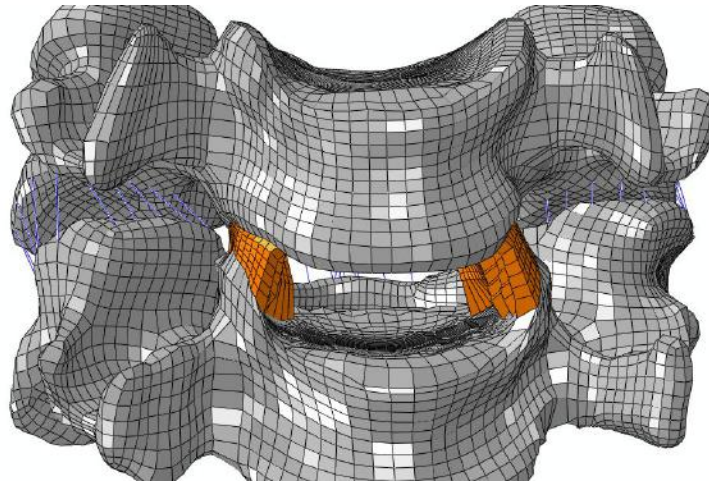


Figure 12: Figure showing the C5-C6 mesh after simulation of milling operations ready for implantation of Bryan disc.

The C5 vertebra was distracted by 1.5mm and the Bryan mesh was then inserted in the disc space (Figure 13). A 16mm disc was used based on the CT image analysis. The prestresses in the discs and the ligaments due to the distraction were exported and fed back into the model as initial conditions. Perfect implant-bone fixation was assumed. This was achieved by using the “TIED” command in ABAQUS which ensured that there was no relative motion between the implant and the vertebral endplates.

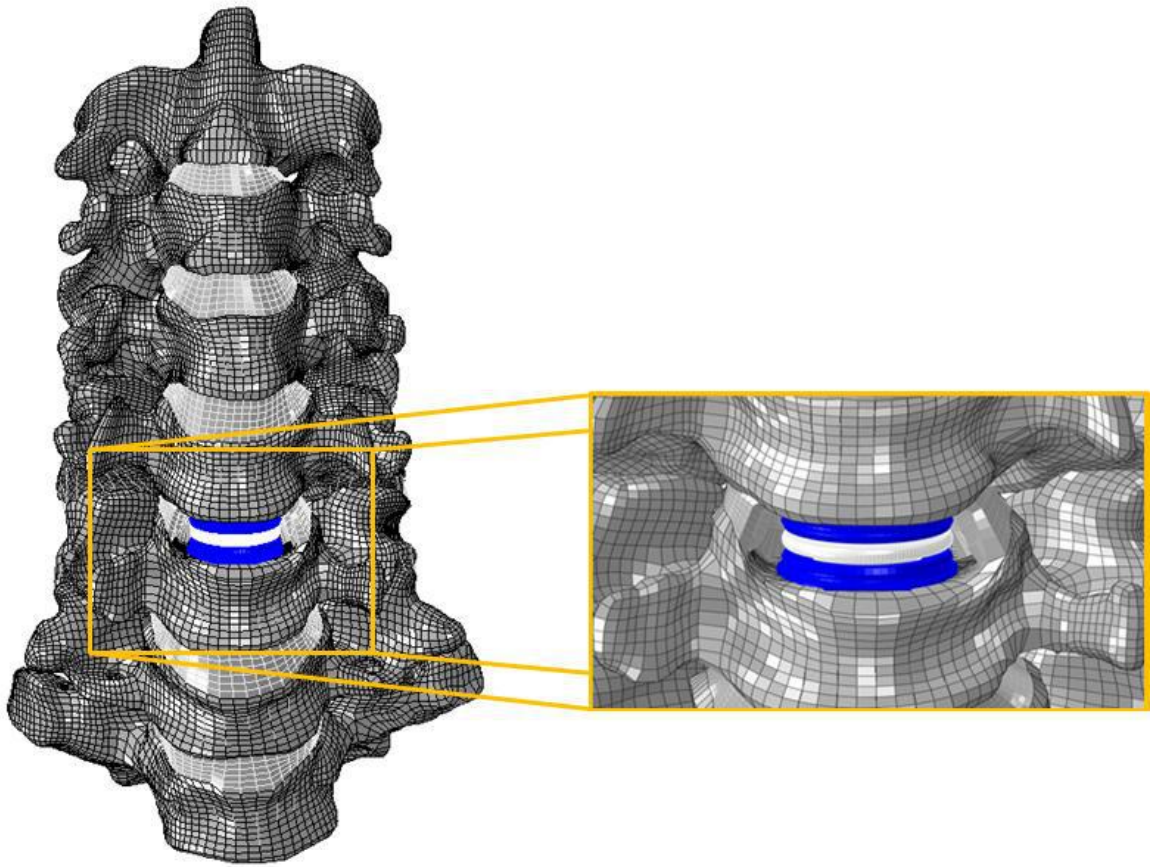


Figure 13: Cervical spine model highlighting the implanted Bryan cervical disc at C5-C6 (left) and a sectioned view of the model (right)

3.1.4.3 Simulation of bi-level TDR surgery

A bi-level disc replacement with Bryan cervical disc system was simulated by modifying the bi-level degenerative model. First a single level TDR at C5-C6 level was performed as described earlier. Then on similar lines, another TDR was performed at the adjacent C6-C7 level. Both C5-C6 and C6-C7 disc spaces were distracted by 1.5 mm and the pre-stresses in the ligaments and the discs were fed back as initial conditions. Once again, a 16mm disc was chosen based on CT analysis. A “TIED” contact was again used for all four endplate-shell contacts to simulate osteointegration.

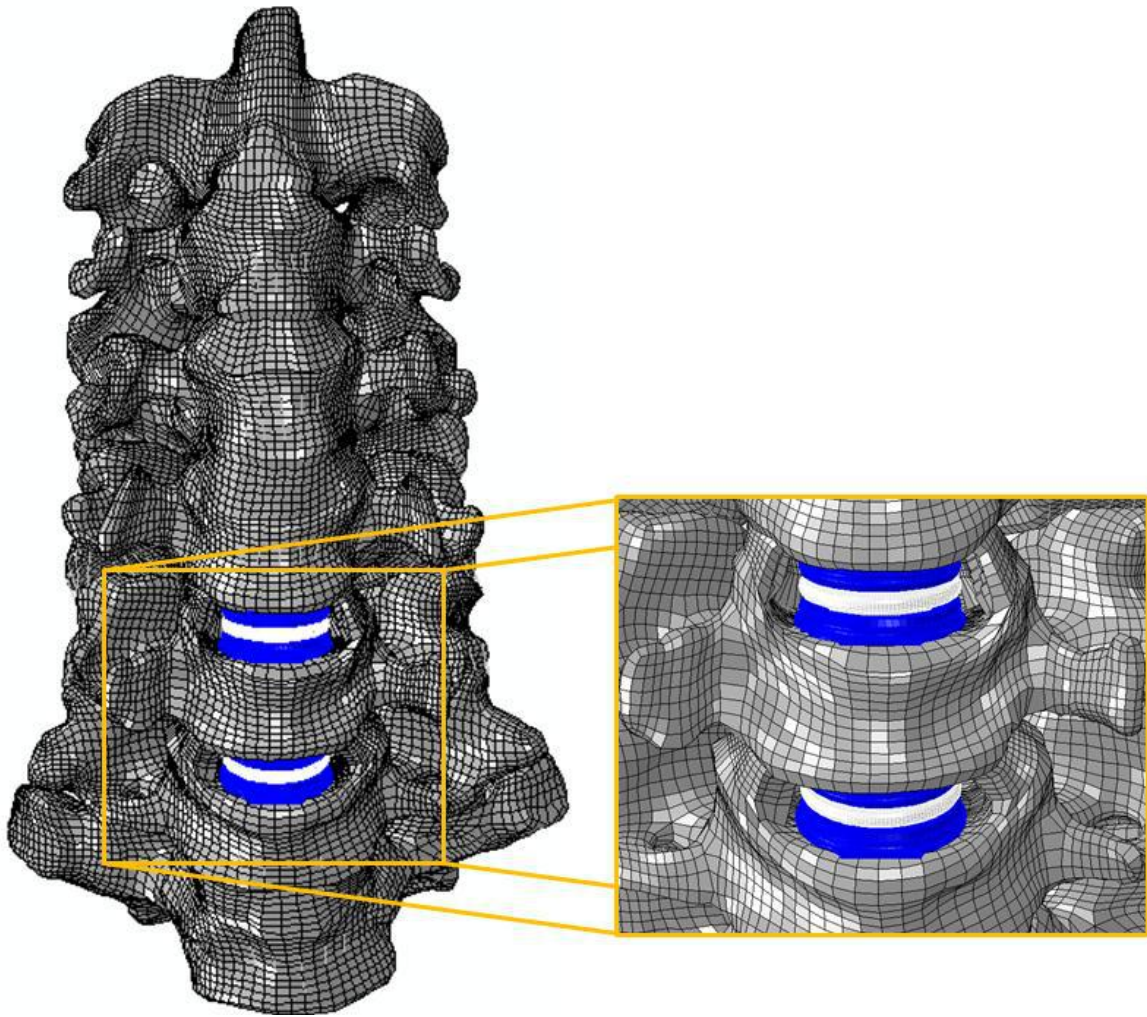


Figure 14: : C2-T1 FE mesh with bi-level TDR using Bryan discs at C5-C6 and C6-C7

3.1.5 Simulation of TDR: Prestige LP

3.1.4.4 Modeling the Prestige LP Disc

The Prestige LP is a titanium ceramic composite device with two articulating components (ball on top & trough on the bottom) that attach to the vertebral bodies. It is a fifth generation device based on the Bristol-Cummins disc. The main highlights of this disc are its low profile and use of rails to provide initial friction against migration of the

implant. It also has a plasma spray coating on its superior and inferior surfaces to allow bony ingrowth from the vertebral endplates.

A 3D FE mesh of the Prestige LP disc was created in IA-FEMesh using the surfaces provided by Medtronic (Medtronic Sofamor Danek, Memphis, TN) [62]. Both components of the disc were meshed with hexahedral elements (Figure 15). The rails and plasma coating were not included in the mesh since we assumed the disc to be osteointegrated with the endplates. The two components of the disc were assigned an elastic modulus of 110GPa and Poisson's Ratio of 0.3. The contact between the ball and trough was modeled as finite sliding with a coefficient of friction of 0.1 to simulate a realistic articulation between the two parts (Figure 15).

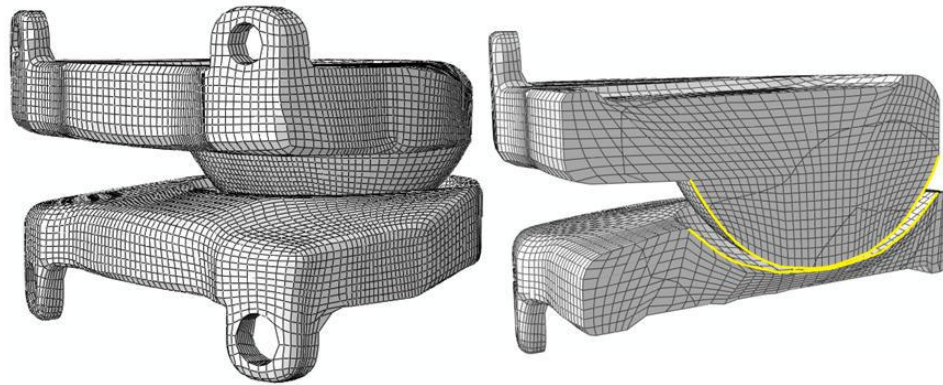


Figure 15: 3D FE model of the Prestige LP cervical disc (left) and section view of the Prestige LP disc showing the contact pair

3.1.4.5 Simulation of single level TDR surgery

A single level arthroplasty was simulated at the C5-C6 level by modifying the C5-C6 degenerative model. Following the instructions in the Prestige LP surgical technique manual, the single level TDR was performed. Based on the CT measurements, an appropriately sized implant was selected (8 x 16mm) and meshed as described earlier.

The anterior longitudinal ligament was removed followed by the nucleus and anterior and posterior parts of the annulus fibrosus creating space for the disc. The maximum possible portions of the lateral annulus and the uncinata processes were preserved. The endplates were prepared as per the manual. The cutting operation was simulated using an in house Surgical Simulation Suite (Figure 16) [72].

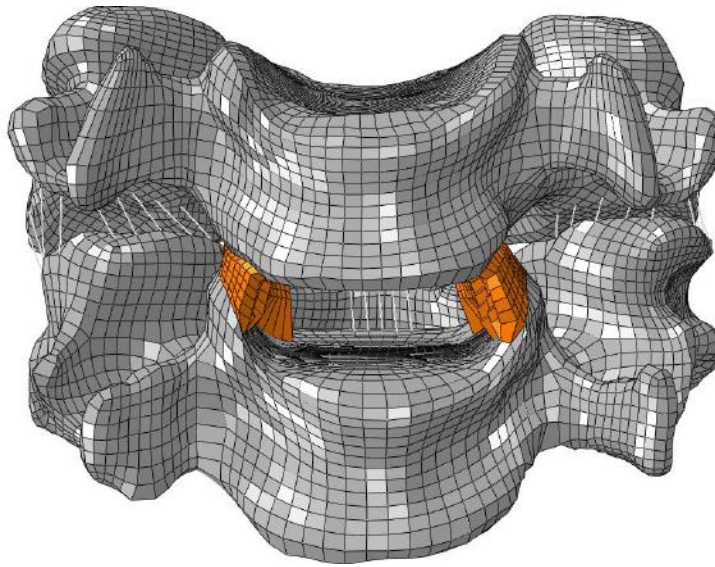


Figure 16: Figure showing the C5-C6 mesh after simulation of cutting operations ready for implantation of Prestige LP disc

The C5 vertebra was distracted by 1.5 mm and the Prestige LP disc mesh was inserted in the disc space (Figure 17). The prestresses in the discs and the ligaments due to the distraction were exported and fed back into the model as initial conditions. Both the superior and inferior components of the implants were attached to the respective endplates of the vertebral bodies to simulate complete osteointegration of the implant with the bone. Thus, the interaction between the implant and the vertebral bodies were modeled as “TIED” contact.

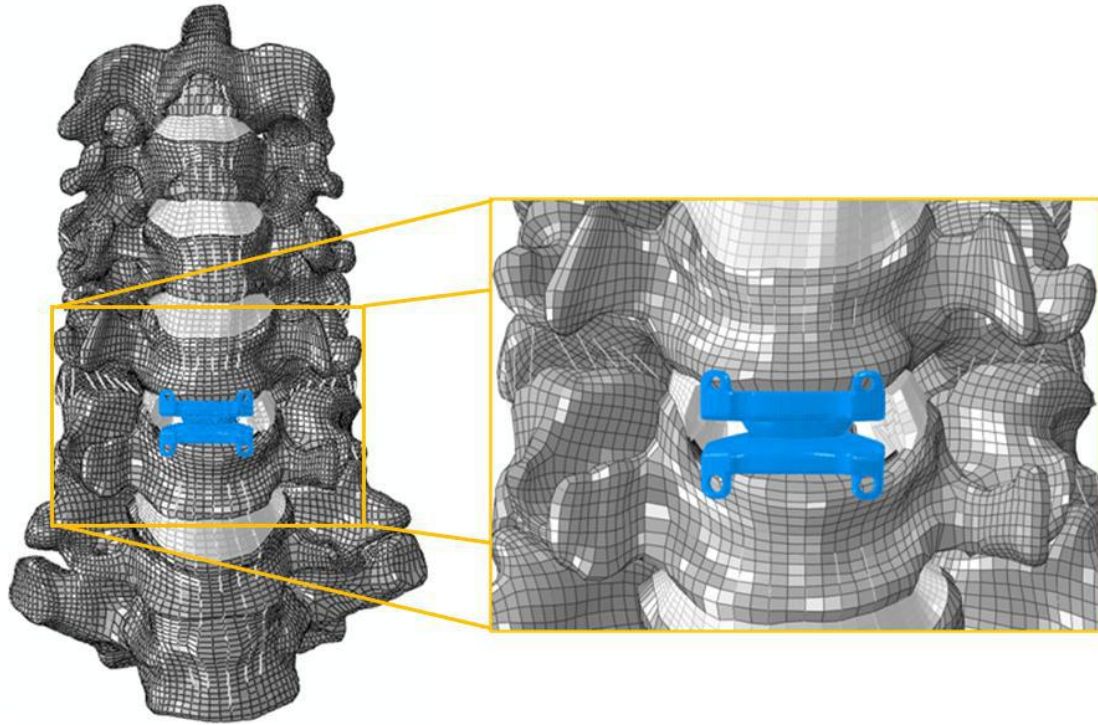


Figure 17: C2-T1 FE model with Prestige LP disc implanted at C5-C6

3.1.4.6 Simulation of bi-level TDR surgery

A bi-level arthroplasty was simulated at the C5-C6 and C6-C7 levels by modifying the C5-C6-C7 degenerative model (Figure 18). The single level approach was expanded to two levels. Once again CT images were analyzed for disc measurements and since the disc space of C5-C6 and C6-C7 were similar, the same 8 x 16mm sized Prestige LP disc was chosen for both the levels. The surgical operations were exactly the same as the single level approach (i.e. removal of ALL, nucleus pulposus, anterior and posterior sections of annulus and some portion of lateral annulus). Both levels were distracted 1.5mm and the prestresses in the discs and the ligaments due to the distraction were exported and fed back into the model as initial conditions. The contact between the ball and trough was modeled as finite sliding with a coefficient of friction of 0.1 and that between the discs and bodies was “TIED”.

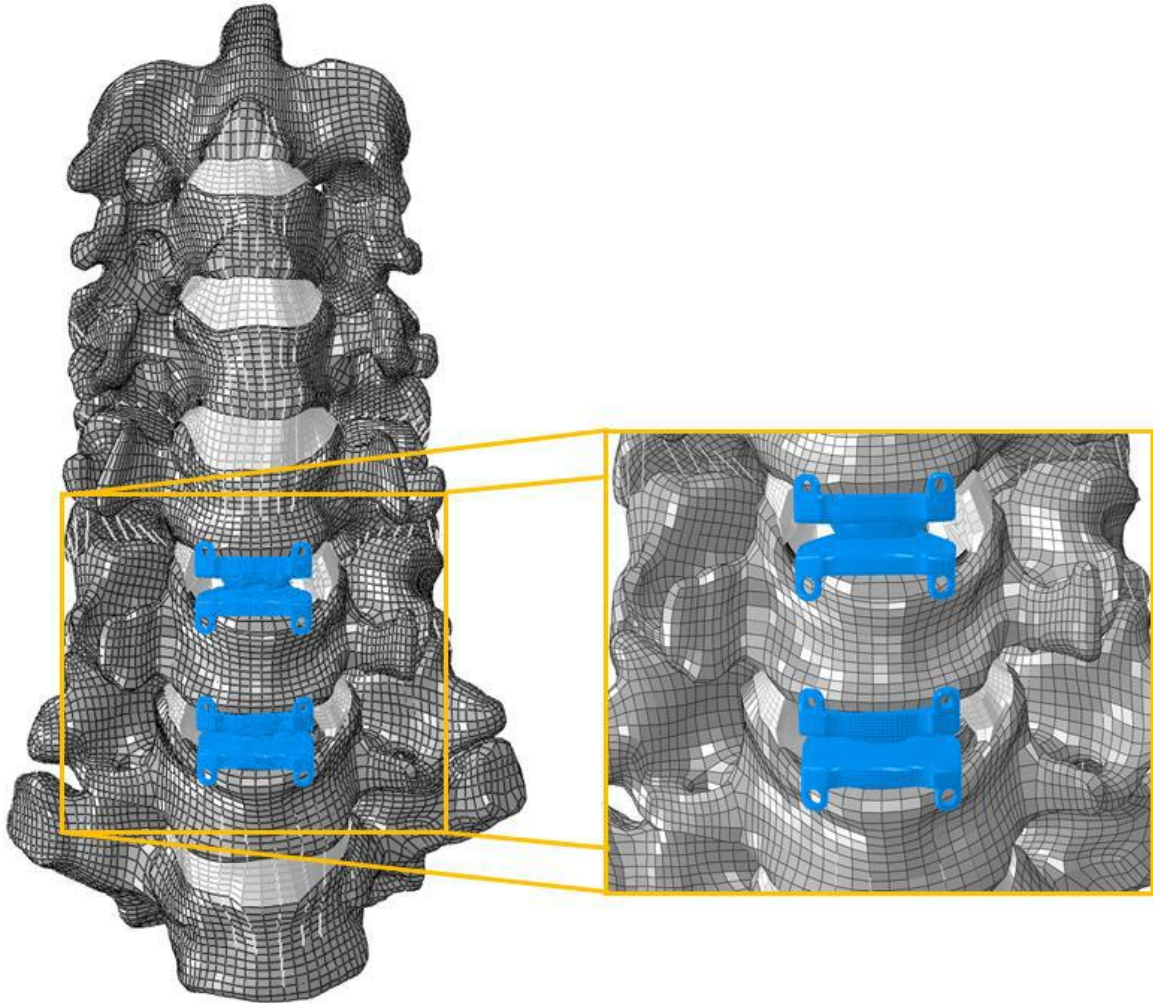


Figure 18: C2-T1 FE mesh with bi-level TDR using Prestige LP discs at C5-C6 and C6-C7 levels

3.1.6 Simulation of TDR adjacent to Fusion

Anterior cervical discectomy and fusion (ACDF) has been established as a successful surgical treatment for radiculopathy and/or myelopathy resulting from degenerative disc disease. There are, however, negative consequences to fusion after anterior cervical decompression, including such complications as pseudarthrosis, and the potential for adjacent segment biomechanical alterations and degeneration. Researchers estimated that more than 25% of patients will develop adjacent segment disease during

the first 10 years after the initial fusion and a risk of repeat operation [23,73]. It is likely that another fusion at adjacent level will accentuate the deleterious effects of fusion on the remaining mobile segment biomechanics. Thus, the concept of a disc replacement, at the symptomatic level adjacent to a prior fusion represents an appealing reconstructive alternative.

There is a lack of biomechanical studies on TDR adjacent to fusion. Clinically though, Phillips et al. [74] conducted a 6 center prospective study to evaluate the outcomes of cervical disc replacement with Porous Coated Motion (PCM) performed adjacent to a prior cervical fusion and obtained favorable results.

The bi-level degenerative model was modified to simulate a fusion at the C5-C6 level and a TDR at C6-C7 level. Fusion was simulated using the technique described in “Simulation of fusion” section earlier. Disc replacement will be done using both Bryan and Prestige LP discs as described in earlier sections.

3.1.7 Flexibility Test

The intact model was subjected to a pure moment of 2 Nm under physiologic flexion/extension ($\pm MX$), right/left lateral bending ($\pm MZ$), and right/left axial rotation ($\pm MY$) modes. The inferior nodes of T1 vertebra were fixed in all directions and a moment of 2Nm was applied to the superior surface of C2. The motion in each direction was noted and the other models were loaded in flexion-extension, lateral bending, and axial rotation by increasing the moment until the primary C2-T1 motion matched that of the intact (healthy) C2-T1 motion (Hybrid Control). ABAQUS will be used to perform all the FE analysis.

The range of motion data at each level, stresses in the discs and facet forces will be used for analyzing the biomechanics and load transfer mechanism in the various

surgical constructs. The peak moment required to achieve the primary motion will also be recorded and used for analysis.

3.2 In-vitro cadaveric testing

A total of 11 fresh frozen human cervical spines were used in this study. All specimens were scanned using a CT to ensure that they are free from gross deformities and provide adequate bone quality following which they were randomly assigned to one of the two treatment groups:

Group 1: TDR using Bryan® Cervical Disc (6 specimens)

Group 2: TDR using Prestige® LP Cervical Disc (5 specimens)

Prior to scanning and testing, the specimens were thawed to room temperature, and the paravertebral musculature was carefully removed, leaving all ligamentous structures intact. The spines were then scanned using CT imaging. Prior to testing, the specimens were wrapped in saline drenched gauze and stored in double freezer bags at -20°C. In preparation for biomechanical testing, the specimens were thawed on the day of testing and the most cephalad and caudal vertebra of each specimen were mounted in polyester resin casts (Bondo Corp., Atlanta, GA).

The flexibility tests consisted of applying pure moments in flexion, extension, right and left lateral bending and right and left axial rotation. This was done using an MTS 858 Bionix System configured with two Spine Simulators (MTS Corp., Minneapolis, MN) and a passive XZ table allowing pure, unconstrained load application in all 6 degrees of freedom (Figure 19). The bottom gimbal acts as a slave and follows the motion of top gimbal to which the moments are applied. In order to account for shear forces, we added a passive XZ table below the bottom gimbal that offsets the high shear forces by translating in the required direction.

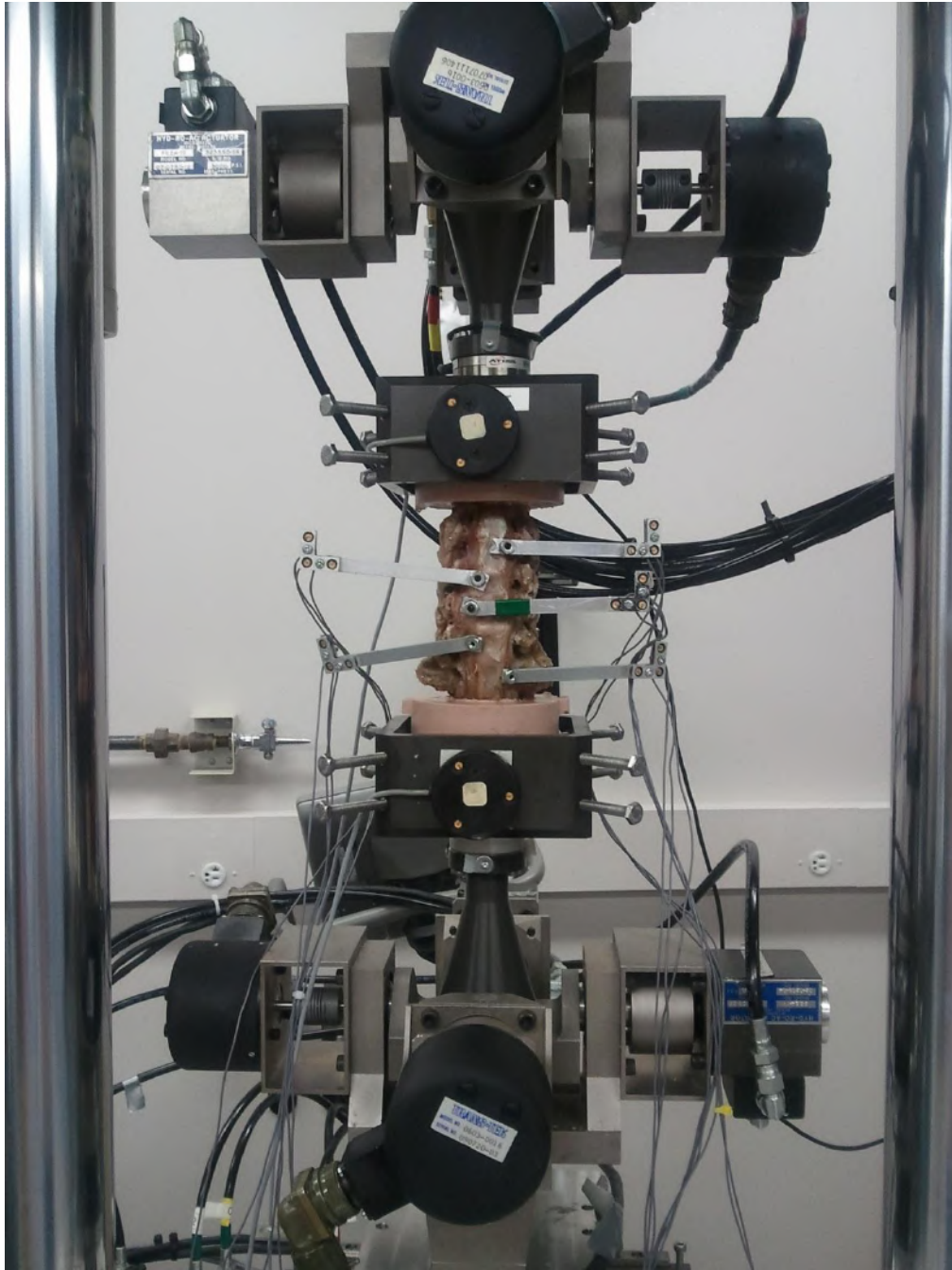


Figure 19: Human cervical spine in the MTS Bionix System with two Spine Simulators

Intersegmental motions will be ascertained via specialized markers rigidly affixed to each vertebral level. Each marker consists of three non collinear infrared light emitting diodes detectable by an optoelectronic motion analysis system (Optotrak 3020,

Northern Digital Inc., Waterloo, Ontario, Canada). Data was captured and analyzed using MotionMonitor ® (Innovative Sports Training, Inc, Chicago, IL, USA). The total and segmental rotations for all the specimens after each test were exported using Euler angle sequence which was dependent on the primary and secondary motion of interest.

There are currently no standardized testing protocols for evaluating total disc replacements. Panjabi proposed a new method of testing called “hybrid control” which consists of two steps. In the first step, the intact specimen is loaded using flexibility protocol to a known moment and the resulting motions are noted. In the second step after some intervention at one of the levels (disc replacement), the load that is applied to the spine is adjusted in such a way to obtain the same overall range of motion as the intact specimen [75]. This kind of protocol helps in determining the effect of the surgical intervention on the adjacent levels as well as the intervened level.

Thus, in the first flexibility test, the intact cervical spine segments were tested nondestructively in flexion and extension (x-axis, ± 2.0 Nm), bilateral axial rotation (y-axis, ± 2.0 Nm), and bilateral lateral bending (z-axis, ± 2.0 Nm) via the pure moment loading system. It should be noted that a maximum moment of 2.00 Nm was chosen for the multi-segment specimens, due to the fact that this loading magnitude has been judged to be sufficient to produce physiological motions but small enough not to injure the specimen [76]. Each test will be repeated for three loading and unloading cycles, with the data from the third cycle contributing to the computational analyses.

In the later flexibility tests, the specimens were loaded in order to obtain the same range of motion as that of the original flexibility test. Again, each test was repeated for three loading and unloading cycles, with the data from the third cycle contributing to the analyses.

To prevent dehydration, the specimens were routinely irrigated with a 0.9% sodium chloride solution throughout the test period.

3.2.1 Testing Protocol

All specimens were first tested nondestructively in their intact state in flexion-extension, bilateral axial rotation, and bilateral lateral bending up to a moment of 2Nm. From this point forward, all subsequent tests were performed using the hybrid protocol, where specimens were loaded in order to obtain the same overall range of motion as that of the intact flexibility test. Next, a TDR was performed at the C5-C6 level; then another TDR at the C6-C7 level. Next, the artificial disc at C5-C6 will be replaced by a fusion to emulate a disc replacement adjacent to a fusion. Subsequently, each of the implanted levels will be subjected to fusions by inserting rods into the polyaxial pedicle screws previously implanted. After each of these interventions, hybrid flexibility tests will be performed. A flow chart of the experimental protocol and details of important steps are provided below (Figure 20).

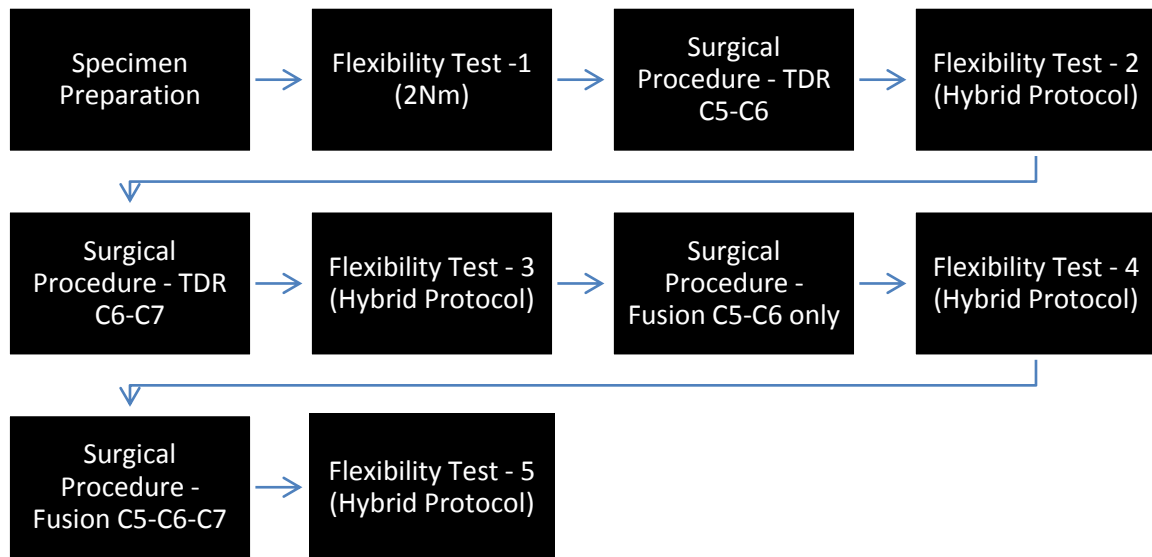


Figure 20: Flowchart of the Experimental Protocol

3.2.1.1 Specimen Preparation

After the specimen was thawed to room temperature, the C2 and T1 levels were potted in Bondo ((Bondo Corp, Atlanta, GA) in order to prepare them for mounting in the testing fixture. In addition, screws were inserted in the vertebral bodies of C3-C7 levels for fixing Ired markers.



Figure 21: Specimen ready to be tested with C2 and T1 levels potted in Bondo.

3.2.1.2 Surgical Procedure: Total Disc Replacement

A total disc replacement surgery was performed at the C5-C6 level. Based on CT measurement, the specimen was implanted with an appropriately sized Bryan or Prestige LP disc depending on the group it was assigned to. The surgery was performed as per the Bryan or Prestige LP surgical technique manual. Details of the surgery are provided in Appendix A.

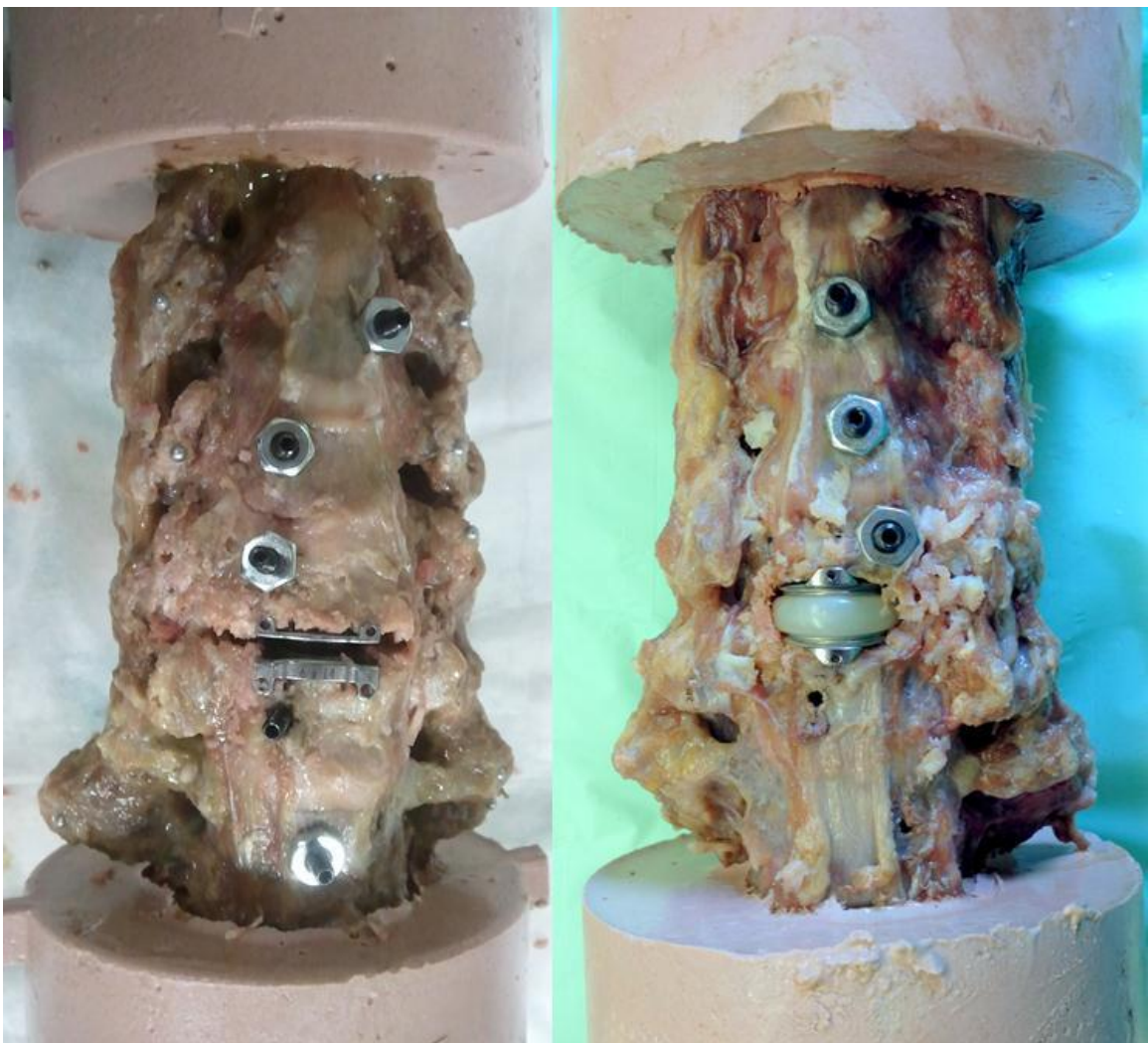


Figure 22: Specimens implanted with Prestige LP (left) and Bryan (right) discs at the C5-C6 level

3.2.1.3 Surgical Procedure: Total Disc Replacement – Bi-level

A total disc replacement surgery was performed at the adjacent C6-C7 level. With artificial discs at C5-C6 and C6-C7 levels, this represented a bi-level disc replacement construct. Again depending on the group, the specimen was implanted with either a Bryan or Prestige LP disc making sure that both discs in one spine were the same.

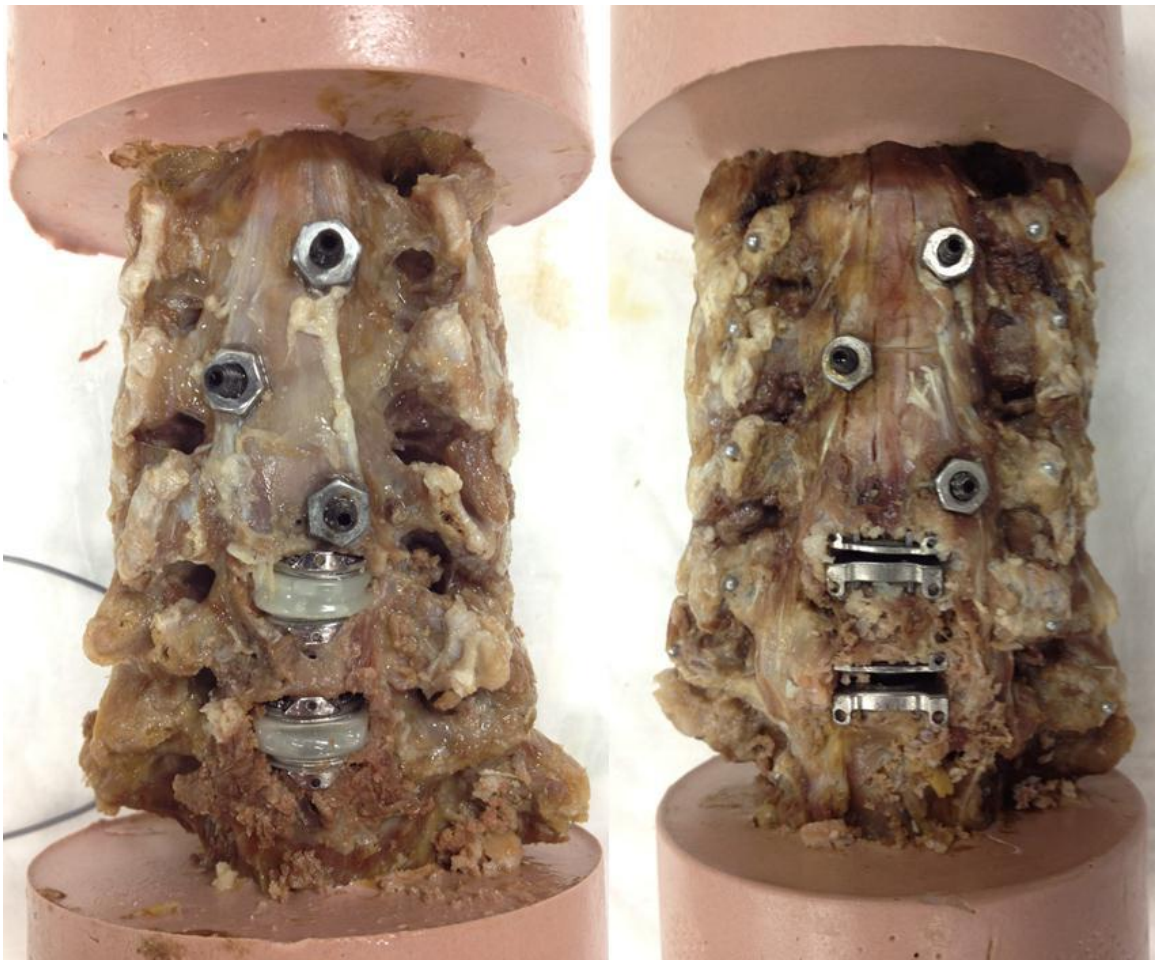


Figure 23: Bi-level disc replacement with Bryan (left) and Prestige LP (right) discs

3.2.1.4 Surgical Procedure: Disc replacement adjacent to fusion

The artificial disc at the C5-C6 level was then be replaced by an appropriate size spacer and an anterior plate (Zephyr or Atlantis Vision Cervical Plating system (Medtronic Sofamor Danek, Memphis, TN, USA)). In addition, Vertex Max (Medtronic Sofamor Danek, Memphis, TN, USA) polyaxial screws were implanted in the lateral mass with rods making it a 360 fusion. This was done to ensure the C5-C6 level was mechanically fused. This construct represented a disc replacement adjacent to an existing fusion; also known as the Hybrid construct.

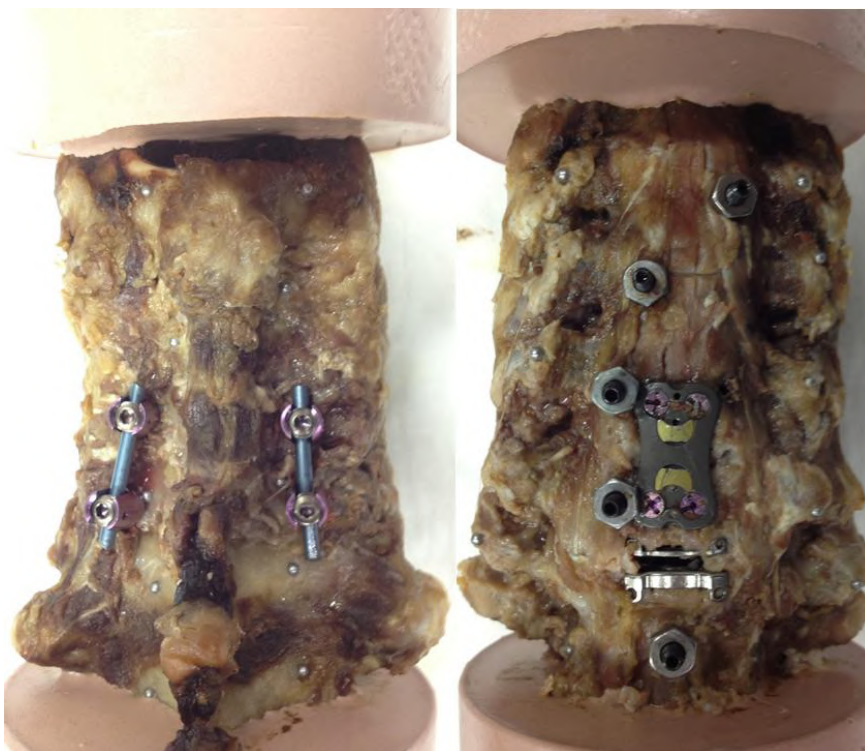


Figure 24: Specimen with a 360 fusion at C5-C6 level and a disc replacement at C6-C7 level

3.2.1.5 Surgical Procedure: Bi-level Fusion

Next, the artificial disc at the C6-C7 level, single level anterior plate at C5-C6 and the posterior fusion rods were removed. The C6-C7 disc space was filled with a spacer and a bi-level fusion plate was then implanted at the C5-C6-C7 levels. Lateral mass screws were added at the C7 level and rods were inserted from C5-C7 levels making it a bi-level 360 fusion.

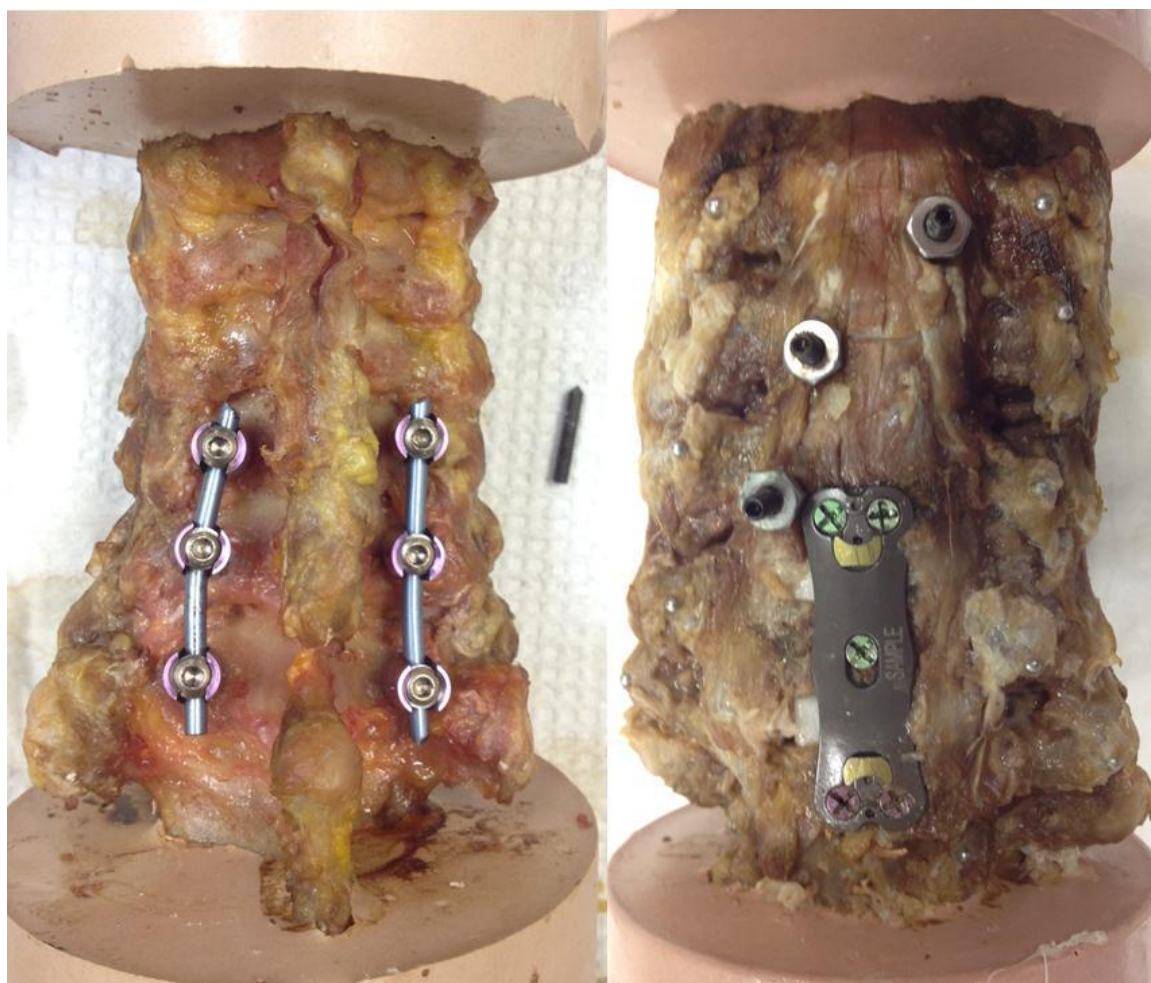


Figure 25: Specimen with a bi-level 360 fusion at C5-C6-C7 levels.

3.2.2 Data Analysis

A three-dimensional coordinate system was used where the positive X axis was defined towards the left, positive Y axis superiorly and positive Z axis anteriorly [77]. The total and segmental rotations were each exported using the Euler angle sequence which was dependent on the primary and secondary motion of interest. For example, during a flexion-extension test, XZY Euler angle sequence was chosen since the dominant off axis motion was lateral bending [65]. Statistical analysis was performed using a paired t-test for analysis within the group and homoscedastic t-test for analysis between the two discs. Statistical significance was assigned at a probability level of less than 0.05 ($p < 0.05$).

CHAPTER 4: RESULTS

This chapter discusses the results obtained from both the finite element analysis and the cadaveric testing. Results from cadaveric testing were used solely for kinematic analysis and the results from FEA were used for kinematic analysis as well as analyzing disc stresses and facet forces.

4.1 Finite Element Analysis Results

The results obtained from the finite element analysis are presented in this section. Each of the following subsections discusses range of motion, moments, disc stresses and facet forces.

Inter-segmental rotations and the effects of various alterations/surgeries on the rotations are presented in the range of motion section. Hybrid control was used across all models which meant that the overall C2-T1 range of motion was the same. The moments required to achieve the intact C2-T1 ranges of motion are presented in the Moments section.

The disc stresses section details the changes in adjacent level annular stresses after modification / surgical intervention. Stresses were recorded in the anterior and posterior regions during flexion and extension, respectively. The left region of annulus was analyzed during left lateral bending and left axial rotation, whereas the right portion of the annulus was examined during right lateral bending and right axial rotation.

Changes in the facet loads at the altered and adjacent levels are presented in the Facet forces section.

4.1.1 Comparison of Intact and Degenerative Models

This section compares the FE analysis of the Intact and Degenerative (single and bi-level) models. In case of single level degenerative model, the modified level was C5-

C6 whereas in case of bi-level degenerative model, C5-C6 and C6-C7 levels were modified to simulate disc degeneration.

4.1.1.1 Range of Motion

The predicted range of motion of the three finite element models; intact, single level degeneration at C5-C6 and bi-level degeneration at C5-C6 and C6-C7 in the six loading directions is shown in Figure 26. Since hybrid control was used, the overall range of motion (C2-T1) was the same across all models.

The C5-C6 degenerative model predicted a decrease in motion at the moderately degenerated level in all directions. A decrease in ROM of ~32% was observed in Flexion, ~33% in extension, ~45% in left/right lateral bending and ~29% in left/right axial rotation at the C5-C6 level. The decrease in motion at the degenerated level was compensated by the remaining levels. The level above (C4-C5) showed an increase in motion of 10.5% in flexion, ~11% in extension, ~9.5% in left/right lateral bending and ~8.5% in left/right axial rotation whereas the level below showed an increase of ~11.5% in flexion, ~11% in extension, ~8% in left/right lateral bending and ~8% in left/right axial rotation. In most cases, it was the level above or below that showed the maximum increase in motion.

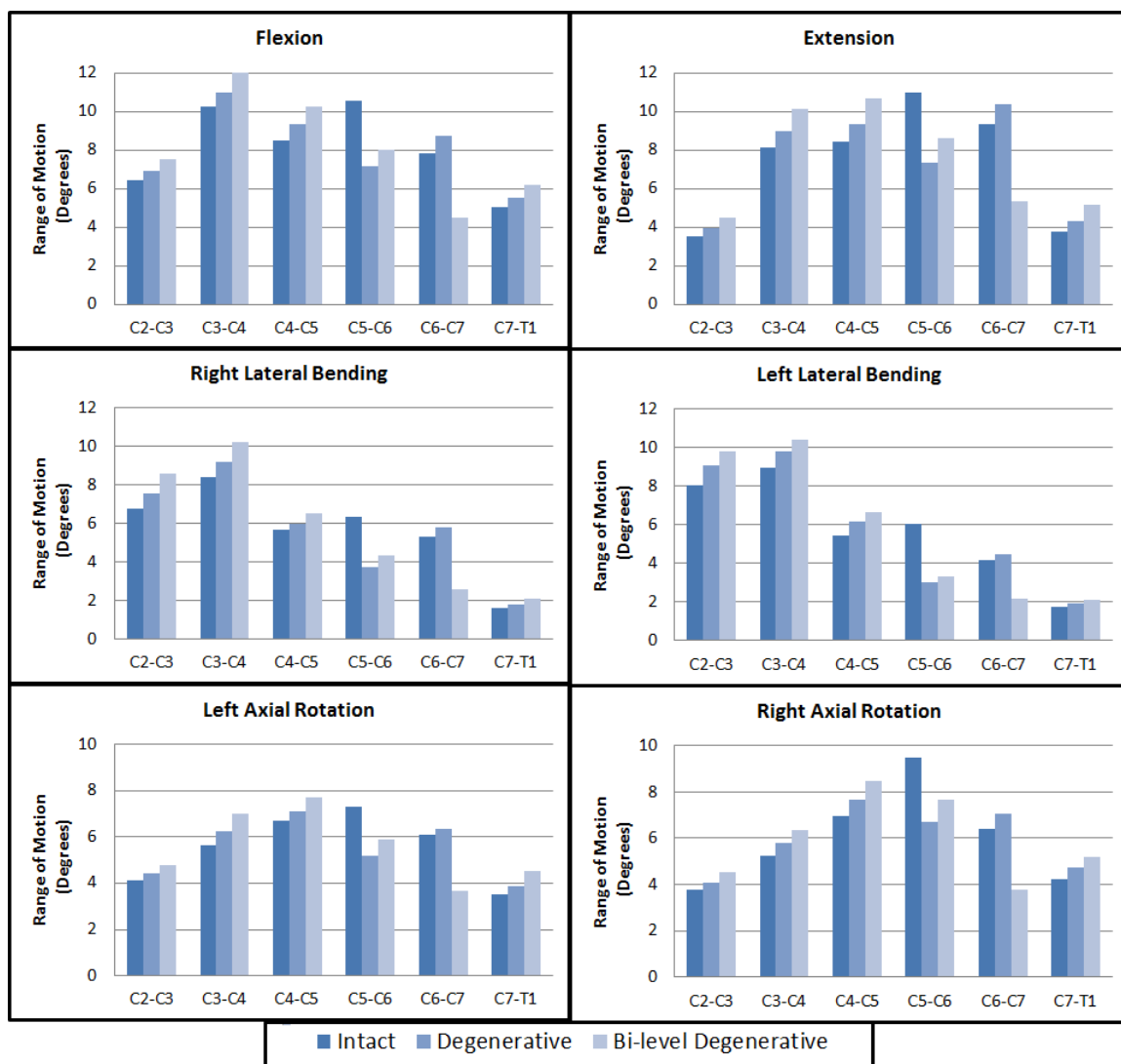


Figure 26: Comparison of Range of Motion in all 6 directions between intact (non-degenerative), single level degenerative and bi-level degenerative models.

In the bi-level degenerative model, both the degenerated levels showed a decrease in motion in all directions. The C5-C6 and C6-C7 levels showed a decrease of ~24% and ~42% in flexion, ~22% and ~42% in extension, ~39% and ~49% in left/right lateral bending and ~19% and ~40% in left/right axial rotation when compared to the intact/non-degenerative model. Once again, like the single level degenerative model, although the decrease in motion was compensated by all the remaining levels the levels above and

below showed the maximum increase in motion. The cranial level (C4-C5) showed a ~21% increase in flexion, ~26% increase in extension and ~19% increase in left/right lateral bending and left/right axial rotation. The caudal level (C7-T1) showed an increase of ~23% in flexion, 38% in extension, ~27% in left/right lateral bending and ~23% in left/right axial rotation.

4.1.1.2 Disc Stresses

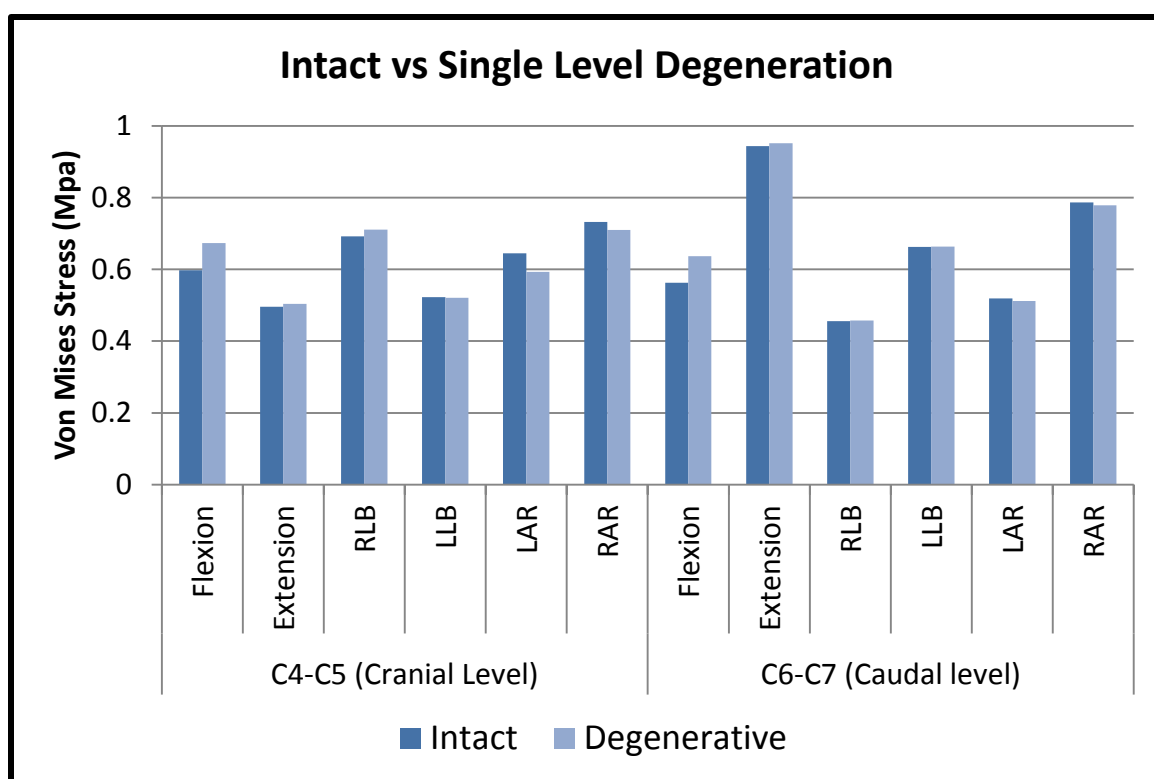


Figure 27: Comparison of annular stresses between Intact and single level degenerative models at the levels cranial and caudal to the degenerated level

Figure 27 compared the disc stresses predicted by the intact and single level degenerative models at the levels immediately above and below the degenerative level. Single level degeneration had minimal effect on the annular stresses at the adjacent

levels. The cranial level showed an average increase in stress by a mere 1% while the caudal level stresses increased by 2%. In both cases, the maximum increase was observed during flexion where the stresses increased by approximately 13%.

Disc stresses predicted by the intact and bi-level degenerative models at the levels immediately above and below the degenerative level are shown in Figure 28. In contrast to the single level degenerative model, the change in stresses at the adjacent levels was far greater. The cranial level showed an average increase in disc stresses of 31% while the caudal level stresses increased by 35%.

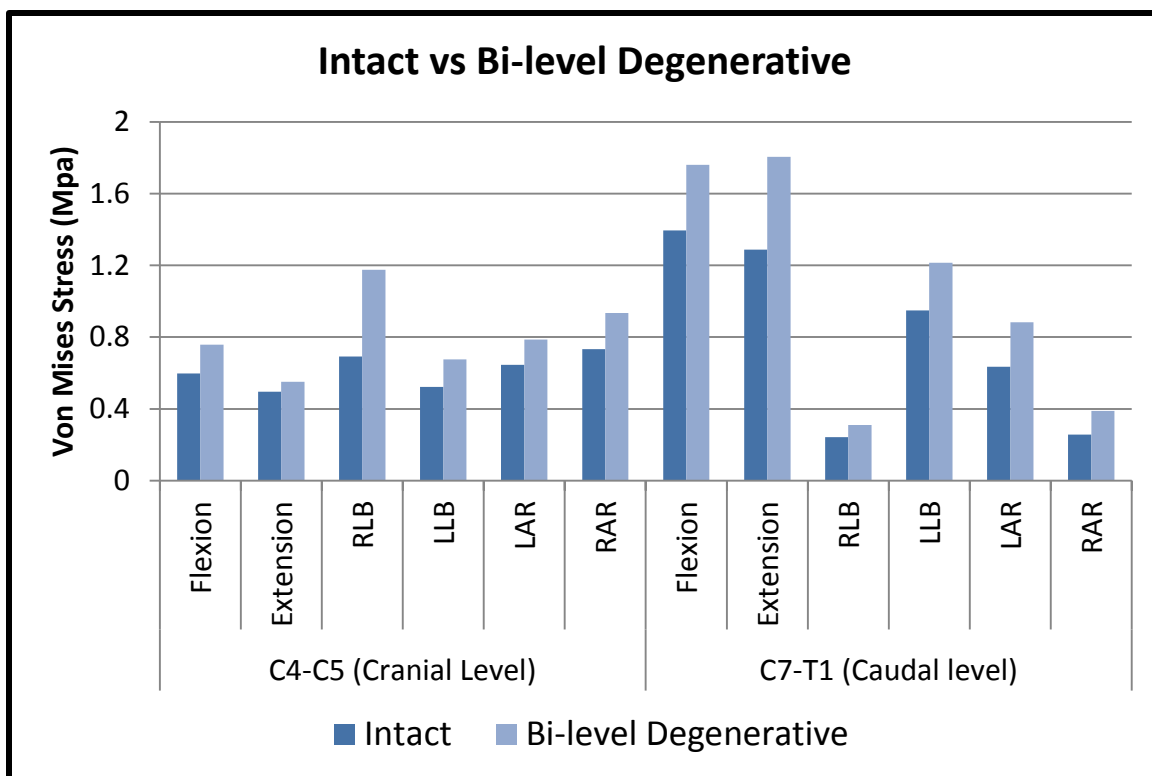


Figure 28: Comparison of annular stresses between Intact and bi-level degenerative models at the levels cranial and caudal to the degenerated levels

4.1.2 Comparison of single level degenerative, disc replacement and fusion models

FE analysis results comparing the single level constructs i.e. single level degeneration, disc replacement (both Bryan and Prestige LP) and fusion are presented in this section. In all cases, the modified level is C5-C6.

4.1.2.1 Range of Motion

Figure 29 compares the change in range of motion about the 3 axes after arthroplasty and fusion. The change in motion is represented as a percent change with respect to the single level degenerative model. Detailed range of motion values are provided in Appendix B.

Arthroplasty with both the Bryan and Prestige LP showed an increase in motion at the implanted level and a decrease in motion at the adjacent levels. TDR with Bryan showed an increase of ~15%, ~21% and ~4% in flexion-extension, lateral bending and axial rotation respectively at the implanted level. The decrease in motion at the other levels after implantation of the Bryan cervical disc ranged from 4-7% in flexion-extension, 1-2% in lateral bending and ~1% in axial rotation with maximum reduction at adjacent levels.

Implantation of the Prestige LP resulted in an increase in motion by ~24% in flexion-extension, ~13% in lateral bending and ~10% in axial rotation. The increase in motion at the implanted level resulted in a decrease in motion at the other levels especially at the adjacent levels. The decrease in motion at the other levels was similar to that of Bryan, ranging from 3-6% in flexion-extension, 1-2% in lateral bending and axial rotation.

Fusion on the other hand resulted in a huge decrease in motion at the implanted level and a considerable increase in motion at all other levels. The decrease in motion at the fused level was around 98% in all three directions. This large decrease in motion was

compensated by an average increase in motion per level of ~18% in flexion-extension, ~10% in later bending and ~20% in axial rotation.

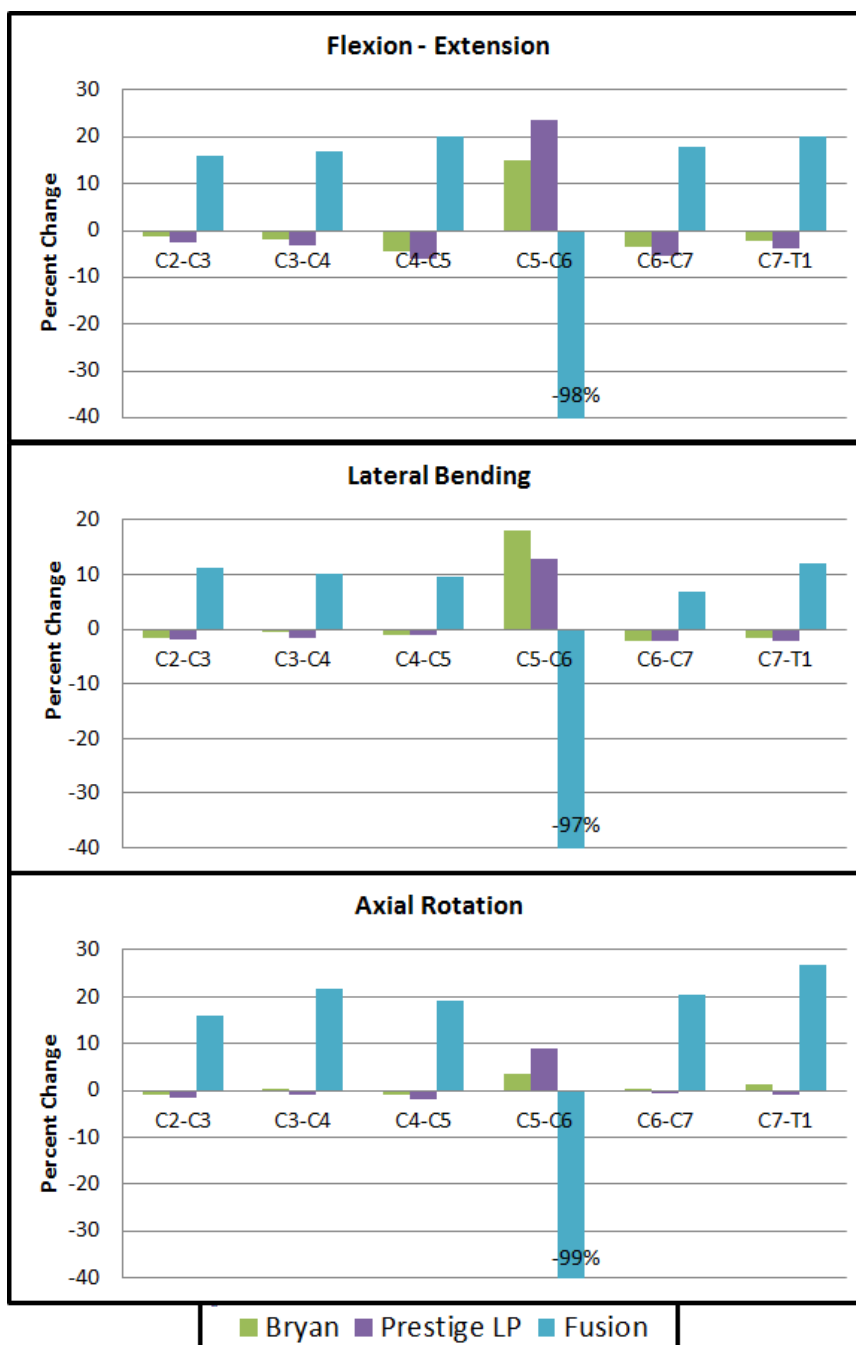


Figure 29: Percent change in motion after fusion and arthroplasty with Bryan and Prestige LP with respect to degenerated motion (C5-C6 level).

4.1.2.2 Moments

Table 2: Hybrid moments (Nm) required in various single level models to achieve overall range of motion equal to the intact model.

	Intact	Degenerative	Bryan	Prestige LP	Fusion
Flexion	2.0	2.3	2.3	2.3	3.0
Extension	2.0	2.5	2.3	2.2	3.5
RLB	2.0	2.4	2.3	2.2	3.0
LLB	2.0	2.5	2.5	2.5	2.9
LAR	2.0	2.3	2.5	2.4	3.4
RAR	2.0	2.5	2.4	2.3	3.9

Moments required to achieve the overall intact range of motion in all single level models is listed in 4.1.2.2 Moments

Table 2. All the modified models (i.e. C5-C6 Degenerative, C5-C6 fusion, and C5-C6 TDR with Bryan and Prestige) required moments greater than 2.0 Nm to obtain the same overall motion as the intact/healthy model for each mode of loading. The moment required for the fused model was the maximum (mean 3.29Nm); over 64% more than the Intact model. The degenerative model required an average moment of 2.4 Nm to achieve the intact ROM. TDR models needed a reduced moment (~2.3Nm) when compared to the degenerative model.

4.1.2.3 Disc Stresses

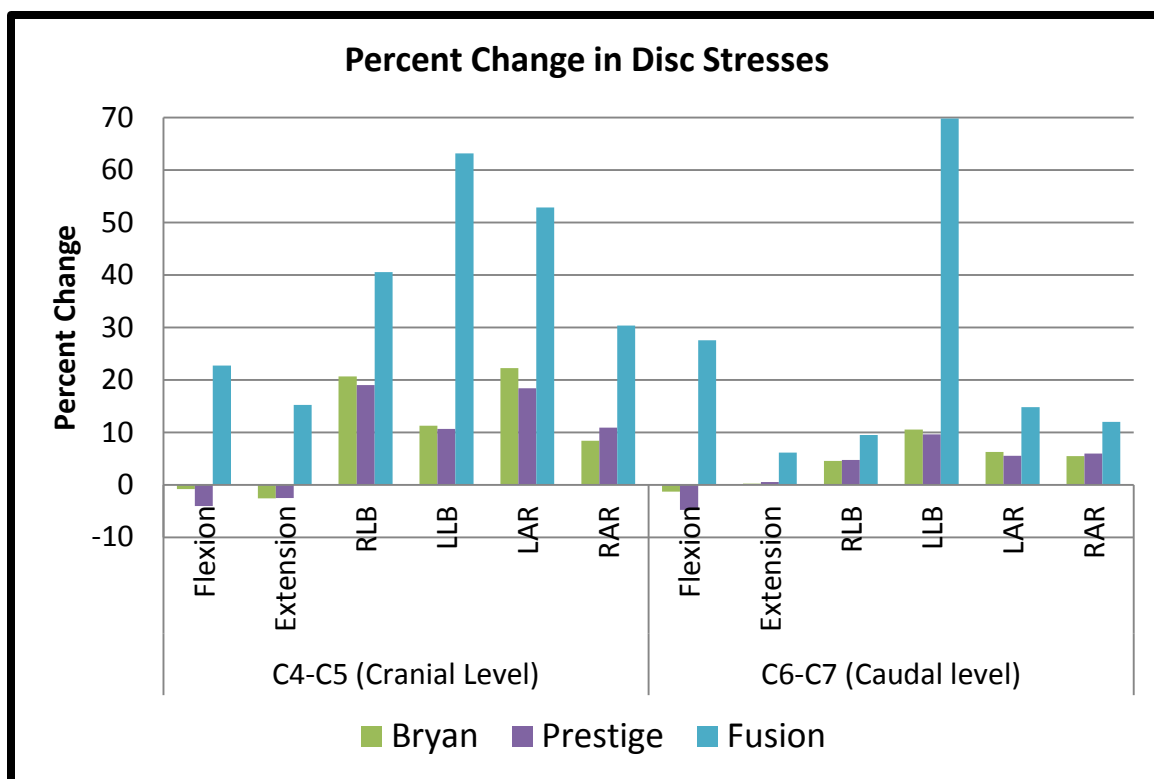


Figure 30: Percent change in disc stresses after disc replacement (Bryan and Prestige LP) and fusion in comparison to the degenerative model at the cranial and caudal levels

Figure 30 depicts the percent change in disc stresses at the level above and below the implanted level after arthroplasty (Bryan and Prestige) and fusion. This percent change is with respect to the single level degenerative model. As expected, the disc stresses increased considerably in all six directions at both the cranial (~37%) and caudal (~23%) levels after fusion. In case of disc replacement, both Bryan and Prestige LP discs resulted in an increase in disc stress in lateral bending and axial rotation. The stresses decreased slightly in flexion and extension. In all cases, the increase in stresses due to fusion was much more than the increase due to disc replacement.

4.1.2.4 Facet Forces

Table 3: Magnitude of facet contact forces at the altered and adjacent levels for intact and various single level models under hybrid moments

	C4-C5 (Cranial Level) Facet Forces (N)				
	Intact	Degenerative	Bryan	Prestige LP	Fusion
Extension	50	65	55	56	101
RLB	26	36	22	31	49
LLB	26	33	34	36	43
LAR	31	35	39	33	53
RAR	19	26	27	27	48
	C5- C6 Facet Forces (N)				
	Intact	Degenerative	Bryan	Prestige LP	Fusion
Extension	48	31	82	84	0
RLB	12	10	20	18	0
LLB	34	29	39	27	0
LAR	20	20	34	39	0
RAR	16	18	30	32	0
	C6-C7 (Caudal Level) Facet Forces (N)				
	Intact	Degenerative	Bryan	Prestige LP	Fusion
Extension	21	33	25	27	65
RLB	37	46	36	41	59
LLB	33	46	47	47	58
LAR	38	42	44	41	55
RAR	28	35	33	32	48

Facet contact forces for the altered level (C5-C6) and adjacent levels for intact, single level degenerative, single level Bryan & Prestige, and single level fusion models are listed in Table 3. In comparison to the intact model, the degenerative model showed a decrease in contact force at the degenerated level and an increase in force at the adjacent levels. The TDR models on the other hand showed an increase in facet contact forces at the implanted level and decrease at the adjacent levels in comparison to the degenerative model. This increase in contact force at the implanted level was largest in extension.

In case of fusion, the facets did not come into contact at the fused level. Hence all forces were zero. At the adjacent level though; the contact forces were highest amongst all models.

4.1.3 Comparison of bi-level degenerative, disc replacement and fusion models

This section compares the FE predictions of bi-level degenerative, bi-level Bryan, bi-level Prestige LP and bi-level fusion models. In all models, the altered levels are C5-C6 and C6-C7.

4.1.3.1 Range of motion

Figure 31 compares the percent change in segmental range of motion in flexion-extension, lateral bending and axial rotation, after simulated surgical procedures of bi-level arthroplasty and bi-level disc replacement with Bryan and Prestige LP discs. The percent change is in comparison with the bi-level degenerative model. In all cases, the level modified were C5-C6 and C6-C7. Since hybrid control was used, the total C2-T1 range of motion was same across all models.

In all cases, bi-level fusion resulted in almost zero motion at the two fused levels. This drop in motion resulted in a substantial increase in motion across all unaltered levels. On an average, the unaltered levels showed an increase in range of motion by 37% in flexion-extension, 22% in lateral bending and 43% in axial rotation.

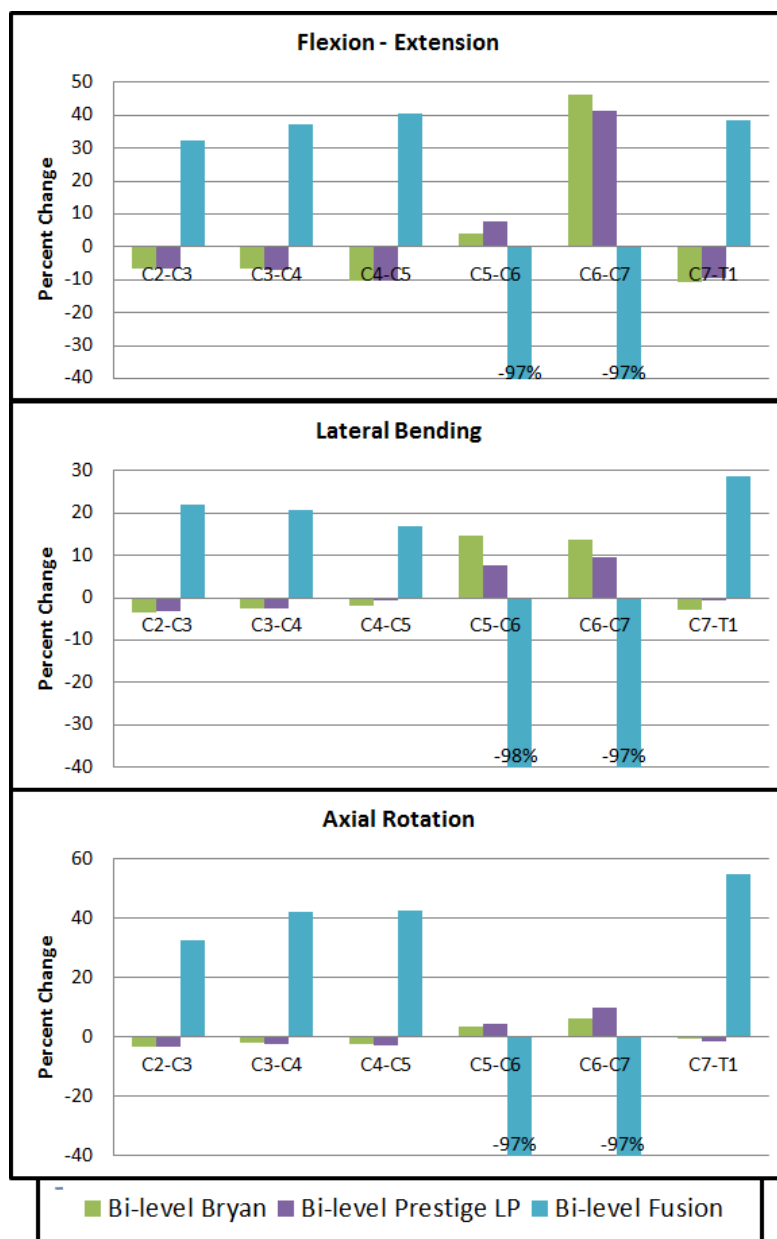


Figure 31: Percent change in motion after bi-level fusion and bi-level arthroplasty with Bryan and Prestige LP discs.

Similar to the single level results, bi-level disc replacement showed an increase in motion at the operated levels which resulted in a decrease in motion at all other levels. This trend was consistent in all six directions. Segmental range of motions predicted for

the two bi-level disc replacement models; bi-level Bryan and bi-level Prestige LP were very similar.

4.1.3.2 Moments

Moments required for the bi-level degenerative, bi-level Bryan, bi-level Prestige LP and bi-level fusion models to achieve the intact range of motion in all six directions are listed in Table 4. All altered models required more moment to achieve the intact range of motion. As expected, bi-level fusion model required the most moment (5Nm average). Clearly, the bi-level fusion stiffened the models significantly. The bi-level degenerative model required an average 50% more moment than the intact model. Similar to the single level results, the moments required for the TDR models were lower than the bi-level degenerative model but higher than the intact model. Both bi-level Bryan and bi-level Prestige LP models required 35% more moment than the intact model. The lower hybrid moments for the bi-level TDR models suggests that the model becomes less stiff following a bi-level TDR compared to the bi-level degenerative model.

Table 4: Hybrid moments (Nm) required in various bi-level models to achieve overall range of motion equal to the intact model.

	Intact	Bi-level Degenerative	Bi-level Bryan	Bi-level Prestige LP	Bi-level Fusion
Flexion	2	2.72	2.62	2.52	4.25
Extension	2	3.17	2.4	2.54	5.5
RLB	2	3.02	2.60	2.54	4.36
LLB	2	2.82	2.87	2.93	3.90
LAR	2	2.90	3.0	2.94	5.5
RAR	2	3.03	2.91	2.81	6.5

4.1.3.3 Disc Stresses

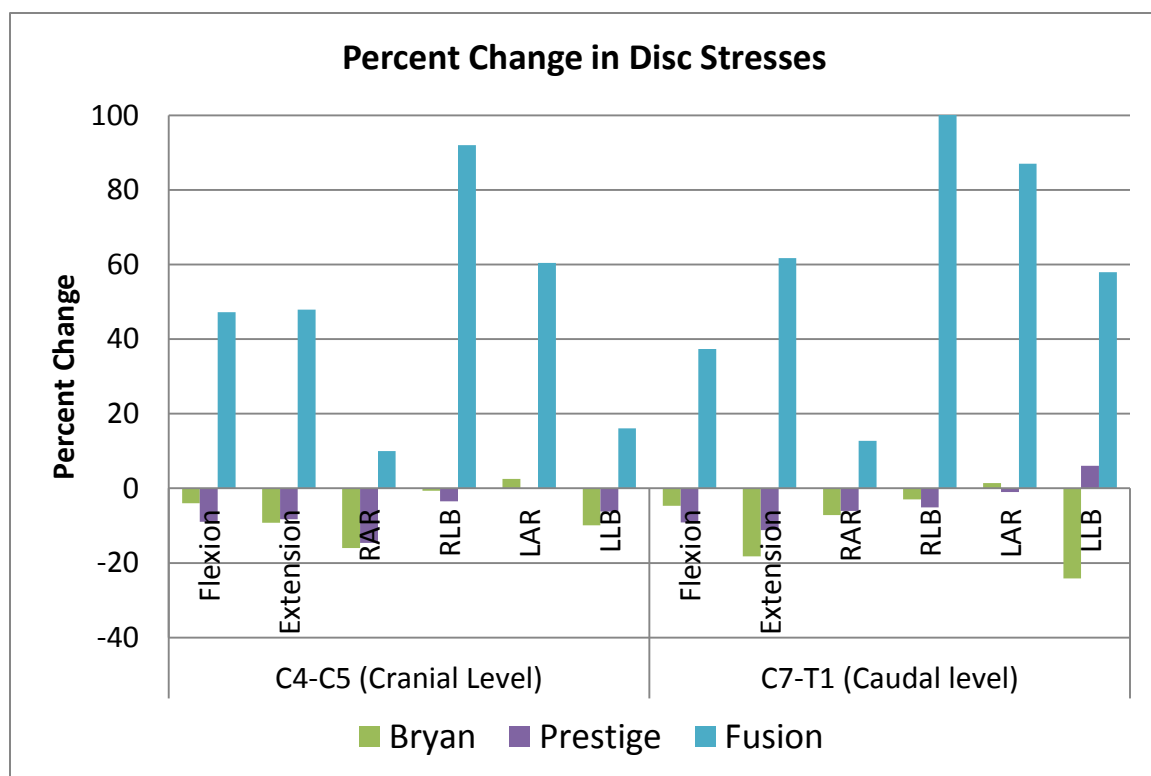


Figure 32: Percent change in disc stresses after bi-level disc replacement (Bryan and Prestige LP) and bi-level fusion in comparison to the bi-level degenerative model at the cranial and caudal levels.

Figure 32 compares the percent change in disc stress after bi-level fusion and bi-level disc replacement at the levels immediately above and below the altered levels. Similar to the trends observed with range of motion, the adjacent level discs showed a huge increase after bi-level fusion in all six directions. An average of 45% and 60% more stresses were predicted by the bi-level fusion model at the level above and below respectively. Following a bi-level disc replacement, disc stresses at the adjacent levels dropped in almost all cases.

4.1.3.4 Facet Forces

Facet contact forces for the altered levels (C5-C6 -C7) and adjacent levels for intact, bi-level degenerative, bi-level Bryan & Prestige, and bi-level fusion models are listed in Table 5. The bi-level degenerative model showed a decrease in contact forces at the degenerated levels and an increase in force at the adjacent levels, in comparison to the intact model. The bi-level TDR models on the other hand showed an increase in facet contact forces at the implanted levels and decrease at the adjacent levels in comparison to the degenerative model.

The increase in contact forces at the adjacent levels was largest in case of bi-level fusion. As the facets did not come into contact at the fused levels, all forces at these levels were zero.

Table 5: Magnitude of facet contact forces at the altered and adjacent levels for intact and various bi-level models under hybrid moments

	Intact	Bi-level Degenerative	Bi-level Bryan	Bi-level Prestige LP	Bi-level Fusion
	C4-C5 (Cranial Level) Facet Forces (N)				
Extension	50	90	64	68	174
RLB	26	49	35	31	80
LLB	26	40	39	40	64
LAR	31	45	48	44	84
RAR	19	32	37	41	99
	C5-C6 (Modified level - 1) Facet Forces (N)				
Extension	48	39	92	78	0
RLB	12	11	21	23	0
LLB	34	26	47	34	0
LAR	20	19	52	42	0
RAR	16	13	40	21	0

Table 5 continued

	C6-C7 (Modified Level – 2) Facet Forces (N)				
Extension	21	17	51	42	0
RLB	37	26	45	31	0
LLB	33	20	47	47	0
LAR	38	32	66	73	0
RAR	28	22	34	42	0
	C7-T1 (Caudal Level) Facet Forces (N)				
Extension	29	55	39	38	111
RLB	45	68	55	39	93
LLB	46	66	57	60	93
LAR	29	41	32	39	77
RAR	15	25	20	21	68

4.1.4 Comparison of bi-level degenerative, fusion and hybrid models

4.1.4.1 Range of Motion

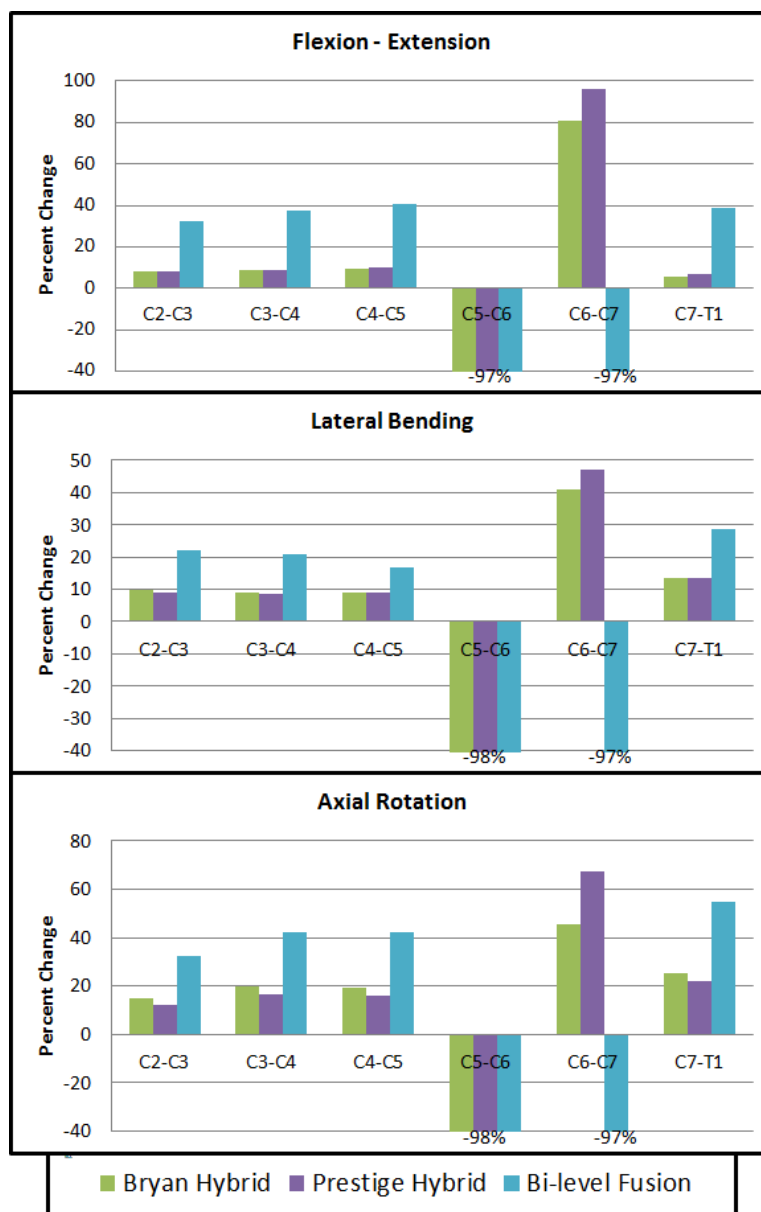


Figure 33: Comparison of percent change in motion between Bryan Hybrid, Prestige LP Hybrid and bi-level fusion models.

A comparison of percent change in motion for the hybrid and bi-level fusion models is presented in Figure 33. The percent change is in comparison to the bi-level degenerative model. The segmental motions predicted for the two hybrid models were very similar. In both hybrid models, the level with arthroplasty showed a large increase in motion. This increase was the most during flexion-extension motion (80% +). The increase in motion at the arthroplasty level resulted in a lesser increase in motion at the unaltered levels. As expected, the increase in motion at the unaltered levels in case of the bi-level fusion model was much more than the hybrid models. In all cases, a fusion resulted in almost zero motion at the fused level.

4.1.4.2 Moments

Table 6: Hybrid moments (Nm) required in various bi-level degenerative, fusion and hybrid models to achieve overall range of motion equal to the intact model.

	Intact	Bi-level Degenerated	Bryan Hybrid	Prestige LP Hybrid	Bi-level Fusion
Flexion	2	2.72	3.36	3.20	4.25
Extension	2	3.18	3.34	3.63	5.50
RLB	2	3.03	3.50	3.47	4.37
LLB	2	2.83	3.40	3.37	3.91
LAR	2	2.91	4.10	3.87	5.50
RAR	2	3.03	4.70	4.48	6.50

Table 6 depicts the hybrid moments for the FE models. In order to achieve the overall intact model motion, all the altered models; bi-level degenerative, bi-level fusion

and the two hybrid models, required a moment greater than intact. This suggests that the alterations stiffened the models. Bi-level fusion required the most moment; an average of 5Nm. For hybrid models, the moments fell between the bi-level degenerative and bi-level fusion models. Bryan hybrid model required an average moment of 3.73Nm whereas Prestige needed an average moment of 3.66Nm to achieve the intact motion.

4.1.4.3 Disc Stresses

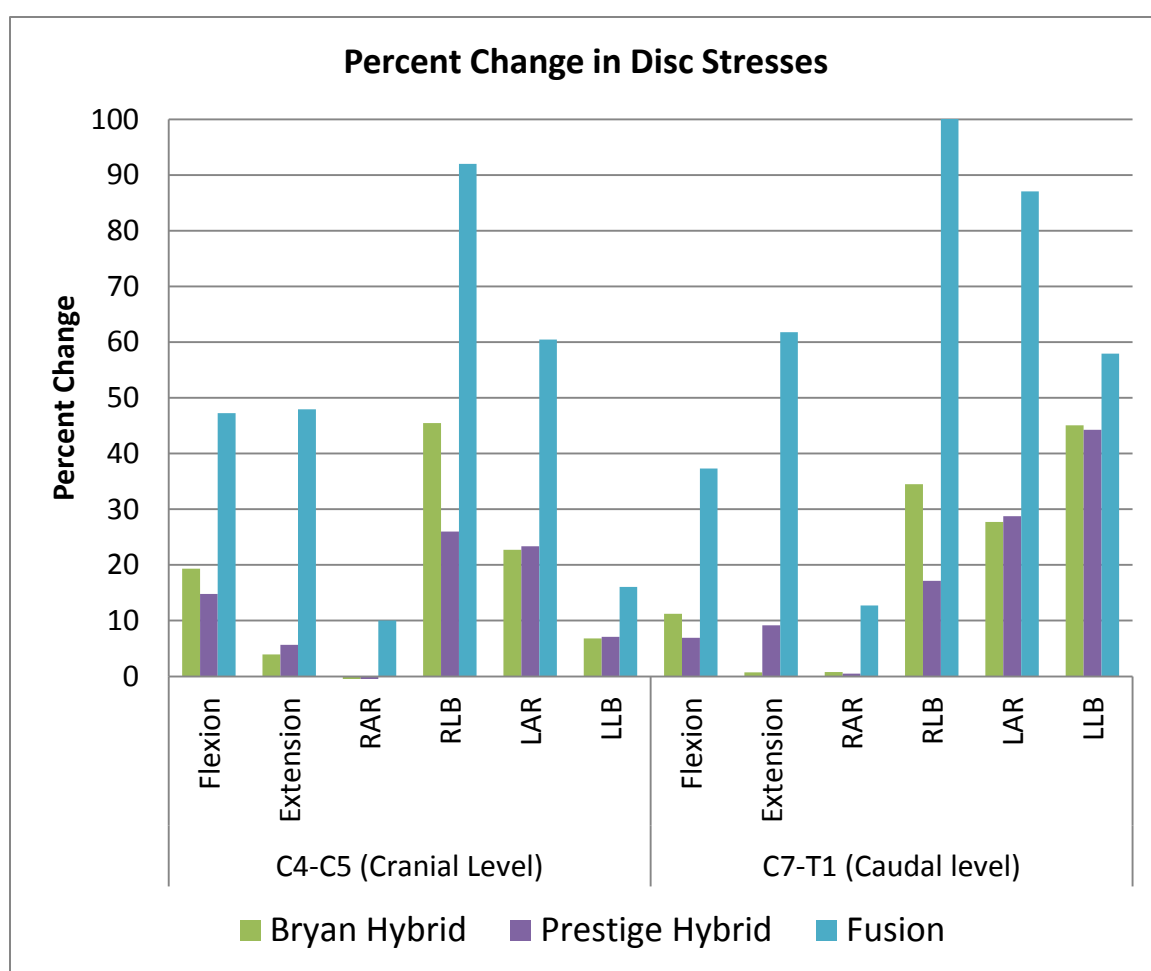


Figure 34: Percent change in disc stresses after a hybrid surgery (Bryan and Prestige LP) and bi-level fusion in comparison to the bi-level degenerative model at the cranial and caudal levels.

Figure 34 compares the percent change in disc stress at the levels immediately above and below the altered levels between bi-level fusion and the two hybrid models. In all cases, the stresses at the cranial and caudal level increased after surgery. Analogous to the kinematic trends, the increase in stresses was larger for the bi-level fusion model. The increase in stresses due to a disc replacement + fusion construct was considerably less when compared to the bi-level fusion model. In most cases, the stresses predicted for the two hybrid models were very similar.

4.1.4.4 Facet Forces

Hybrid models consisted of a fusion at the C5-C6 level and a disc replacement (Bryan or Prestige) at the C6-C7 level. The facet forces at the C5-C6 level for both the hybrid models were zero due to fusion. At the C6-C7 level (Bryan and Prestige LP), the facet forces were considerably higher in comparison to both, intact and bi-level degenerative models. At the adjacent levels however, the forces were between the bi-level fusion and bi-level degenerative models.

Table 7: Magnitude of facet contact forces at the altered and adjacent levels for intact, bi-level degenerative, hybrid (Bryan and Prestige) and bi-level fusion models under hybrid moments

	Intact	Bi-level Degenerative	Bryan Hybrid	Prestige Hybrid	Bi-level Fusion
	C4-C5 (Cranial Level) Facet Forces (N)				
Extension	50	90	95	103	174
RLB	26	49	59	57	80
LLB	26	40	50	48	64
LAR	31	45	59	58	84
RAR	19	32	70	65	99
	C5-C6 (Modified Level -1) Facet Forces (N)				
Extension	48	39	0	0	0
RLB	12	11	0	0	0
LLB	34	26	0	0	0
LAR	20	19	0	0	0
RAR	16	13	0	0	0
	C6-C7 (Modified Level - 2) Facet Forces (N)				
Extension	21	17	67	62	0
RLB	37	26	63	59	0
LLB	33	20	52	54	0
LAR	38	32	76	82	0
RAR	28	22	55	59	0
	C7-T1 (Caudal Level) Facet Forces (N)				
Extension	29	55	61	63	111
RLB	45	68	75	75	93
LLB	46	66	81	79	93
LAR	29	41	53	54	77
RAR	15	25	44	40	68

4.2 *In-vitro* Cadaveric Testing Results

In-vitro cadaveric testing results are presented in this section. Cadaveric testing results are limited to changes in kinematics due to various surgical procedures.

4.2.1 TDR using Bryan Cervical Disc

The mean intersegmental rotations for the five tested conditions for the Bryan group during flexion/extension, lateral bending and axial rotation are shown in Figure 35. In general, a disc replacement increased the motion at the implanted level whereas a fusion resulted in a drop in the motion. Following a single level disc replacement, the motion at C5-C6 increased in all directions. This increase was significant only in flexion/extension (22% increase).

Similar trend was observed with a bi-level disc replacement. In comparison with the intact state, motion at all implanted levels increased. The increase was significant only at C5-C6 level in flexion/extension.

The hybrid construct consisted of a fusion at C5-C6 level and a disc replacement at the C6-C6 level. In comparison to the intact state, C5-C6 level showed a significant drop in motion in all directions. The C6-C7 level with an artificial disc showed an increase in motion. This increase was significant in flexion/extension only.

Comparing the bi-level fusion construct to with intact, both the fused levels (C5-C6 and C6-C7) showed a significant decrease in motion and all unaltered levels showed a significant increase in motion in all directions.

Figure 36 depicts the intersegmental rotations for all bi-level constructs (bi-level TDR, hybrid and bi-level fusion). In comparison to the bi-level Bryan construct, fusion decreased the motion significantly at the C5-C6 level in case of hybrid and at C5-C6 and C6-C7 levels in case of bi-level fusion. Most of the unaltered levels in hybrid and bi-level fusion states showed a significant increase in motion in comparison to the bi-level TDR

state. All un-operated levels in bi-level fusion state had significantly more motion in comparison to the hybrid state as well.

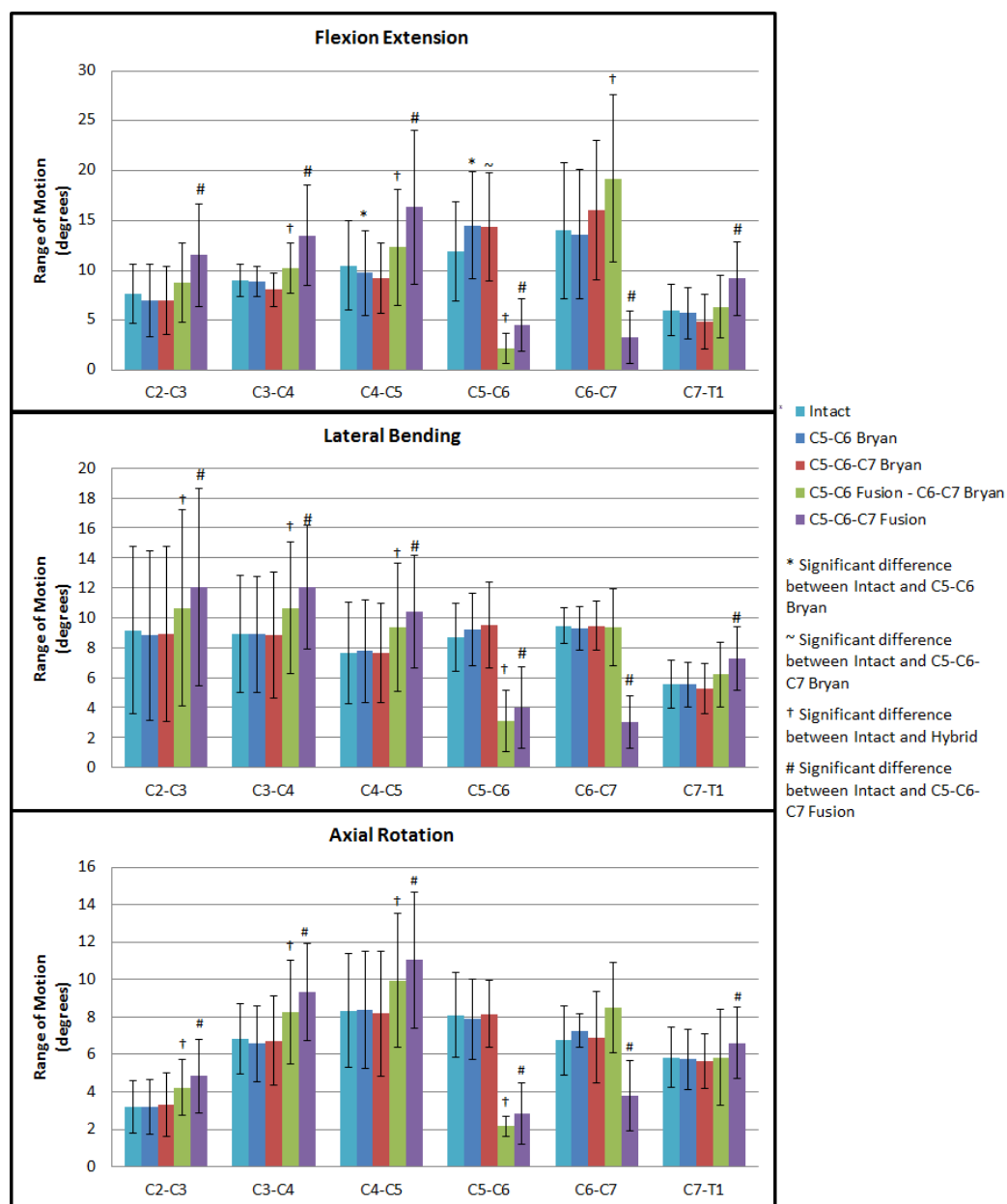


Figure 35: Mean intervertebral rotations (\pm standard deviation) for various surgical constructs (Bryan) for each level during Flexion-Extension, lateral bending and axial rotation

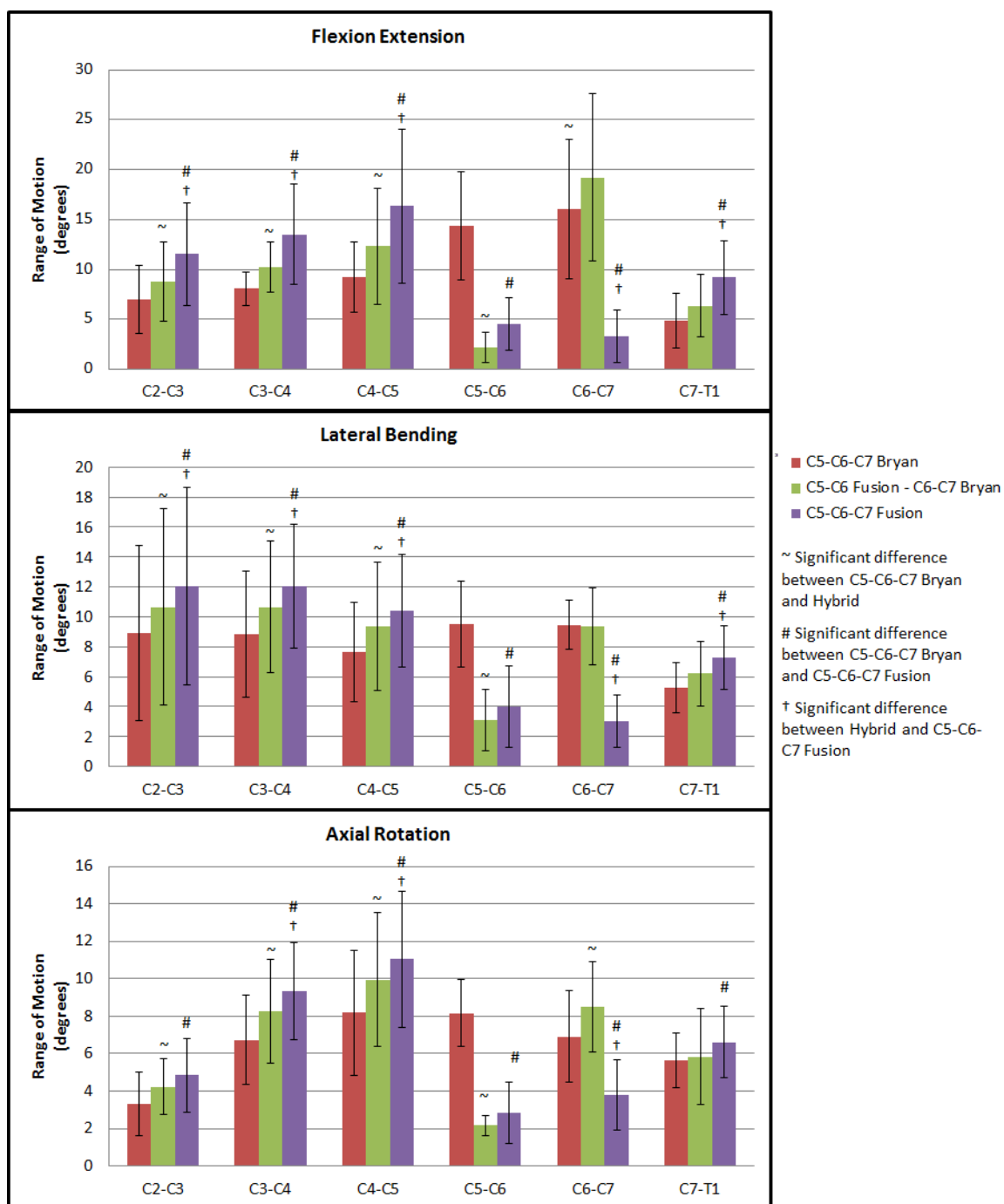


Figure 36: Mean intervertebral rotations (\pm standard deviation) for various bi-level surgical constructs (Bryan)

Table 8: Hybrid moments (Nm) required after various surgeries to achieve overall range of motion equal to the intact state.

	Flexion/Extension	Lateral Bending	Axial Rotation
Intact	± 2	± 2	± 2
C5-C6 Bryan	± 1.93	± 1.91	± 1.94
C5-C6-C7 Bryan	± 2.02	± 1.79	± 1.98
Bryan Hybrid	± 2.59	± 3.14	± 2.95
C5-C6-C7 Fused	± 4.22	± 5.39	± 3.65

The hybrid moments required for single level TDR, bi-level TDR, hybrid and bi-level fusion constructs in the Bryan group to achieve the intact range of motion are listed in Table 8. Compared to 2Nm moment in all intact models, the single level Bryan construct required 1.93Nm, 1.91Nm and 1.94Nm and bi-level construct required 2.02, 1.79 and 1.98Nm in flexion/extension, lateral bending and axial rotation respectively. The lower hybrid moments suggest that the specimen becomes less stiff following a TDR.

On the other hand, a bi-level fusion required 4.22Nm in flexion/extension, 5.39Nm in lateral bending and 3.65 Nm in axial rotation. Clearly, the bi-level fusion stiffened the specimens significantly leading to higher hybrid moments. For the hybrid construct, the moments fell between the bi-level TDR and bi-level fusion moments.

4.2.1 TDR using Prestige LP Cervical Disc

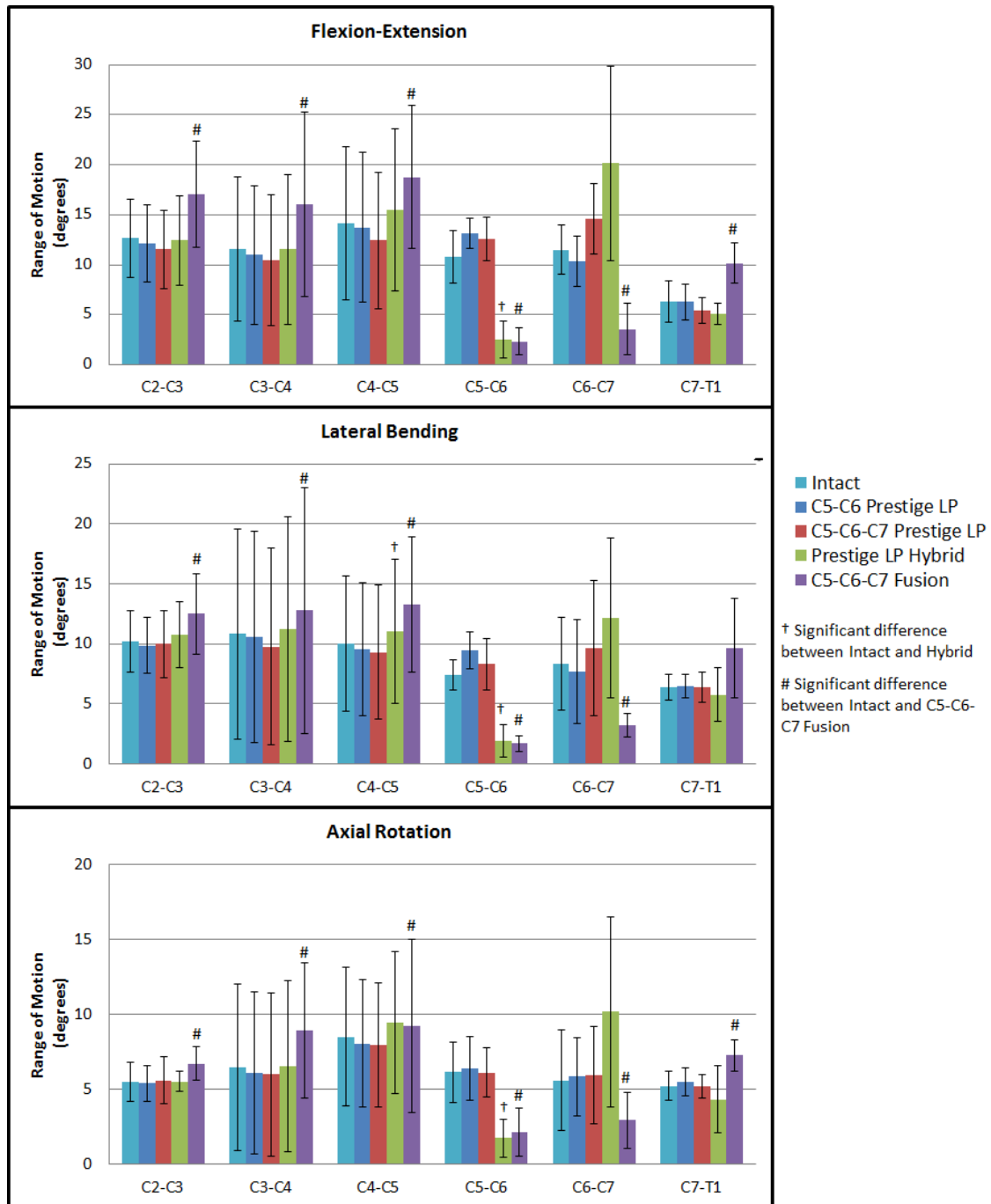


Figure 37: Mean intervertebral rotations (\pm standard deviation) for various surgical constructs (Prestige LP) for each level during Flexion-Extension, lateral bending and axial rotation

The mean intersegmental rotations for the Prestige LP group during flexion/extension, lateral bending and axial rotation for the five tested conditions are shown in Figure 37. In general, a disc replacement increased the motion at the implanted level and decreased the motion at unaltered levels; whereas a fusion resulted in a decrease in the motion at the fused level and an increase at un-fused levels. The changes in motion were not significant when comparing single and bi-level disc replacement with the intact state.

Comparing hybrid construct (fusion at C5-C6 level and Prestige LP at the C6-C6 level) with the intact state, the only statistically significant change in motion was a decrease in motion at the C5-C6 level. The other levels showed a non-significant increase in motion.

Comparing the bi-level fusion construct to with intact, both the fused levels (C5-C6 and C6-C7) showed a significant decrease in motion and all unaltered levels showed a significant increase in motion in all directions.

Figure 38 depicts the intersegmental rotations for all bi-level constructs (bi-level TDR, hybrid and bi-level fusion. In comparison to the bi-level Prestige LP construct, fusion decreased the motion significantly at the C5-C6 level in case of hybrid and at C5-C6 and C6-C7 levels in case of bi-level fusion. Apart from the fused level (C5-C6) there was no significant change in motion from the bi-level TDR to hybrid state. Most of the unaltered levels in bi-level fusion states showed a significant increase in motion in comparison to the bi-level TDR state.

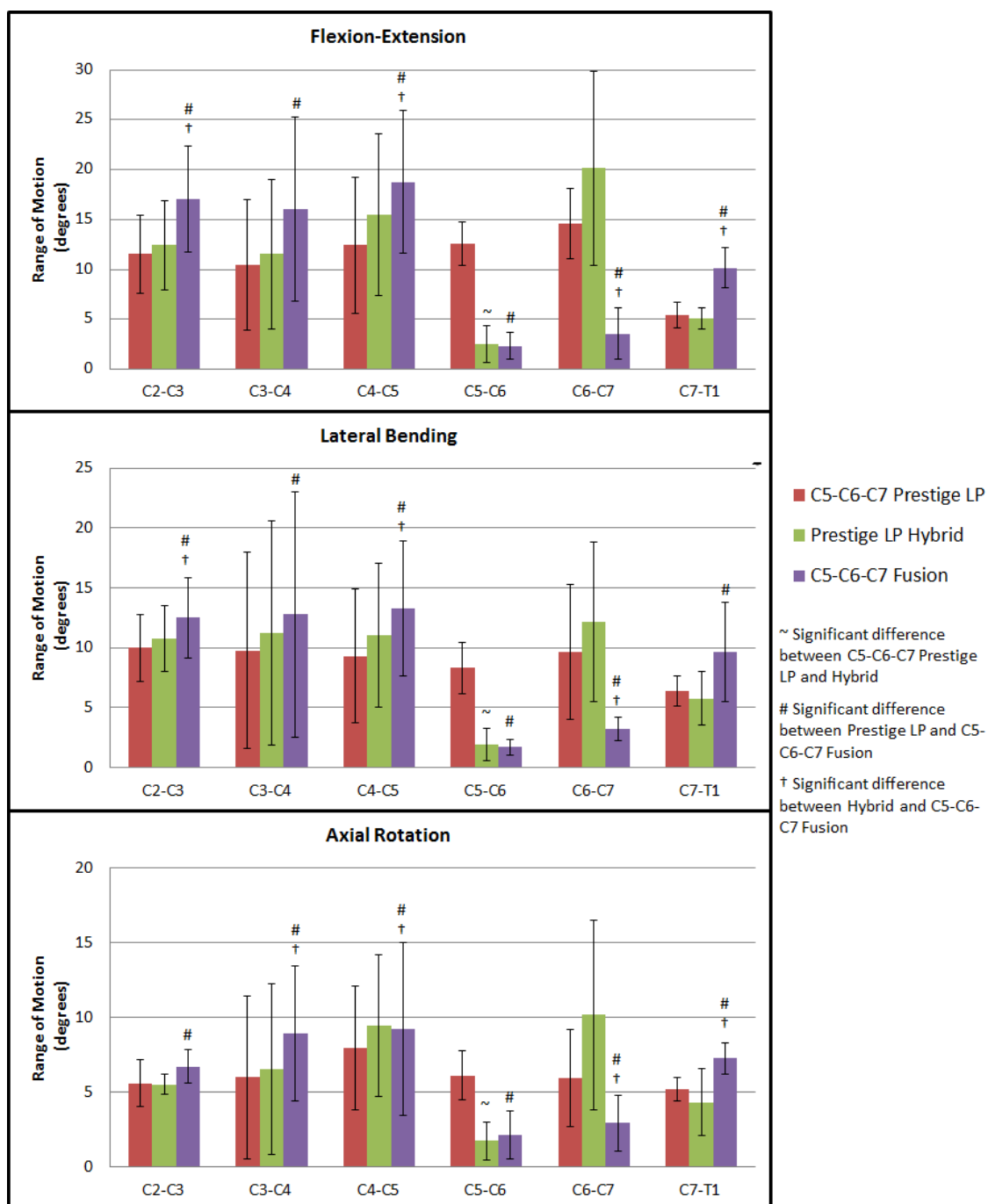


Figure 38: Mean intervertebral rotations (\pm standard deviation) for various bi-level surgical constructs (Bryan)

Table 9: Hybrid moments (Nm) required after various surgeries to achieve overall range of motion equal to the intact state.

	Flexion/Extension	Lateral Bending	Axial Rotation
Intact	± 2	± 2	± 2
C5-C6 Prestige LP	± 2.22	± 1.91	± 1.95
C5-C6-C7 Prestige LP	± 2.02	± 1.67	± 1.98
Prestige LP Hybrid	± 2.44	± 2.78	± 2.45
C5-C6-C7 Fused	± 4.78	± 4.59	± 3.33

The hybrid moments required for single level TDR, bi-level TDR, hybrid and bi-level fusion constructs in the Prestige LP group to achieve the intact range of motion are listed in Table 9. The single level Prestige LP construct required 2.22Nm, 1.91Nm and 1.95Nm and bi-level construct required 2.02, 1.67 and 1.98Nm in flexion/extension, lateral bending and axial rotation respectively compared to the 2Nm moment required for the intact state. This suggests that the specimen becomes less stiff in lateral bending and axial rotation and stiffer in flexion/extension following a TDR with Prestige LP.

On the other hand, a bi-level fusion required 4.78Nm in flexion/extension, 4.59Nm in lateral bending and 3.33 Nm in axial rotation. For the hybrid construct, once again, the moments fell between the bi-level TDR and bi-level fusion moments.

There was no significant difference in motion at the operated or un-operated levels between the Bryan and Prestige LP groups. This was true for both single and bi-level TDR constructs.

CHAPTER 5: DISCUSSION

The aim of this study was to compare biomechanics of the cervical spine following a combination of arthroplasty and fusion surgeries. Both *in-vitro* cadaveric testing and finite element analyses were used in this study.

5.1 Finite Element Analysis

Modeling a complex structure such the spine is very challenging. Certain assumptions are necessary to reduce the complexity without compromising the outcomes. This section summarizes the assumptions and limitations of the various FE models.

5.1.1 Intact Model

A previously validated C2-T1 finite element model of spine was used in this study [65, 78]. This model was validated with specimen-specific experimental data. As with most other FEA studies, this study has the general limitation where the effect of muscles on the stability of spine is ignored. Some studies apply a compressive load to mimic the weight of the head on the cervical spine. However, no compressive load was applied in this study in order to maintain consistent loading conditions between experimental and computational studies.

5.1.2 Degenerative Model

In-vitro cadaveric testing and computational models are commonly used to study the biomechanics of the spine. To investigate the biomechanical effects due to disc degeneration, *in-vitro* human cadavers are not particularly useful. Although the specimens could be dissected after experimentation to look at the amount of disc degeneration, the assessment is not quantitative. In contrast, finite element models are well suited to study such phenomena as appropriate material properties can be assigned representing the various stages in the degeneration process.

From a biomechanical perspective, the intervertebral disc is the connecting medium between the vertebrae for transmission of majority of load taken up by the spine along with facilitating mobility [79]. During the degenerative process, the disc undergoes progressive structural changes in the form of desiccation of the nucleus pulposus and disintegration of the annulus fibrosus resulting in decreased disc height [80,81]. These structural changes affect the overall and internal biomechanical responses. Dehydration of the nucleus increases the compression stiffness (overall response) and reduces disc fiber strain (internal response) at the degenerated level [82]. There have been very few studies that look at the effect of degeneration on the biomechanics of the cervical spine. Kumaresan et al. [83] used a C4-C6 FE model to simulate disc degeneration at the C5-C6 level. However this study was more focused on the contribution of disc degeneration to osteophyte formation rather than the change in biomechanics due to disc degeneration. The results of this study indicated that the overall stiffness increased with the severity of disc degeneration.

Two degenerative models were created in this study; a single level degenerative model at the C5-C6 level and a bi-level degenerative model at the C5-C6-C7 levels. In both cases, degeneration resulted in stiffening of the degenerated levels and in turn the entire model. As a result of this stiffness, the facet forces at the level decreased while the motion, facet forces and disc stresses at the adjacent levels increased.

5.1.3 Single, Bi-level and Hybrid Models

Several experimental and limited number of finite element studies have been done to look at the effect of arthroplasty on the biomechanics of the cervical spine. FE studies by Galbusera et al [37, 38], Faizan et al [84], Womack et al [85], have confirmed that cervical arthroplasty devices preserve motion better than fusion. All of these studies however modified the intact model to simulate a disc replacement surgery. Since a disc

replacement is mostly performed to alleviate pain and other complications due to disc degeneration, we decided to use a degenerative model.

In this study, the implanted level motions did not vary much between the two implants. With both the artificial discs, the motion at the implanted level increased and the motion at the nonoperative levels decreased. In both; single and bi-level TDR models, the largest increase in motion was during flexion/extension. In most cases, the reduction in motion at the adjacent levels was less than 10%.

A fusion resulted in complete loss of motion at the fused level and a substantial increase in motion at the adjacent levels. In the case of a single level fusion, the motion at the un-fused levels increased by ~16% whereas for the bi-level fusion, the motion at the un-fused levels increased by ~35%. In case of the hybrid models however, the increase in motion at the nonoperative levels was just 12%. This suggests that an arthroplasty procedure may be preferable to a fusion adjacent to a pre-existing fusion.

The resulting moments followed the motion trends. A TDR model required a hybrid moment less than the corresponding degenerative model. A fused model required the greatest moment; especially the bi-level fusion, where the moment required was more than two times the intact model. The hybrid models fell between the bi-level TDR and the bi-level fusion models supplementing the theory of an arthroplasty being a better alternative to a second fusion.

Previous studies have had inconsistent results with facet forces. Some studies have shown no change in facet forces after arthroplasty while others have shown significant increase in facet forces at the implanted level. Chang et al. [86] reported that following an arthroplasty, the facet loads increased at the index level in all directions with maximum increase during extension motion. Metzger et al. [87] also conducted *in-vitro* studies to investigate the changes in the facet load profile with the variation in the device positioning in the disc space. The authors reported that facet forces were sensitive to the device placement location and thereby indicated that improper positioning could

potentially lead to higher facet loads following TDR. Contrary to these results, a similar study conducted by Steiber et al. [88] using ovine spines reported no significant increase in the facet loading after disc replacement. A computational study by Faizan et al. [84] which included a C3-C7 human finite element model also concluded that under hybrid loading conditions TDR maintains facet loads similar to the intact values in most cases.

In this study, the facet forces at the implanted level increased considerably after a TDR. This could be attributed to disc placement. Although extra care was taken during implant placement and analysis, the FE models have some limitations that might have influenced the results of the study. The FE model results are strong functions of the inputs such as material properties, loading conditions, and implant locations etc. The cervical biomechanics is affected by alteration in the location of the implant in the disc space. For example, by shifting the implant in the anterior, posterior or in the lateral directions, or by changing the orientation of the implant in the disc space, the resulting biomechanics might get influenced as predicted by the studies in both lumbar and cervical spine [84,89]. More work needs to be done with respect to disc positioning in order to address these issues.

The articulation between the two components of the disc implant was modeled as finite sliding, surface to surface contact with a friction coefficient of 0.1. Although there have been studies that have used the exact same contact formulation, it is possible that it may vary *in-vivo* [37, 38, 84].

5.2 In-vitro Cadaveric Testing

The in-vitro cadaveric testing was carried out in the following sequence; intact, single level TDR, bi-level TDR, hybrid and bi-level fusion. A total of 11 specimens were used in the experimental study; 6 for the Bryan group and 5 for the Prestige LP group. The intact specimen was tested up to a pure moment of 2.0Nm. Hybrid loading protocol was used for testing specimens after surgical intervention. We decided to opt for a 360

fusion (anterior plate + posterior screws and rods) as opposed to the clinically popular anterior fusion in order to simulate mechanical fusion.

The cadaveric testing results had trends similar to the FE results. A disc replacement resulted in a slight increase in motion at the implanted level and a reduction in motion at the un-operated levels. The hybrid moment required to obtain intact motion reduced after disc replacement. A fusion resulted in reduction of motion at the fused level and an increase in motion at the un-fused levels. The hybrid moment was considerably higher in case of fusion. Just like the FE study, the hybrid construct was in between bi-level TDR and bi-level fusion indicating that a hybrid construct is a better alternative to bi-level fusion.

In spite of a 360 fusion, the motion at the fused levels was not eliminated completely. There was a significant reduction in motion to a mean of 2.5° , which may be representative of immediate postsurgical results. *In-vivo*, it is expected that as the fusion mass matures the residual motion at the fused segment will further reduce. A further reduction in the residual motion at the fused segment may increase the motion demand on the adjacent mobile segments.

The use of fresh frozen human spines has been shown to not significantly affect the material properties of ligaments, bone, annulus and the general motion of spine itself [90-93]. However, the cost and challenge involved in obtaining cadaveric specimens can be a limitation. It is also common that most readily available specimens are older and therefore exhibit signs of physical degeneration. This raises a valid question of how representative the specimens are of the general population. The cervical specimens used in this study had an average age of 74 years which has implications to bone quality, ligament strength and disc degeneration. Although, all specimens were screened for abnormalities and only those that appeared to be 'normal' were selected for biomechanical testing a lot of specimens did have degenerated discs and at times osteophytes in the disc

space. This could be the reason the average intact range of motion of cadaveric specimens was considerably lower in comparison to the FE model.

Muscle forces tend to have a 'stiffening' effect on the cervical spine. Therefore, in order to achieve a desired amount of motion a higher bending moment must be applied. A similar result has been reported in the presence of an axial compressive load [76, 94]. It is desirable to test the spine in the presence of an appropriate preload. However, the application of an axial compressive load in the absence of muscular forces tends to create a highly unstable spine. The cervical spine tends to go into extension upon the application of a preload which is why we decided to carry out our tests under "no preload" conditions (under pure moment of up to 2.0Nm).

Inter-specimen variability is a problem with all biomechanical spine studies. Each spine is architecturally different from the next and material properties may slightly vary between two specimens. It becomes difficult to take all these variables into account when determining, for example, the stabilizing potential of a disc replacement system. For these reasons, each spine was first tested in the intact state. This test served as the baseline measurement, effectively making each specimen its own control. Subsequent motions of the instrumented spine were reported in comparison with the intact spine. Means and standard deviations were computed to study the general trend in the results. This method reduces inter-specimen variability resulting from the specimen population.

In spite of these limitations, cadaveric testing is the most direct and obvious way to obtain biomechanical data. It has been used for years to test and validate the use of various implants.

5.3 Comparison of computational and experimental results

Comparing the motion pattern between the computational and experimental studies, the overall trends were very similar. The actual motion however, had a lot of variation. In some cases, the segmental rotations of the intact FE model were more than

one standard deviation greater than the intact motion values of the cadaveric specimen. The primary reason for this difference is the specimen quality. However, the goal of the study was to look at trends and changes as opposed to exact numbers.

Inter-specimen variability is a problem with experimental studies and that's where computational models have an advantage. By changing the material properties, we modified the FE model of a healthy spine to simulate moderate degeneration and subsequent surgical procedures. Clinically interbody fusion has been known to completely eliminate motion at the fused level within 12 months after surgery [95,96]. However, in spite of opting for a 360 fusion, the reduction in motion in cadavers was not satisfactory. The poor bone quality of the specimens was most likely the reason for poor fusion. The FE model on the other hand eliminated motion completely.

The changes in motion between the computational and experimental studies following various surgeries had similar trends. After a disc replacement, the cadaveric specimens tended to settle in a slightly extended position. Similar behavior was observed with the FE model as well. There is a variation in results reported in clinical studies. Some studies report a post-op kyphosis while others report a lordosis [97-99]. We think the lack of muscles and the absence of ALL is the reason for the model and the cadaveric specimens settling in the extended position.

To conclude, this study highlighted that cervical disc replacement with both Bryan and Prestige LP discs not only preserved the motion at the operated level, but also maintained the normal motion at the adjacent levels. Under hybrid loading, the motion pattern of the spine with a TDR was closer to the intact motion pattern in comparison to the degenerative or fusion models. Also, in case of an existing fusion, this study shows that a disc replacement is a better alternative to a second fusion.

CHAPTER 6: FUTURE WORK

This study aimed at studying the changes in biomechanics of the cervical spine following disc replacement and fusion. Using a combination of arthroplasty using two discs, fusion and two levels, various surgical constructs were analyzed in detail. Range of motion, disc stresses and facet forces were used for analysis. The results of this study suggest that disc replacement is a better alternative to fusion. Based on the analysis, various pros and cons of each surgical procedure have been discussed. Several areas for additional research have been generated from this study. Future study opportunities are presented below.

It is known that muscles provide additional stability to the spine. However incorporating muscles in a computational model is a challenging task. The model in this study is made up of osteoligamentous components and ignores muscles. Addition of muscles/muscle forces would enable a better understanding of *in-vivo* conditions.

Also, the FE model or the cadaveric testing done in this study did not include a preload simulating head weight. A preload could significantly alter the biomechanics of the spine, but loading the spine axially caused instability the testing system due to which ‘no preload’ condition was used. Loading the spine using a follower load is an alternative, but that requires special loading apparatus [100].

Only moderate degeneration was modeled in the FE model in this study. In future, various grades of degeneration could be modeled. The results of a disc replacement in a severely degenerated disc with minimal disc height could vary.

Another potential area that needs more research is disc placement. It is discussed that there is a variation in facet forces and curvature of the spine after disc replacement. Disc placement could be a very important factor and an optimal disc placement could potentially eliminate high facet forces and abnormal curvatures.

APPENDIX A: SURGICAL TECHNIQUE FOR IMPLANTATION

A.1 Bryan® Cervical Disc system

The following section describes and illustrates the placement of the BRYAN® Cervical Disc at C5-C6 in a cadaveric spine.

Step 1: Fixing and positioning the cadaveric spine

Implantation of a Bryan disc involves multiple drilling and milling operation which are relative to the position and placement of the spine with respect to the surgical table. Hence, securing the specimen to the table is very important. This was done with the use of tape. The two potted ends of the specimen were strapped to the table using tape.

Step 2: Target disc excision

After estimating the center of the disc, width of the incision was determined using template markings. Only the disc between the markings of this incision was excised. This was done using rongeurs and curettes. Lateral portion of the annulus was left intact.

Once all of the desired soft tissue was removed, anterior osteophytes (if any) were removed using a high speed burr.

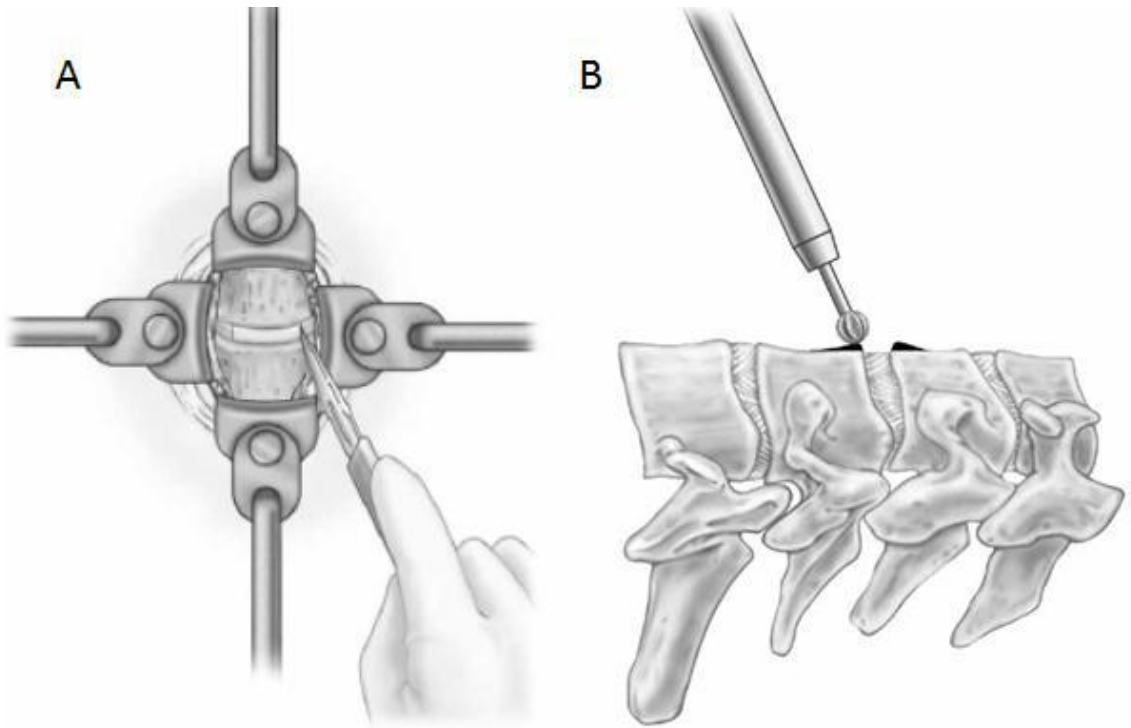


Figure A-1: Excision of disc (A), and removal of osteophytes using a high speed burr (B)

Step 3: Aligning and Centering

Using various alignment and centering tools included in the instruments trays, transverse and sagittal centering was done. Finally a Dual Track Milling Guide was aligned and secured to the vertebral bodies.

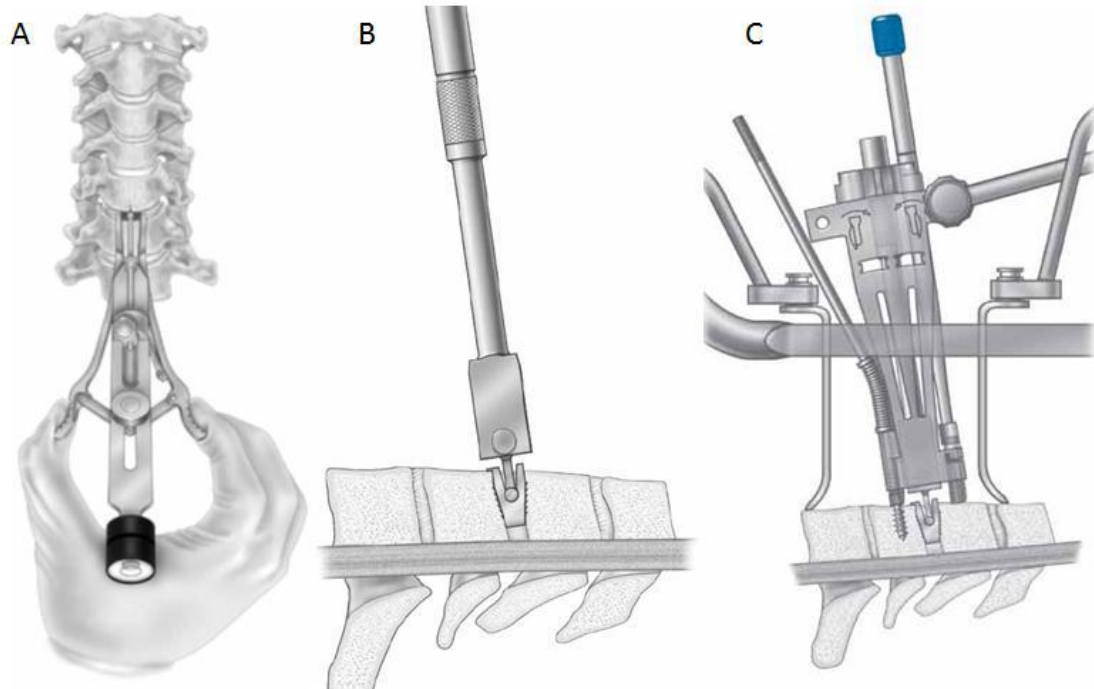


Figure A-2: Figure showing transverse alignment (A), sagittal alignment (B) and securing of the Dual Track Milling Guide.

Step 4: Burring end-plates

Using certain disc size specific tools and a high speed burring block, the two end-plates were burred such that they were parallel to each other.

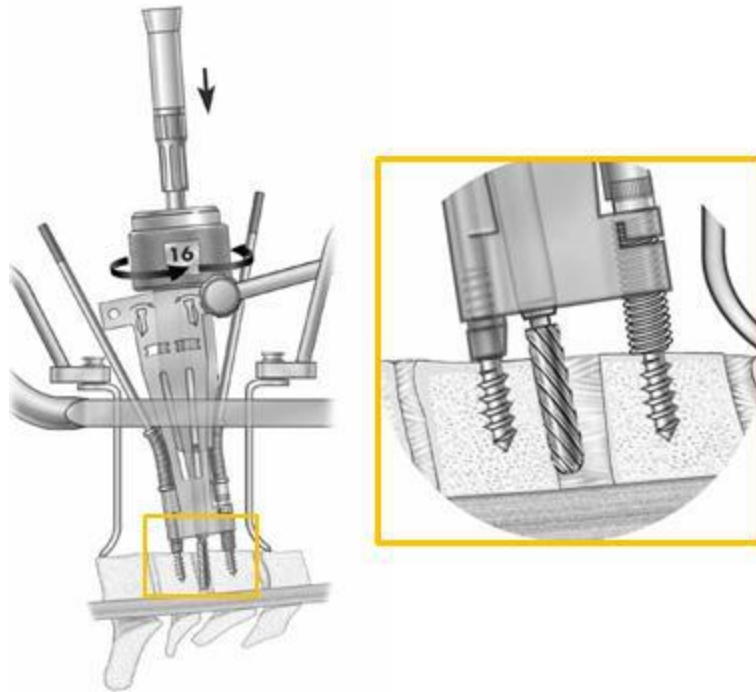


Figure A-3: Figure showing burring of the end-plates

Step 5: End-plate Milling

Bryan disc has convex titanium shells which attach to the vertebral end-plates. In order to achieve a good fixation, the vertebral end-plates need to be machined such that they will match the contour of the disc. This is done using a specialized milling disc.

The milling disc is attached to the handpiece and using the guides in the dual track milling guide, the two end-plates are machined.

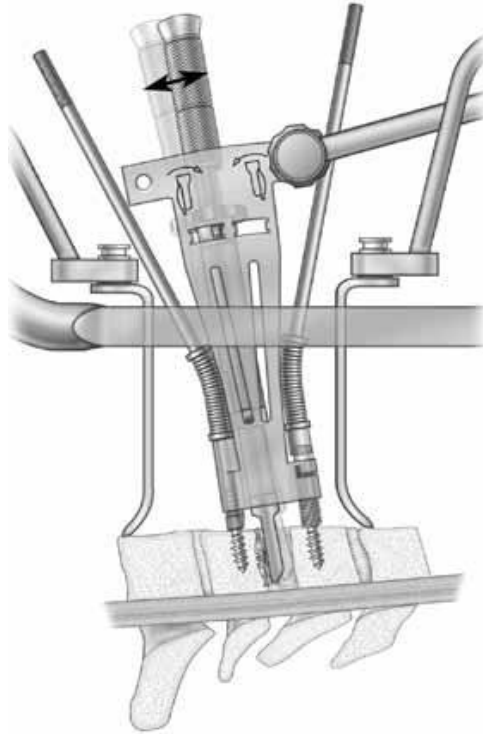


Figure A-4: End-plate milling operation

Step 6: Distraction

Once the end-plates were ready, an appropriate size implant spacer was inserted in the disc space. Once the spacer was engaged with the milled surfaces, the milling guide was removed and a distractor was inserted over the anchor posts. Using the thumb screw, the disc space was distracted.

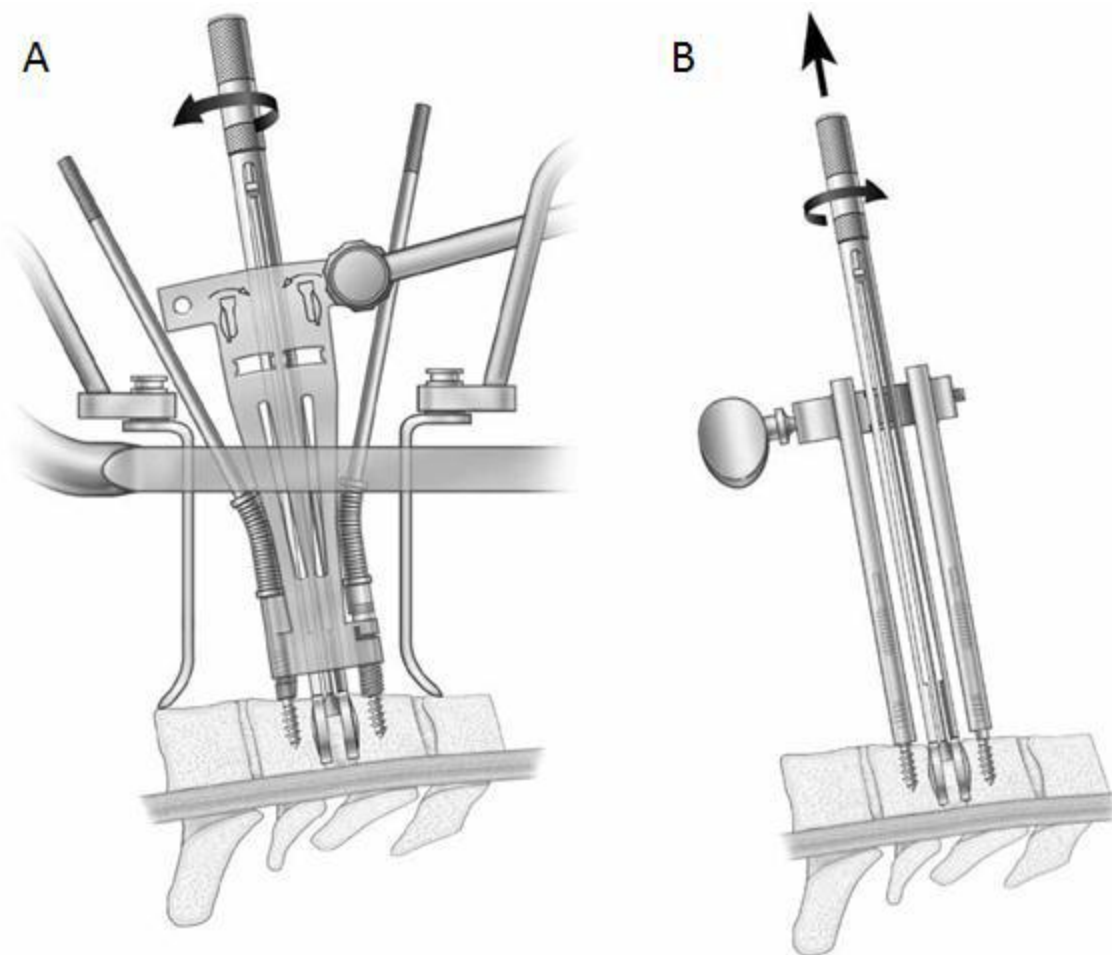


Figure A-5: Insertion of implant spacer (A), and distraction (B)

Step 7: Implant Preparation

Prior to implantation, the prosthesis is filled completely with saline and the seal plugs are tightened.

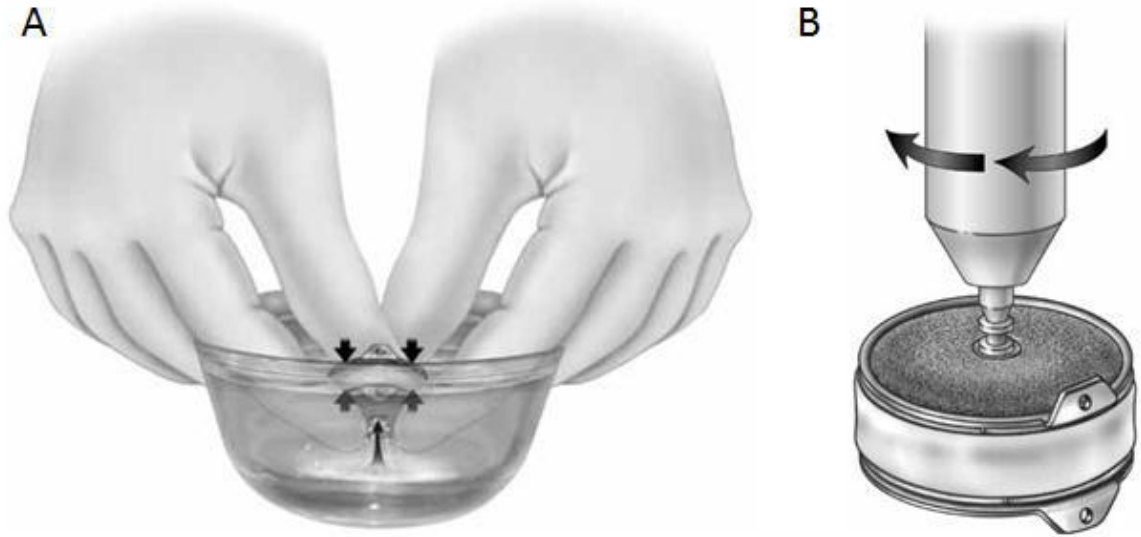


Figure A-6: Bryan disc being filled with saline (A) and tightening of seal plug (B)

Step 8: Prosthesis Placement

After preparing the implant, it was attached to the implant inserter using which it was inserted in the prepared disc space. Slight gentle taps were applied in order to fully seat the implant.

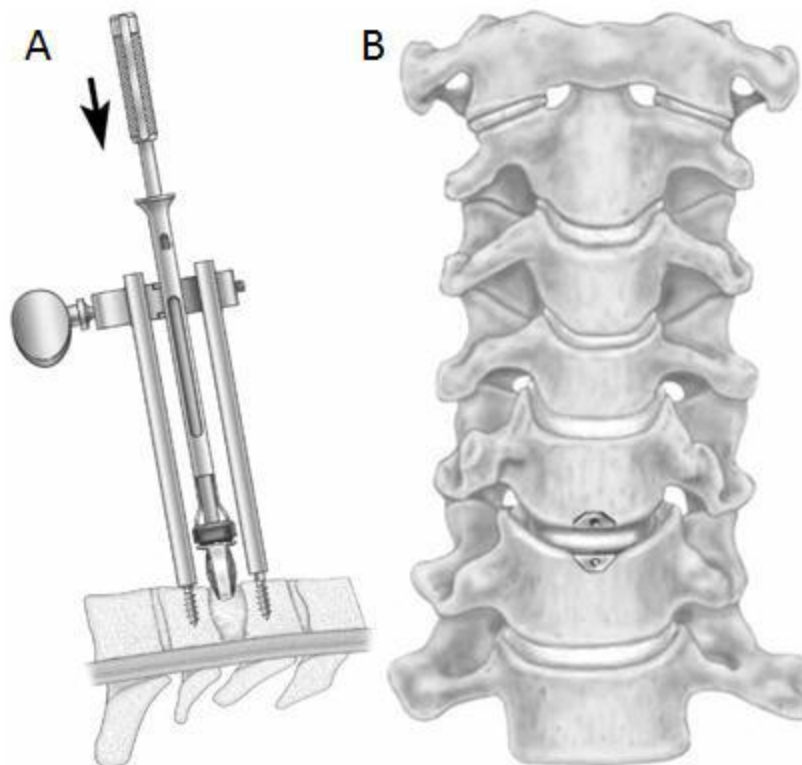


Figure A-7: A: Implant being inserted in the disc space; B: Disc fully seated in the disc space.

A.2 Prestige LP® Cervical Disc system

The following section describes and illustrates the placement of the Prestige LP® Cervical Disc at C5-C6 in a cadaveric spine.

Step 1: Discectomy

A complete discectomy was performed at the C5-C6 level. Pituitaries, curettes, and kerrisons were used to remove the disc material and expose the posterior longitudinal ligament. A high-speed burr (match tip/round) was utilized for removal of osteophytes. The anterior surface of the vertebral bodies was lightly burred to remove any soft tissue and bony protrusions in order to create a flat surface.



Figure A-8: Anterior surface being milled to create a flat surface.

Step 2: End-Plate preparation

An appropriately sized rasp was used to prepare the endplates.



Figure A-9: A rasp being used to prepare the endplates

Step 3: Rail Preparation

Appropriately sized Rail Cutter Guide was centered and then inserted in the prepared disc space. Using a rail cutter bit, four holes were drilled in the bodies using the rail cutting guide.



Figure A-10: Rail cutter guide inserted in the disc space

Step 4: Rail Cutting

After aligning the four cutting blades of the Rail Punch into the four pilot holes made by the Trial/Cutter Guide, the Rail Punch was gently tapped into the disc space. This created four channels in the endplates.



Figure A-11: Rail cutting

Step 5: Implantation

The appropriately sized Prestige LP disc is then attached to the implant inserter and finally inserted in the disc space making sure the ball portion of the disc is positioned superiorly. While inserting, the rails of the disc were aligned to the channels in the endplates and using a mallet. Then the inserter was gently tapped until the anterior tabs of the disc were in contact with the vertebral bodies.

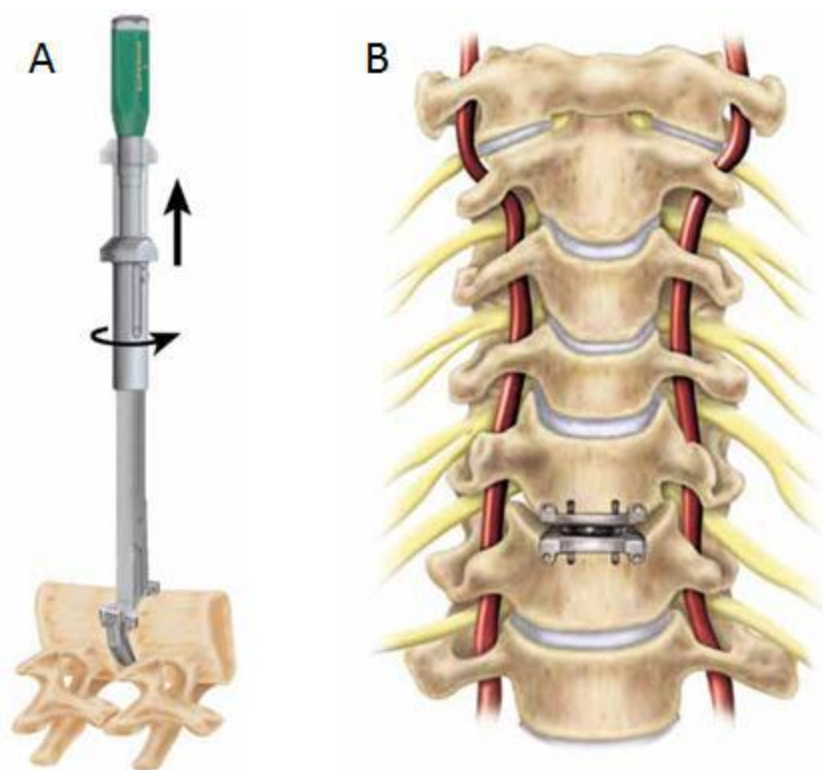


Figure A-12: A: Implant being inserted in the disc space. B: Prestige LP disc fully seated in the disc space.

APPENDIX B: DETAILED FE ANALYSIS RESULTS

B.1 Single Level Models

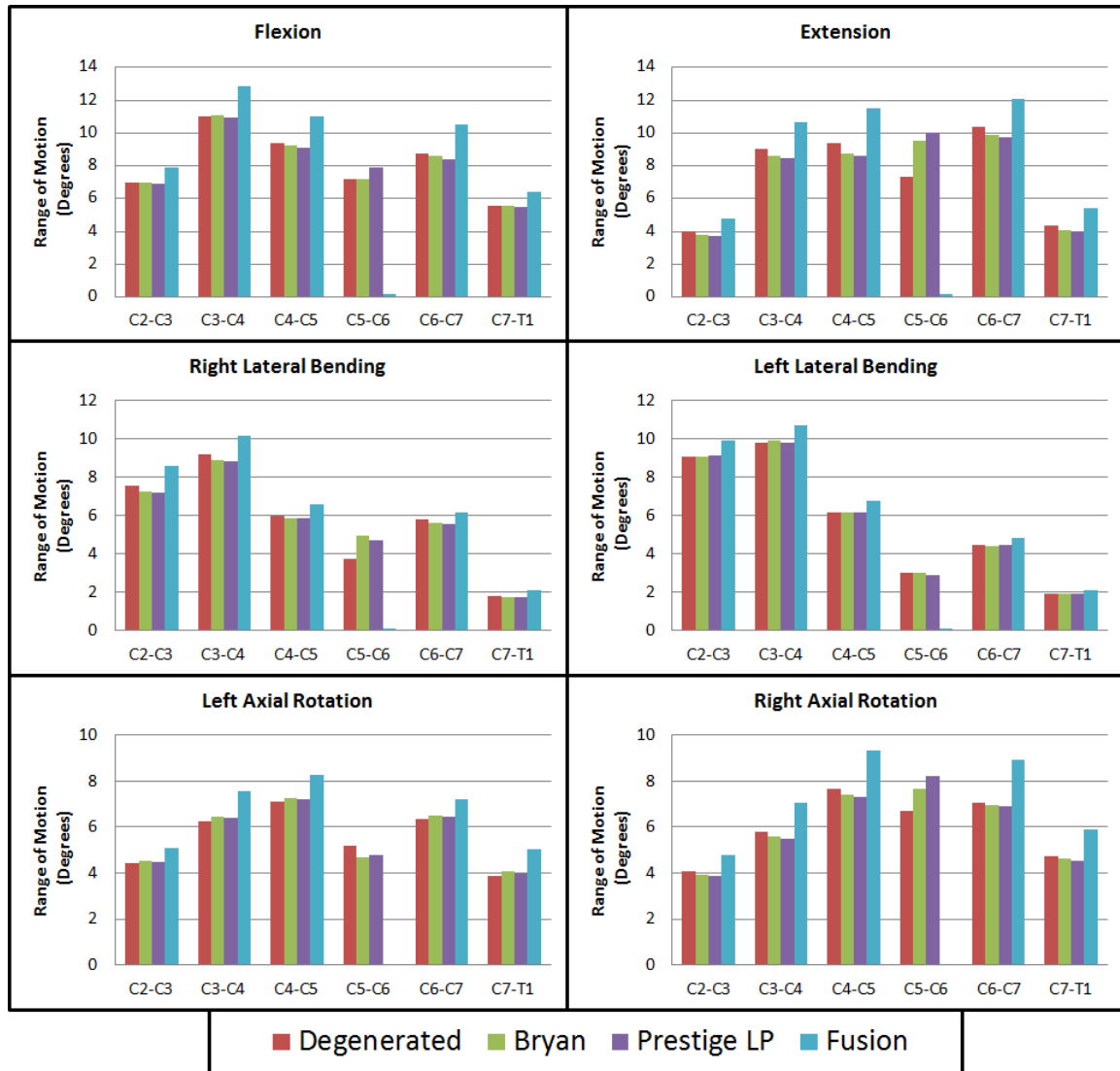


Figure B-1: Comparison of range of motion in all six directions between single level degenerative, Bryan, Prestige LP and fusion models.

Table B-1: Range of motion (degrees) values for all single level models in all six directions.

Flexion		Intact	Degenerative	Bryan	Prestige LP	Fusion
	C2-C3	6.48	6.96	6.99	6.94	7.93
	C3-C4	10.30	11.05	11.11	10.96	12.83
	C4-C5	8.50	9.40	9.24	9.08	11.02
	C5-C6	10.60	7.17	7.22	7.91	0.17
	C6-C7	7.85	8.76	8.60	8.37	10.55
	C7-T1	5.08	5.54	5.56	5.49	6.41
	C2-T1	48.8	48.9	48.7	48.7	48.9
Extension		Intact	Degenerative	Bryan	Prestige LP	Fusion
	C2-C3	3.57	3.98	3.81	3.71	4.76
	C3-C4	8.17	9.04	8.61	8.49	10.67
	C4-C5	8.48	9.40	8.75	8.59	11.53
	C5-C6	11.02	7.36	9.50	10.03	0.16
	C6-C7	9.36	10.41	9.90	9.78	12.07
	C7-T1	3.79	4.34	4.10	4.02	5.46
	C2-T1	44.38	44.53	44.67	44.62	44.64
RLB		Intact	Degenerative	Bryan	Prestige LP	Fusion
	C2-C3	6.75	7.58	7.27	7.21	8.60
	C3-C4	8.39	9.17	8.93	8.84	10.19
	C4-C5	5.66	5.99	5.88	5.88	6.57
	C5-C6	6.35	3.72	4.96	4.69	0.09
	C6-C7	5.34	5.78	5.60	5.59	6.15
	C7-T1	1.61	1.82	1.74	1.72	2.10
	C2-T1	34.09	34.06	34.39	33.92	33.69

Table B-1 Continued

LLB		Intact	Degenerative	Bryan	Prestige LP	Fusion
	C2-C3	8.07	9.09	9.10	9.15	9.95
	C3-C4	8.98	9.80	9.92	9.83	10.70
	C4-C5	5.46	6.17	6.15	6.14	6.78
	C5-C6	6.07	3.02	3.00	2.91	0.08
	C6-C7	4.16	4.46	4.42	4.45	4.81
	C7-T1	1.74	1.91	1.92	1.93	2.07
	C2-T1	34.49	34.45	34.52	34.40	34.40
LAR		Intact	Degenerative	Bryan	Prestige LP	Fusion
	C2-C3	4.11	4.43	4.52	4.51	5.09
	C3-C4	5.64	6.23	6.44	6.39	7.56
	C4-C5	6.71	7.12	7.26	7.19	8.27
	C5-C6	7.31	5.21	4.70	4.78	0.06
	C6-C7	6.08	6.37	6.50	6.47	7.23
	C7-T1	3.52	3.89	4.08	3.97	5.04
	C2-T1	33.36	33.24	33.50	33.31	33.25
RAR		Intact	Degenerative	Bryan	Prestige LP	Fusion
	C2-C3	3.77	4.10	3.92	3.87	4.79
	C3-C4	5.24	5.77	5.59	5.49	7.06
	C4-C5	6.94	7.67	7.40	7.30	9.36
	C5-C6	9.49	6.72	7.66	8.23	0.05
	C6-C7	6.38	7.08	6.97	6.89	8.94
	C7-T1	4.24	4.72	4.65	4.55	5.89
	C2-T1	36.06	36.07	36.19	36.33	36.09

B.1 Bi-level Models

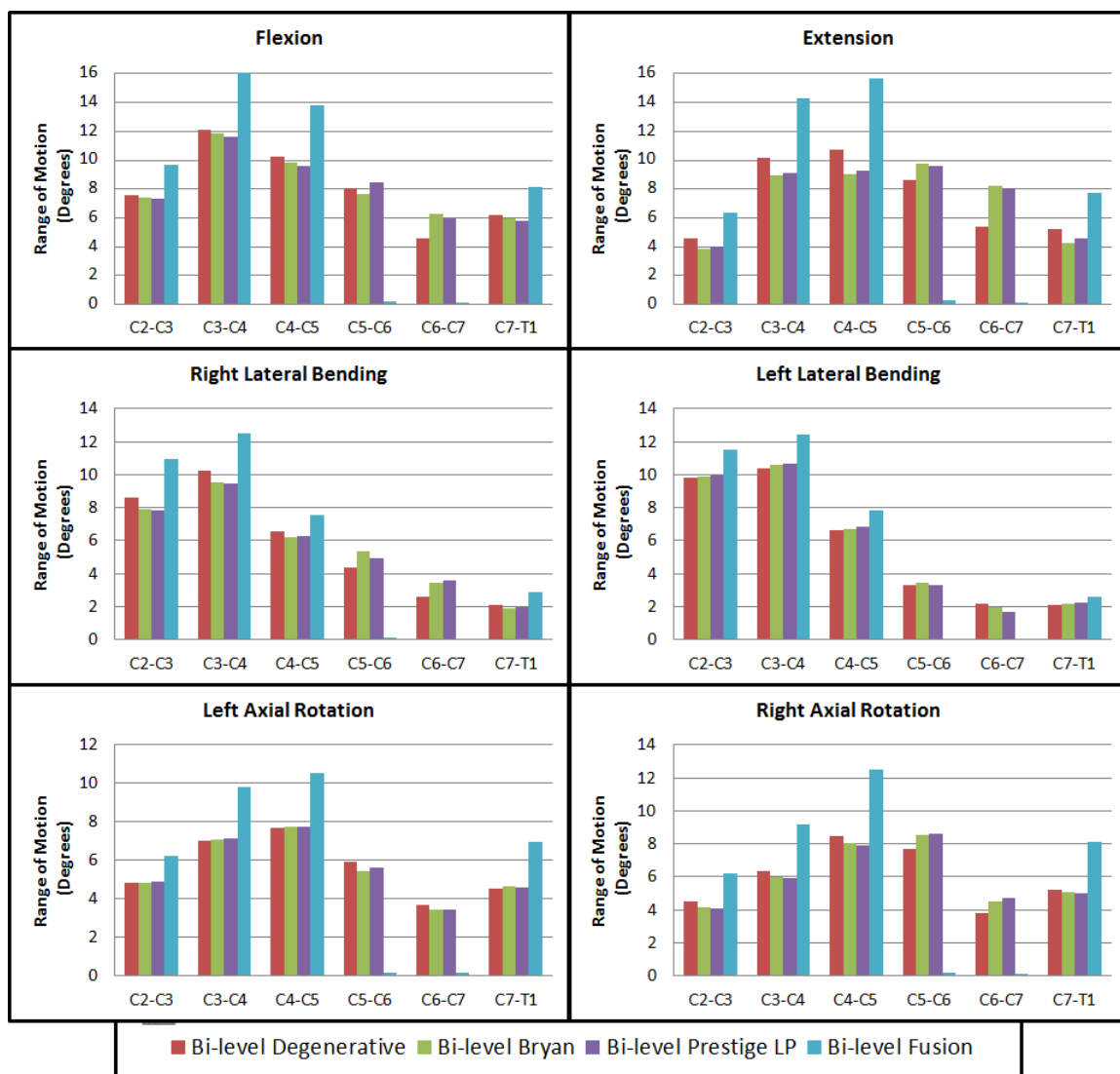


Figure B-2: Comparison of range of motion in all six directions between bi-level degenerative, Bryan, Prestige LP and fusion models.

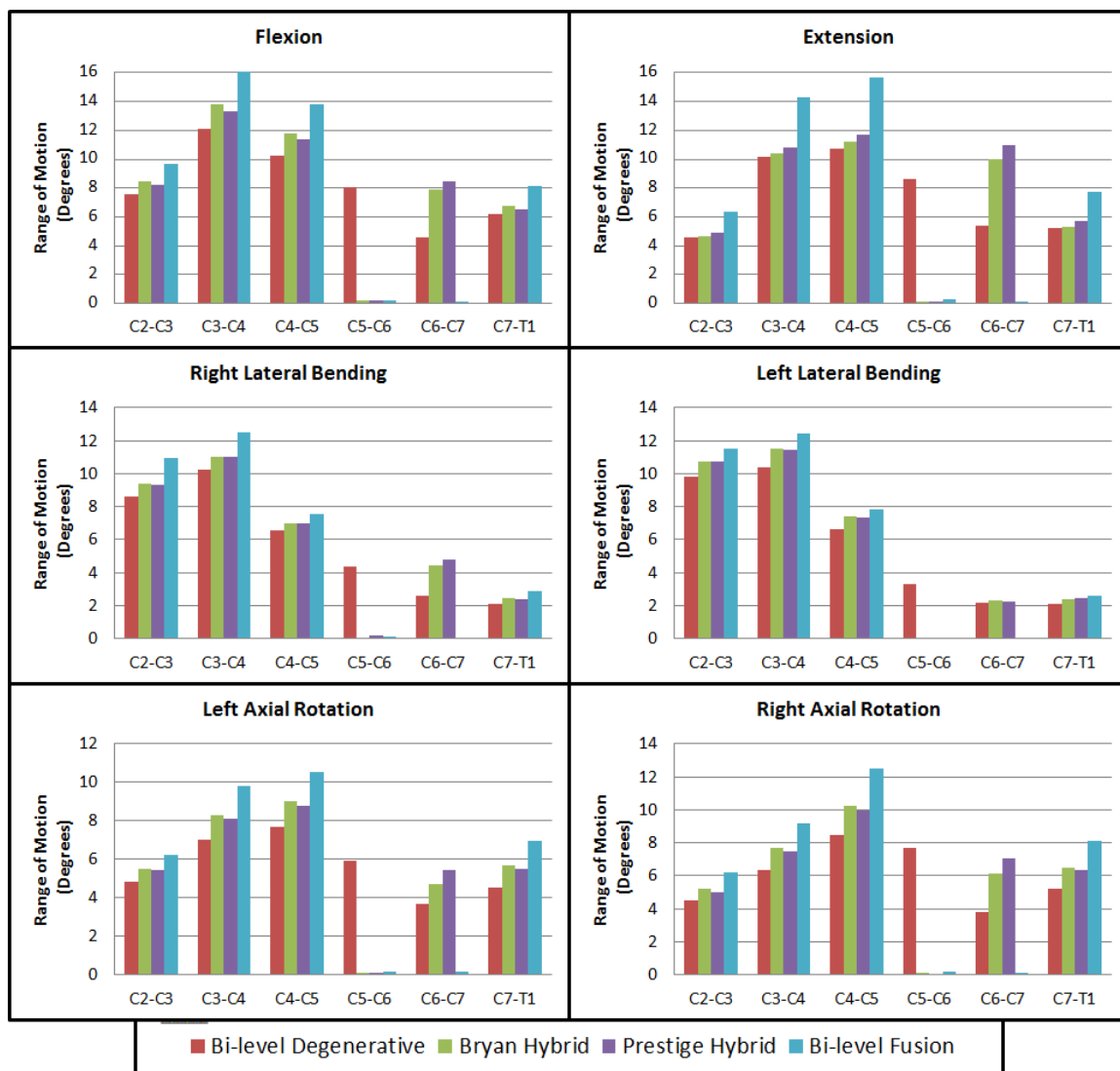


Figure B-3: Comparison of range of motion in all six directions between bi-level degenerative, Bryan Hybrid, Prestige LP Hybrid and bi-level fusion models.

Table B-2: Range of motion (degrees) values for all bi-level models in all six directions.

		Intact	Bi-level Degenerative	Bi-level Bryan	Bi-level Prestige LP	Bryan Hybrid	Prestige Hybrid	Bi-level Fusion
Flexion	C2-C3	6.48	7.56	7.43	7.31	8.44	8.24	9.71
	C3-C4	10.30	12.10	11.85	11.60	13.80	13.36	16.34
	C4-C5	8.50	10.28	9.84	9.56	11.76	11.40	13.77
	C5-C6	10.60	8.07	7.68	8.44	0.17	0.25	0.21
	C6-C7	7.85	4.55	6.28	5.93	7.86	8.49	0.12
	C7-T1	5.08	6.24	5.96	5.79	6.79	6.56	8.13
Extension	C2-C3	3.57	4.55	3.89	4.02	4.65	4.87	6.35
	C3-C4	8.17	10.19	8.94	9.14	10.39	10.83	14.25
	C4-C5	8.48	10.69	9.01	9.25	11.20	11.72	15.70
	C5-C6	11.02	8.66	9.76	9.57	0.17	0.16	0.29
	C6-C7	9.36	5.36	8.22	8.08	10.02	10.94	0.17
	C7-T1	3.79	5.22	4.29	4.59	5.29	5.71	7.74
RLB	C2-C3	6.75	8.59	7.89	7.82	9.39	9.35	10.92
	C3-C4	8.39	10.23	9.53	9.46	11.03	11.00	12.48
	C4-C5	5.66	6.55	6.24	6.28	6.98	7.00	7.56
	C5-C6	6.35	4.34	5.33	4.95	0.05	0.21	0.09
	C6-C7	5.34	2.62	3.47	3.59	4.45	4.80	0.06
	C7-T1	1.61	2.12	1.92	1.96	2.43	2.40	2.87
LLB	C2-C3	8.07	9.79	9.87	9.99	10.75	10.70	11.49
	C3-C4	8.98	10.41	10.60	10.66	11.51	11.45	12.45
	C4-C5	5.46	6.64	6.69	6.81	7.38	7.37	7.86
	C5-C6	6.07	3.30	3.44	3.28	0.07	0.07	0.06
	C6-C7	4.16	2.17	1.98	1.65	2.30	2.24	0.07
	C7-T1	1.74	2.13	2.20	2.26	2.39	2.42	2.59

Table B-2 continued

LAR	C2-C3	4.11	4.81	4.84	4.90	5.51	5.41	6.21
	C3-C4	5.64	7.01	7.05	7.12	8.32	8.12	9.78
	C4-C5	6.71	7.70	7.76	7.75	9.05	8.80	10.56
	C5-C6	7.31	5.91	5.45	5.61	0.10	0.10	0.16
	C6-C7	6.08	3.68	3.44	3.45	4.72	5.45	0.13
	C7-T1	3.52	4.54	4.65	4.59	5.70	5.49	6.96
RAR	C2-C3	3.77	4.52	4.19	4.11	5.19	5.04	6.17
	C3-C4	5.24	6.34	6.02	5.90	7.68	7.46	9.17
	C4-C5	6.94	8.47	8.04	7.93	10.25	9.97	12.48
	C5-C6	9.49	7.67	8.57	8.60	0.10	0.08	0.21
	C6-C7	6.38	3.79	4.49	4.74	6.15	7.05	0.12
	C7-T1	4.24	5.18	5.05	4.97	6.49	6.34	8.08

REFERENCES

- [1] http://1.bp.blogspot.com/_OG2sdI8pIz0/TQ_EkORnu3I/AAAAAAAAABME/o8jppJdgNs/s1600/Web+Spine+1.jpg. Available at: http://1.bp.blogspot.com/_OG2sdI8pIz0/TQ_EkORnu3I/AAAAAAAAABME/o8jppJdgNs/s1600/Web+Spine+1.jpg.
- [2] White AA, Panjabi MM. Clinical biomechanics of the spine. : Lippincott Philadelphia; 1990.
- [3] Goel VK. Biomechanics of the spine: clinical and surgical prospective. ; 1990.
- [4] <http://www.Hughston.com/hha/a.Cspine.Htm>. Available at: <http://www.Hughston.com/hha/a.Cspine.Htm>.
- [5] Singh AP. Surgical Anatomy of Lower Cervical Spine or Subaxial Spine. Available at: <http://boneandspine.com/spine/cervical-spine/surgical-anatomy-of-lower-cervical-spine-or-subaxial-spine/>.
- [6] Bao QB. The artificial disc: theory, design and materials. Biomaterials 1996;17(12).
- [7] Nachemson A. Lumbar intradiscal pressure. Experimental studies on post-mortem material. Acta orthopaedica Scandinavica.Supplementum 1960;43:1-104.
- [8] King AI, Prasad P, Ewing CL. Mechanism of spinal injury due to caudocephalad acceleration. Orthop Clin North Am 1975;6(1):19-31.
- [9] Gruber H, Hanley E. Observations on morphologic changes in the aging and degenerating human disc: secondary collagen alterations. BMC Musculoskeletal Disorders 2002;3(1):9.
- [10] Kurtz SM, Edidin AA. Spine technology handbook. : Elsevier Academic Press; 2006.
- [11] Morishita Y, Hida S, Miyazaki M, Hong SW, Zou J, Wei F, et al. The effects of the degenerative changes in the functional spinal unit on the kinematics of the cervical spine. Spine 2008;33(6):E178.
- [12] Drerup B, Granitzka M, Assheuer J, Zerlett G. Assessment of disc injury in subjects exposed to long-term whole-body vibration. European Spine Journal 1999;8(6):458-467.
- [13] Stokes IAF, Iatridis JC. Mechanical conditions that accelerate intervertebral disc degeneration: overload versus immobilization. Spine 2004;29(23):2724.
- [14] Ala-Kokko L. Genetic risk factors for lumbar disc disease. Ann Med 2002;34(1):42-47.

- [15] Miyazaki M, Hong SW, Yoon SH, Zou J, Tow B, Alanay A, et al. Kinematic analysis of the relationship between the grade of disc degeneration and motion unit of the cervical spine. *Spine* 2008;33(2):187.
- [16] Kelsey JL, Githens P, Walter S, Southwick W, Weil U, Holford T, et al. An epidemiological study of acute prolapsed cervical intervertebral disc. *The Journal of Bone and Joint Surgery* 1984;66(6):907.
- [17] Richard Staehler. Conservative Treatment for a Cervical Herniated Disc. Available at: <http://www.spine-health.com/conditions/herniated-disc/conservative-treatment-a-cervical-herniated-disc>. Accessed 2/24, 2011.
- [18] Cloward RB. The Anterior Approach for Removal of Ruptured Cervical Disks*. *J Neurosurg* 1958;15(6):602-617.
- [19] Smith GW, Robinson RA. The treatment of certain cervical-spine disorders by anterior removal of the intervertebral disc and interbody fusion. *The Journal of Bone and Joint Surgery* 1958;40(3):607.
- [20] Weinhoffer SL, Guyer RD, Herbert M, Griffith SL. Intradiscal pressure measurements above an instrumented fusion: a cadaveric study. *Spine* 1995;20(5):526.
- [21] Bushell G, Ghosh P, Taylor T, Sutherland J, Braund K. The effect of spinal fusion on the collagen and proteoglycans of the canine intervertebral disc. *J Surg Res* 1978;25(1):61-69.
- [22] EMERY SE, BOHLMAN HH, BOLESTA MJ, JONES PK. Anterior cervical decompression and arthrodesis for the treatment of cervical spondylotic myelopathy. Two to seventeen-year follow-up. *The Journal of Bone and Joint Surgery* 1998;80(7):941.
- [23] Hilibrand AS, Carlson GD, Palumbo MA, Jones PK, Bohlman HH. Radiculopathy and myelopathy at segments adjacent to the site of a previous anterior cervical arthrodesis. *The Journal of Bone and Joint Surgery* 1999;81(4):519.
- [24] Goffin J, Geusens E, Vantomme N, Quintens E, Waerzeggers Y, Depreitere B, et al. Long-term follow-up after interbody fusion of the cervical spine. *Journal of spinal disorders & techniques* 2004;17(2):79.
- [25] Anterior Cervical Discectomy with Fusion. Available at: <http://www.melbournespinesurgery.com.au/anterior-cervical-discectomy-with-fusion-graeme-brazenor-neuro-spine-surgeon.html>.
- [26] Vaccaro AR. Early failure of long segment anterior cervical plate fixation. *Journal of spinal disorders techniques* 1998;11(5):410.

- [27] Wang JC. Increased fusion rates with cervical plating for two-level anterior cervical discectomy and fusion. *Spine (Philadelphia, Pa.1976)* 2000;25(1):41.
- [28] Bohlman H, Emery S, Goodfellow D, Jones P. Robinson anterior cervical discectomy and arthrodesis for cervical. *J Bone Joint Surg Am* 1993;75:1298-1307.
- [29] Newman M. The outcome of pseudarthrosis after cervical anterior fusion. *Spine (Philadelphia, Pa.1976)* 1993;18(16):2380.
- [30] Phillips FM. Anterior cervical pseudarthrosis: natural history and treatment. *Spine (Philadelphia, Pa.1976)* 1997;22(14):1585.
- [31] Martin Jr GJ. Anterior cervical discectomy with freeze-dried fibula allograft: Overview of 317 cases and literature review. *Spine (Philadelphia, Pa.1976)* 1999;24(9):852.
- [32] Hilibrand AS. The use of diagnostic imaging to assess spinal arthrodesis. *Orthop Clin North Am* 1998;29(4):591.
- [33] Emery SE. Robinson anterior cervical fusion comparison of the standard and modified techniques. *Spine (Philadelphia, Pa.1976)* 1994;19(6):660.
- [34] Traynelis V. Cervical arthroplasty. *Clin Neurosurg* 2006;53:203-7.
- [35] Sasso RC, Best NM. Cervical kinematics after fusion and bryan disc arthroplasty. *Journal of spinal disorders & techniques* 2008;21(1):19.
- [36] Goffin J, Casey A, Kehr P, Liebig K, Lind B, Logroscino C, et al. Preliminary clinical experience with the Bryan cervical disc prosthesis. *Neurosurgery* 2002;51(3):840.
- [37] Galbusera F, Bellini CM, Raimondi MT, Fornari M, Assietti R. Cervical spine biomechanics following implantation of a disc prosthesis. *Med Eng Phys* 2008;30(9):1127-1133.
- [38] Galbusera F, Fantigrossi A, Raimondi M, Assietti R, Sassi M, Fornari M. Biomechanics of the C5-C6 spinal unit before and after placement of a disc prosthesis. *Biomechanics and Modeling in Mechanobiology* 2006;5(4):253-261.
- [39] Lafuente J, Casey A, Petzold A, Brew S. The Bryan cervical disc prosthesis as an alternative to arthrodesis in the treatment of cervical spondylosis: 46 consecutive cases. *Journal of Bone and Joint Surgery-British Volume* 2005;87(4):508.
- [40] Heller JG, Sasso RC, Papadopoulos SM, Anderson PA, Fessler RG, Hacker RJ, et al. Comparison of BRYAN cervical disc arthroplasty with anterior cervical decompression and fusion: clinical and radiographic results of a randomized, controlled, clinical trial. *Spine* 2009;34(2):101.

- [41] Sasso RC, Smucker JD, Hacker RJ, Heller JG. Artificial disc versus fusion: a prospective, randomized study with 2-year follow-up on 99 patients. *Spine* 2007;32(26):2933.
- [42] Kim SW, Limson MA, Kim SB, Arbatin JJF, Chang KY, Park MS, et al. Comparison of radiographic changes after ACDF versus Bryan disc arthroplasty in single and bi-level cases. *European Spine Journal* 2009;18(2):218-231.
- [43] Cummins BH, Robertson JT, Gill SS. Surgical experience with an implanted artificial cervical joint. *J Neurosurg* 1998;88(6):943-948.
- [44] Wigfield CC, Gill SS, Nelson RJ, Metcalf NH, Robertson JT. The new Frenchay artificial cervical joint: results from a two-year pilot study. *Spine* 2002;27(22):2446.
- [45] Robertson JT, Metcalf NH. Long-term outcome after implantation of the Prestige I disc in an end-stage indication: 4-year results from a pilot study. *Neurosurg Focus* 2004;17(3):E10.
- [46] Porchet F, Metcalf NH. Clinical outcomes with the Prestige II cervical disc: preliminary results from a prospective randomized clinical trial. *Neurosurg Focus* 2004;17(3):E6.
- [47] Mummaneni PV, Burkus JK, Haid RW, Traynelis VC, Zdeblick TA. Clinical and radiographic analysis of cervical disc arthroplasty compared with allograft fusion: a randomized controlled clinical trial. *Journal of Neurosurgery: Spine* 2007;6(3):198-209.
- [48] Peng CWB, Yue WM, Basit A, Guo CM, Tow BPB, Chen JLT, et al. Intermediate Results of the Prestige LP Cervical Disc Replacement: Clinical and Radiological Analysis With Minimum Two-Year Follow-up. *Spine* 2011;36(2):E105.
- [49] Phillips FM, Garfin SR. Cervical disc replacement. *Spine* 2005;30(17S):S27.
- [50] Spinal Fusion. Available at: <http://www.surgeryencyclopedia.com/Pa-St/Spinal-Fusion.html>.
- [51] Azmi H, Schlenk RP. Surgery for postarthrodesis adjacent-cervical segment degeneration. *Neurosurgical Focus* 2003;15(3):1-6.
- [52] Baba H, Furusawa N, Imura S, Kawahara N, Tsuchiya H, Tomita K. Late radiographic findings after anterior cervical fusion for spondylotic myeloradiculopathy. *Spine* 1993;18(15):2167.
- [53] Eck JC, Humphreys SC, Hodges SD. Adjacent-segment degeneration after lumbar fusion: a review of clinical, biomechanical, and radiologic studies. *Am J Orthop (Belle Mead NJ)* 1999 Jun;28(6):336-340.

- [54] Puttlitz CM, Rousseau MA, Xu Z, Hu S, Tay BKB, Lotz JC. Intervertebral disc replacement maintains cervical spine kinetics. *Spine* 2004;29(24):2809.
- [55] Diangelo DJ, Foley KT. An improved biomechanical testing protocol for evaluating spinal arthroplasty and motion preservation devices in a multilevel human cadaveric cervical model. *Neurosurg Focus* 2004;17(3):E4.
- [56] Diangelo DJ, Foley KT, Morrow BR, Schwab JS, Song J, German JW, et al. In vitro biomechanics of cervical disc arthroplasty with the ProDisc-C total disc implant. *Neurosurgical focus* 2004;17(3):44-54.
- [57] Dmitriev AE, Cunningham BW, Hu N, Sell G, Vigna F, McAfee PC. Adjacent level intradiscal pressure and segmental kinematics following a cervical total disc arthroplasty: an in vitro human cadaveric model. *Spine* 2005;30(10):1165.
- [58] Chang UK, Kim DH, Lee MC, Willenberg R, Kim SH, Lim J. Range of motion change after cervical arthroplasty with ProDisc-C and prestige artificial discs compared with anterior cervical discectomy and fusion. *Journal of Neurosurgery: Pediatrics* 2007;7(1).
- [59] Puttlitz CM, DiAngelo DJ. Cervical spine arthroplasty biomechanics. *Neurosurg Clin N Am* 2005 Oct;16(4):589-94, v.
- [60] Swathi Kode, Nicole A. Kallemeyn, Joseph D. Smucker, Douglas C. Fredericks and Nicole M. Grosland. Biomechanical Effects of Laminoplasty and Laminectomy on the stability of Cervical Spine. *ASME 2011 Summer Bioengineering Conference*; June 22-25, 2011; ; 2011.
- [61] DeVries NA, Gassman EE, Kallemeyn NA, Shivanna KH, Magnotta VA, Grosland NM. Validation of phalanx bone three-dimensional surface segmentation from computed tomography images using laser scanning. *Skeletal Radiol* 2008;37(1):35-42.
- [62] Grosland NM. IA-FEMesh: An open-source, interactive, multiblock approach to anatomic finite element model development. *Comput Methods Programs Biomed* 2009;94(1):96.
- [63] Kallemeyn NA, Tadeipalli SC, Shivanna KH, Grosland NM. An interactive multiblock approach to meshing the spine. *Comput Methods Programs Biomed* 2009;95(3):227-235.
- [64] Sharma M, Langrana NA, Rodriguez J. Role of ligaments and facets in lumbar spinal stability. *Spine* 1995;20(8):887.
- [65] Kallemeyn N, Gandhi A, Kode S, Shivanna K, Smucker J, Grosland N. Validation of a C2-C7 cervical spine finite element model using specimen-specific flexibility data. *Med Eng Phys* 2010;32(5):482-489.

- [66] Wheeldon JA, Pinar FA, Knowles S, Yoganandan N. Experimental flexion/extension data corridors for validation of finite element models of the young, normal cervical spine. *J Biomech* 2006;39(2):375-380.
- [67] RubertÃfÂ© LM. Influence of single-level lumbar degenerative disc disease on the behavior of the adjacent segments--A finite element model study. *J Biomech* 2009;42(3):341.
- [68] Natarajan RN, Williams JR, Andersson GB. Modeling changes in intervertebral disc mechanics with degeneration. *J Bone Joint Surg Am* 2006 Apr;88 Suppl 2:36-40.
- [69] Banwart JC, Asher MA, Hassanein RS. Iliac crest bone graft harvest donor site morbidity: a statistical evaluation. *Spine* 1995;20(9):1055.
- [70] Assietti R, Beretta F, Arienta C. Two-level anterior cervical discectomy and cage-assisted fusion without plates. *Neurosurg Focus* 2002;12(1):3.
- [71] Nicole Kallemeyn, Joseph Smucker, Douglas Fredericks, Kiran Shivanna and Nicole Grosland. Single Level Fusion in a C27 Cervical Spine Finite Element Model. 33rd Annual Meeting of the American Society of Biomechanics; August 26-29, 2009; ; 2009.
- [72] Tadepalli SC. Toward the Development of Virtual Surgical Tools to Aid Orthopaedic FE Analyses. *EURASIP Journal on Advances in Signal Processing* 2010;2010.
- [73] Gore DR, Sepic SB. Anterior discectomy and fusion for painful cervical disc disease: a report of 50 patients with an average follow-up of 21 years. *Spine* 1998;23(19):2047.
- [74] Phillips FM, Allen TR, Regan JJ, Albert TJ, Cappuccino A, Devine JG, et al. Cervical disc replacement in patients with and without previous adjacent level fusion surgery: a prospective study. *Spine* 2009;34(6):556.
- [75] MM Panjabi. Biomechanical testing to quantify adjacent-level effects. *Trans IV World Congress of Biomechanics*. Calgary, Canada; 2002.
- [76] Panjabi MM, Crisco JJ, Vasavada A, Oda T, Cholewicki J, Nibu K, et al. Mechanical properties of the human cervical spine as shown by three-dimensional load-displacement curves. *Spine* 2001;26(24):2692.
- [77] Panjabi MM. Biomechanical evaluation of spinal fixation devices: I. A conceptual framework. *Spine (Philadelphia, Pa.1976)* 1988;13(10):1129.
- [78] Swathi Kode. Biomechanical effects of multi-level laminoplasty and laminectomy: An experimental and finite element investigation. Iowa City, IA: University of Iowa; 2011.

- [79] Goel VK. Prediction of load sharing among spinal components of a C5-C6 motion segment using the finite element approach. *Spine (Philadelphia, Pa.1976)* 1998;23(6):684.
- [80] Buckwalter JA. Aging and degeneration of the human intervertebral disc. *Spine (Philadelphia, Pa.1976)* 1995;20(11):1307.
- [81] Goel VK, Ramirez SA, Kong W, Gilbertson LG. Cancellous bone Young's modulus variation within the vertebral body of a ligamentous lumbar spine--application of bone adaptive remodeling concepts. *J Biomech Eng* 1995;117(3):266-271.
- [82] Kim YE. Effect of disc degeneration at one level on the adjacent level in axial mode. *Spine (Philadelphia, Pa.1976)* 1991;16(3):331.
- [83] Kumaresan S. Contribution of disc degeneration to osteophyte formation in the cervical spine: a biomechanical investigation. *Journal of Orthopaedic Research* 2006;19(5):977.
- [84] Faizan A. Adjacent level effects of bi level disc replacement, bi level fusion and disc replacement plus fusion in cervical spine-a finite element based study. *Clin Biomech* 2012;27(3):226.
- [85] Womack W. Finite element modeling of kinematic and load transmission alterations due to cervical intervertebral disc replacement. *Spine (Philadelphia, Pa.1976)* 2011;36(17):E1126.
- [86] Chang UK. Changes in adjacent-level disc pressure and facet joint force after cervical arthroplasty compared with cervical discectomy and fusion. *Journal of neurosurgery.Spine* 2007;7(1):33.
- [87] M. Metzger, F. Acosta, J. Buckley, O. O'Reilly and J. Lotz. Facet forces sensitive to total disc replacement device position. San Francisco, CA: Orthopedics Research Society; 2008.
- [88] Stieber JR. The Facet Joint Loading Profile of a Cervical Intervertebral Disc Replacement Incorporating a Novel Saddle-shaped Articulation. *Journal of spinal disorders techniques* 2011;24(7):432.
- [89] Dooris AP. Load-sharing between anterior and posterior elements in a lumbar motion segment implanted with an artificial disc. *Spine (Philadelphia, Pa.1976)* 2001;26(6):E122.
- [90] Hirsch C. Laboratory conditions for tensile tests in annulus fibrosus from human intervertebral discs. *Acta orthopaedica* 1967;38(1-4):148.

- [91] Panjabi MM. Biomechanical time-tolerance of fresh cadaveric human spine specimens. *Journal of Orthopaedic Research* 1985;3(3):292.
- [92] Sedlin ED. Factors affecting the determination of the physical properties of femoral cortical bone. *Acta orthopaedica* 1966;37(1):29.
- [93] Tkaczuk H. Tensile properties of human lumbar longitudinal ligaments. *Acta Orthop Scand* 1968;Suppl 115:1-Suppl 115:1.
- [94] Goel VK. An in-vitro study of the kinematics of the normal, injured and stabilized cervical spine. *J Biomech* 1984;17(5):363.
- [95] Park SA. Correlation of radiostereometric measured cervical range of motion with clinical radiographic findings after anterior cervical discectomy and fusion. *Spine (Philadelphia, Pa.1976)* 2009;34(7):680.
- [96] Wang JC. Increased fusion rates with cervical plating for two-level anterior cervical discectomy and fusion. *Spine (Philadelphia, Pa.1976)* 2000;25(1):41.
- [97] Yoon DH. Clinical and radiological results following cervical arthroplasty. *Acta Neurochir* 2006;148(9):943.
- [98] Fong SY. Design limitations of Bryan disc arthroplasty. *The spine journal* 2006;6(3):233.
- [99] Yanbin Z. Sagittal Alignment Comparison of Bryan Disc Arthroplasty With ProDisc-C Arthroplasty: A Prospective, Randomized Controlled Clinical Trial. *Journal of spinal disorders techniques* 2011;24(6):381.
- [100] Patwardhan AG. Load-carrying capacity of the human cervical spine in compression is increased under a follower load. *Spine (Philadelphia, Pa.1976)* 2000;25(12):1548.